

Log-normal Stochastic Volatility Model with Quadratic Drift: Applications to Assets with Positive Return-Volatility Correlation and to Inverse Martingale Measures

Artur Sepp* Parviz Rakhmonov†

15th September, 2022

Abstract

We show that the application of conventional stochastic volatility (SV) models may not be feasible for the arbitrage-free valuation of derivative securities on assets with positive return-volatility correlation under the money-market account (MMA) measure and under the inverse price measure. The existence of the inverse martingale measure, where an asset is used as the numeraire itself, is critical for valuation of options on cryptocurrencies, where most traded options have inverse payoffs.

We introduce the log-normal SV model with a quadratic drift, which allows for the arbitrage-free valuation of options on assets with positive return-volatility correlation under both the MMA and the inverse measures. We show that the proposed volatility process has a strong solution. We then develop an analytic approach to compute an affine expansion for the moment generating function of the log-price, its quadratic variance (QV) and the instantaneous volatility.

We finally demonstrate application of our model and the accuracy of our solution for valuation and calibration of listed options on assets with positive return-volatility correlation and for inverse options on Bitcoin cryptocurrency.¹

Keywords: Log-normal stochastic volatility, Non-affine models, Closed-form solution, Moment generating function, cryptocurrency derivatives, Quadratic variance

1 Introduction

Empirical studies strongly support evidence that the volatility of price returns is itself a stochastic process (see, for an example, [Shephard \(2005\)](#) for a comprehensive survey). It is accepted that the celebrated model by [Black and Scholes \(1973\)](#) and [Merton \(1973\)](#), which assumes a constant volatility, cannot explain implied volatility surfaces observed in option markets, which are inhomogeneous in strike and maturity dimensions. In contrast, stochastic volatility (SV) models are able to fit to implied volatility surfaces and their dynamics.

1.1 Evidence of Log-normality of Implied and Realized Volatilities

Applications of log-normal SV models, which are based either on the log-normal dynamics for the instantaneous volatility or on the Gaussian dynamics for the logarithm of the volatility, are widespread in practice. Predominantly, SABR model by [Hagan et al \(2002\)](#) is widely used among practitioners for fitting implied volatility surfaces. However, for modeling the dynamics of volatility

*Syngnum Bank, Zurich, Switzerland, artursepp@gmail.com

†Citigroup, London, United Kingdom, parviz.msu@gmail.com

¹Github project <https://github.com/ArturSepp/StochVolModels> provides Python code with the implementation of option valuation using the affine expansion and examples of model calibration to implied volatility data applied in this paper.

surfaces, we need to account for the mean-reversion of the volatility process like in conventional SV models. The mean-reversion implies that the distribution of the volatility has a stationary long-run distribution and simulated paths of model dynamics by Monte-Carlo do not explode.

In an excellent study [Christoffersen, Jacobs and Mimouni \(2010\)](#) examine the empirical performance of Heston, log-normal and 3/2 SV models using three sources of market data: the VIX index, the implied volatility for options of the S&P500 index, and the realized volatility of returns on the S&P500 index. They found that, for all three sources of data, the log-normal SV model outperforms its alternatives. [Tegner and Poulsen \(2018\)](#) report similar finding using realized volatilities.

We note that conventional [Hull and White \(1988\)](#), [Heston \(1993\)](#), and 3/2 ([Lewis \(2000\)](#), [Carr and Sun \(2007\)](#)) SV volatility models specify the dynamics for the stochastic variance of returns. [Hagan et al \(2002\)](#) and [Karasinski and Sepp \(2012\)](#) specify the log-normal dynamics for the stochastic volatility. In another widely used specification, the so called Exp-OU specification, the stochastic process is defined for the logarithm of the volatility². In fact, all three specifications for the stochastic driver of the volatility may result in the “loss of martingality” of the price process when the return-volatility correlation is positive (see, for example, [Lewis \(2000, 2016, 2018\)](#) and [Lions and Musiela \(2007\)](#)). Then, market has a strong bubble as the price process is a strict a local martingale, see [Herdegen and Schweizer \(2016\)](#), which may lead to arbitrages.

In a related research, [Lewis \(2018\)](#) introduces a log-normal SV model with a quadratic drift without a constant term and suggests to apply the model only when return-volatility correlation is negative because of the loss of martingality when return-volatility correlation is positive. [Carr and Willems \(2019\)](#) introduce the log-normal SV model with the quadratic drift, similar to our model, and specify the condition for the mean-reversion parameter of the quadratic term so that the price process is a true martingale. In our paper we augment the log-normal SV model with the linear drift term introduced in [Karasinski and Sepp \(2012\)](#) to include the quadratic drift term. We contribute to studies of [Lewis \(2018\)](#) and [Carr and Willems \(2019\)](#) by defining the martingale conditions under both MMA measure and inverse measures. We also develop an analytic approach for valuation of vanilla and inverse options.

1.2 Dynamics with Positive Return-Volatility Correlation

[Carr and Wu \(2017\)](#) propose three economic factors behind negative return-volatility correlation, which is most typically observed in the dynamics of stock prices and stock indices: aggregate financial leverage, systematic risk, positive auto-correlation of negative shocks. However, in many markets we actually observe asset dynamics with positive return-volatility correlation either on a permanent basis or on a temporary basis.

In Figure 1, we use the market data of four assets to illustrate their term structures of implied volatility skews, displayed as function of corresponding option deltas. In the legend, we show the corresponding 25-delta skews, which equal the difference between implied volatilities of +25-delta calls and -25-delta puts. Positive skew is indicative of positive return-volatility correlation.

1. Assets providing protection against increases in equity index volatilities (such as the VIX index which is linked to the volatilities of the S&P 500 index) have persistent and strong positive skews. During equity market corrections, the VIX index may increase significantly because of strong negative correlation between its returns and returns of the S&P500 index. As a result, out-of-the-money calls on the VIX index provide protection against equity risk and, thus, demand higher implied volatilities, as shown in Subplot (A).

2. Assets with either short or leveraged short exposure to equity indices have significant positive skews because of their anti-correlation to underlying equity indices. In Subplot (B), we illustrate

²Exp-OU SV models are studied in [Fouque, Papanicolaou and Sircar \(2000\)](#), [Detemple and Osakwe \(2000\)](#), [Masoliver and Perelló \(2006\)](#), [Perelló, Sircar and Masoliver \(2008\)](#), [Bormetti, Cazzola, Montagna and Nicrosini \(2008\)](#), [Drimus \(2012\)](#), [Bayer, Gatheral and Karlsmark \(2013\)](#). Exp-OU SV models are widespread in industry as a basis for local SV models ([Lipton \(2002\)](#)), see [Jonsson and Sircar \(2002\)](#), [Bergomi \(2015\)](#), [Bühler \(2006\)](#), [Ren, Madan and Qian \(2007\)](#), [Henry-Labordère \(2009\)](#), [Bergomi and Guyon \(2012\)](#), [Kaye \(2012\)](#).

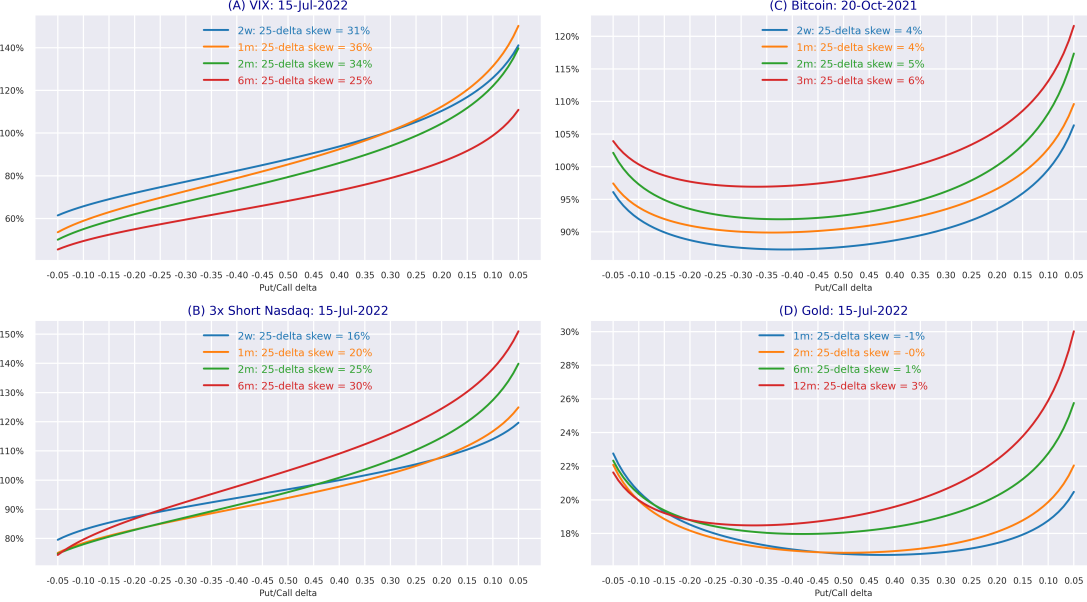


Figure 1: Implied volatilities of assets with positive return-volatility correlation with x-axis being corresponding Black-Scholes option delta. Subplot (A) shows skews of options on the VIX index, (B) shows skews of 3x short Nasdaq ETF (NYSE ticker is SQQQ), (C) shows skews on Bitcoin cryptocurrency (using Deribit options exchange data taken on 20-Oct-2022), (D) shows skews of gold ETF (GLD). Market data for (A), (B), (D) are taken on 15-Jul-2022. 2w stands for options with two weeks to maturity; 1m, 2m, 3m, 6m, 12m stands for 1, 2, 3, 6, 12 months to maturity, respectively. For each maturity, the label displays 25-delta skew which is the difference between implied volatilities for +25-delta call and -25-delta put at that maturity.

the implied skews of 3x Short Nasdaq exchange-traded fund (ETF) (with NYSE ticker SQQQ), which is the largest short ETF in US equity market and which has very liquid listed options market.

3. Assets with demand for leveraged upside exposures and with somewhat speculative dynamics may exhibit positive skews during regimes of persistent price increases. In Subplot (C), we show positive skews on options on Bitcoin cryptocurrency observed during the most recent all time highs in late October 2021 using Deribit options exchange data. For this type of dynamics, the pattern of positive skews may change to negative skews once a “greed” regime is followed by a “fear” regime, where the demand for defensive puts increases due to the risk-aversion³.

4. Assets with time-inhomogeneous supply-demand imbalances may exhibit implied volatility skews with different signs for different options maturities. In Subplot (D), we show the implied volatility skews of gold ETF (with NYSE ticker GLD). Options with short-term maturities exhibit a higher demand for puts, while longer maturities exhibit a higher demand for calls due to hedging demand against macro instabilities. Such patterns of implied skews are most typical for commodities, where positive or negative implied skews may be dependent on the supply-demand and seasonality patterns.

In Table 1, we show that the parameters of our proposed log-normal model, which are calibrated to implied volatilities of these four assets, imply positive return-volatility correlation. As a result, the application of conventional SV models may be infeasible, which we address in Section 2.3.

³Interestingly, similar patters are also typical during greed regimes of the so-called “meme” stocks and emerging market indices. For an example, using the dynamics observed in the Chinese stock market, Wu *et al* (2018) argue that the positive return-volatility correlation during such periods could be due to, firstly, short selling constraints, including inability to sell short and high borrowing costs; and, secondly, self-feeding price increases, especially involving leveraged players.

1.3 Inverse Martingale Measure

For inverse options, the payoff is defined in the units of the underlying asset, so that both option premium and final payoff are quoted in the units of the underlying asset. In fact, options with inverse payoffs are dominant in the cryptocurrency options market. The advantage of inverse payoffs for crypto markets is that all option-related transactions can be handled using units of underlying cryptocurrencies, such as Bitcoin or Ether, without using fiat currencies (see [Lucic \(2021\)](#) for a connection between the valuation of the inverse cryptocurrency options and FX options). Importantly, when both inverse option payoffs (on Deribit, which is the largest crypto exchange) and vanilla payoffs (on CBOE, which is the second most liquid venue) are traded in the market, a SV model must satisfy the martingale condition for both MMA and inverse measures to exclude arbitrage opportunities between vanilla and inverse options.

Also, the inverse measure can be applied for the analysis of explosions in SV models, see [Sin \(1998\)](#), [Lewis \(2000\)](#), [Andersen and Piterbarg \(2007\)](#). In fact, [Sin \(1998\)](#) relates the loss of martingale property for the price process to explosions in finite time of the “auxiliary volatility process”, which coincides with the dynamics of the volatility process under the inverse measure.

In Section 4, we contribute to the literature by introducing the inverse measure and examining conditions under which the inverse measure exists as a martingale measure. This result is important for the arbitrage-free valuation of options with inverse payoffs, such as options on cryptocurrencies.

1.4 Analytical Tractability

Log-normal SV models cannot be handled by semi-analytic Fourier methods available for affine SV models. The analytical intractability may have resulted in a slow adaptation of log-normal SV models in spite of their empirical support.

We note that the log-normal SV model with the quadratic drift does not belong to the family of affine diffusions because the so-called admissible set of parameters is not satisfied, see [Duffie, Filipović and Schachermayer \(2003\)](#), [Filipović and Mayerhofer \(2009\)](#). Further, because of the quadratic drift, the model does not belong to a general family of polynomial diffusions, see [Filipović and Larsson \(2016\)](#), [Cuchiero, Keller-Ressel and Teichmann \(2012\)](#). We note that [Carr and Willems \(2019\)](#) introduce measure change and relate the model to the class of polynomial diffusions, which comes at cost of introducing an additional state variable. Authors then approximate the payoff function using an orthogonal polynomial expansion, see [Ackerer and Filipović \(2020\)](#), for option pricing applications. A related approach for computing the moments under SV models using expansions is developed by [Alòs-Gatheral-Radoicic \(2020\)](#).

We contribute with a closed-form approximate and very accurate solution for the log-normal SV model to circumvent its analytical intractability. In Section 5, we develop an affine expansion to derive a closed-form solution for the moment generating function (MGF) of the log-price process, the its quadratic variance (QV), and the volatility. We show that our solution to the MGF produces valid probability density functions of the state variables which are aligned with Monte Carlo (MC) simulations. In Section 6, we derive closed-form solution for pricing vanilla and inverse options, which are applied for fast calibration of model parameters to market data.

1.5 Organization of the Paper

In Section 2, we provide the framework and introduce the log-normal beta SV model with quadratic drift. We introduce the MMA and the inverse measures and derive conditions for no-arbitrage pricing within SV models. In Section 3, we establish important properties of the volatility process and study unconditional return distribution under stationary distribution of the volatility. In Section 4, we study conditions for price dynamics to be martingales under MMA and inverse measures. In Section 5, we present first- and second-order affine expansion for the MGF of the log-price process, the QV and the volatility. In Section 6, we apply affine expansion to derive

close-form solutions for option valuation problem under the MMA and the inverse measures. In Section 7 we apply our method for model calibration to market data and demonstrate the accuracy of both the model specification and our proposed solution methods. Technical proofs are provided in Appendix A.

2 Framework and Key Results

2.1 Vanilla and Inverse payoffs

While a payoff of (cash-settled) vanilla options is settled in the units of cash, a payoff of an inverse option is settled in the units of the underlying asset using asset price fixed at the option maturity. In particular, options with inverse payoffs are prevalent in cryptocurrency option markets. Deribit exchange, which is the most liquid crypto exchange with over 90% of total options volume, incorporates trading in inverse options on Bitcoin and Ethereum with premiums quoted and traded using Bitcoin and Ethereum units, respectively. The rationale for the inverse payoff is that all transactions for premium and payoff settlements are handled using Bitcoin or Ethereum rather than fiat, which is an attractive feature for transactions between crypto exchanges and wallets.

We denote the spot price at time T by S_T , and we assume that the price is quoted in United State Dollar (USD). We consider vanilla call and puts payoffs settled in USD cash at maturity time T , respectively by

$$u^{\text{call}}(S_T) = \max \{S_T - K, 0\}, \quad u^{\text{put}}(S_T) = \max \{K - S_T, 0\}. \quad (1)$$

payoffs of inverse call and put options are converted to units of the underlying asset at maturity T as follows

$$r^{\text{call}}(S_T) = \frac{1}{S_T} \max \{S_T - K, 0\}, \quad r^{\text{put}}(S_T) = \frac{1}{S_T} \max \{K - S_T, 0\}. \quad (2)$$

2.2 Valuation under Equivalent MMA and Inverse Measures

We consider a continuous-time market with a fixed horizon date $T^* > 0$ with uncertainty modeled on probability space $(\Omega, \mathbb{F}, \mathbb{P})$ equipped with filtration $\{\mathbb{F}\}_{0 \leq t \leq T^*}$. We assume that filtration satisfies usual conditions of right-continuity and completeness.

2.2.1 Spot Markets

We make the following assumption.

Assumption 2.1. *Risk-free rate $r(t)$ is deterministic with the value of one units of the money market account $M(T)$ given by*

$$M(T) = e^{\bar{r}(0,T)}, \quad \bar{r}(t, T) = \int_t^T r(s) ds. \quad (3)$$

We assume that the market is complete and satisfies the so-called *No Free Lunch with Vanishing Risk* (NFLVR) and *No Dominance* (ND) conditions. By choosing M as a numéraire, we consider an equivalent martingale measure \mathbb{Q} , induced by M . Accordingly, the time- t value of an option, denoted by $U(t, S)$, with payoff function $u(S_T)$ at time T , equals to

$$U(t, S) = M(t) \mathbb{E} \left[\frac{1}{M(T)} u(S_T) \mid \mathcal{F}_t \right], \quad (4)$$

where expectation \mathbb{E} is taken under the MMA martingale measure \mathbb{Q} .

Next, by choosing S as a numéraire, we consider an inverse martingale measure $\tilde{\mathbb{Q}}$, induced by S . The option value function, denoted by $\tilde{U}(t, S)$, with the payoff paid in units of S , equals to

$$\tilde{U}(t, S) = S_t \tilde{\mathbb{E}} \left[\frac{1}{S_T} u(S_T) \mid \mathcal{F}_t \right], \quad (5)$$

where expectation $\tilde{\mathbb{E}}$ is taken under the inverse martingale measure $\tilde{\mathbb{Q}}$.

Theorem 2.1. *We assume that a complete market satisfying NFLVR and ND conditions. We assume that both the MMA measure \mathbb{Q} and the inverse measure $\tilde{\mathbb{Q}}$ are equivalent martingale measures. Then the values of options under the MMA measure in Eq (4) and under the inverse measure are in Eq (5) are unique and satisfy*

$$M(t) \mathbb{E} \left[\frac{1}{M(T)} u(S_T) \mid \mathcal{F}_t \right] = S_t \tilde{\mathbb{E}} \left[\frac{1}{S_T} u(S_T) \mid \mathcal{F}_t \right]. \quad (6)$$

Proof. As shown in Theorem 3.2 of [Jarrow and Larsson \(2012\)](#) and Theorem 2.17 of [Herdegen and Schweizer \(2018\)](#), the market satisfies NFLVR and ND conditions if and only if \mathbb{Q} is a true martingale measure. Hence, asset prices, discounted by numéraire M are true \mathbb{Q} -martingales. Consequently, due to the uniqueness of price, we can write (6). To justify the equality of both sides, we also used the existence and uniqueness of equivalent inverse (true) martingale measure $\tilde{\mathbb{Q}}$ for the numéraire S , see Theorem 4.4 and Corollary 3.11 in [Herdegen and Schweizer \(2018\)](#). \square

2.2.2 Futures Markets

Since most option markets for commodities and cryptocurrencies are based on futures, we also adopt our methodology for futures options. We consider a set of futures contracts settled at times $\{T_k\}_{k=1,\dots,K}$ with prices $\{F_t^{T_k}\}_{k=1,\dots,K}$.

Assumption 2.2. *The convenience yield $q(t)$ of futures prices is deterministic with the integrated convenience yield given by*

$$\bar{q}(t, T) = \int_t^T q(s) ds. \quad (7)$$

Definition 2.1. *Measure $\tilde{\mathbb{Q}}^T$ induced by price F_t^T with futures maturity at T , $T \in \{T_k\}$, chosen as a numeraire is called the inverse T -futures measure.*

Corollary 2.1. *We assume that the market is complete and satisfies NFLVR and ND conditions. We assume that both the MMA measure \mathbb{Q} and the inverse futures measure $\tilde{\mathbb{Q}}^T$ are equivalent martingale measures. Then option values under the MMA and the inverse measures are unique and satisfy*

$$M(t) \mathbb{E} \left[\frac{1}{M(T)} u(F_T) \mid \mathcal{F}_t \right] = F_t \tilde{\mathbb{E}}^T \left[\frac{1}{F_T} u(F_T) \mid \mathcal{F}_t \right]. \quad (8)$$

For markets, where both vanilla and inverse options are tradable, such as cryptocurrency markets, any SV model applied for joint valuation of options across several exchanges and contract specifications must satisfy the conditions (6) and (8). For this purpose, we may need to impose certain conditions on model parameters, which we will address in Section 4.

2.3 Log-normal Model Dynamics

2.3.1 The MMA Measure

We consider the log-normal beta SV model introduced by [Karasinski and Sepp \(2012\)](#) and augment it with the quadratic drift in the volatility process as introduced by [Lewis \(2018\)](#) and [Carr and](#)

Willems (2019). The SV model is specified for the spot price S_t , the instantaneous volatility σ_t and the QV I_t under the MMA measure \mathbb{Q} as follows

$$\begin{aligned} dS_t &= r(t)S_t dt + \sigma_t S_t dW_t^{(0)}, \quad S_0 = S, \\ d\sigma_t &= (\kappa_1 + \kappa_2 \sigma_t)(\theta - \sigma_t)dt + \beta \sigma_t dW_t^{(0)} + \varepsilon \sigma_t dW_t^{(1)}, \quad \sigma_0 = \sigma, \\ dI_t &= \sigma_t^2 dt, \quad I_0 = I, \end{aligned} \tag{9}$$

where $r(t)$ is the deterministic risk-free rate; $W_t^{(0)}$ and $W_t^{(1)}$ are uncorrelated Brownian motions, $\beta \in \mathbb{R}$ is the volatility beta which measures the sensitivity of the volatility to changes in the spot price, and $\varepsilon > 0$ is the volatility of residual volatility. We denote by ϑ^2 , $\vartheta^2 = \beta^2 + \varepsilon^2$, the total instantaneous variance of the volatility process.

The mean-reversion of the volatility process is specified using the mean level of the volatility θ , $\theta > 0$, and the mean-reversion speed which is the linear function of the volatility $\kappa_1 + \kappa_2 \sigma_t$, $\kappa_1 \geq 0$, $\kappa_2 \geq 0$. As a result, the quadratic drift of the volatility process is given by

$$\mu(\sigma) \equiv (\kappa_1 + \kappa_2 \sigma)(\theta - \sigma) = \kappa_1 \theta - (\kappa_1 - \kappa_2 \theta)\sigma - \kappa_2 \sigma^2. \tag{10}$$

In addition to modeling advantages that we employ in our development, Bakshi *et al* (2006) find that the presence of non-linear terms, including the quadratic term, in the volatility drift is significant when using econometric estimation of the dynamics of the VIX index.

We introduce the zero-drift stochastic driver Z_t , $Z_t = e^{-\int_0^t r(t')dt'} S_t$ and its inverse process R_t , $R_t = Z_t^{-1}$, with the following dynamics

$$\begin{aligned} dZ_t &= Z_t \sigma_t dW_t^{(0)}, \quad Z_0 = S_0, \\ dR_t &= \sigma_t^2 R_t dt - R_t \sigma_t dW_t^{(0)}, \quad R_0 = 1/Z_0. \end{aligned} \tag{11}$$

We introduce the log of the zero-drift price process X_t , $X_t = \ln Z_t$, driven by

$$dX_t = -\frac{1}{2} \sigma_t^2 dt + \sigma_t dW_t^{(0)}, \quad X_0 = \ln S_0. \tag{12}$$

Using X_T , we can represent the spot price S_T under the MMA measure by

$$S_T = e^{\bar{r}(0,T)} e^{X_T}. \tag{13}$$

Under the assumption (2.1) and (2.2), and using Eq (13), we represent the price of the futures settled at time T under the MMA measure by

$$f_T(T) = e^{\bar{r}(0,T) - \bar{q}(0,T)} e^{X_T}. \tag{14}$$

Accordingly, for modeling purposes, we focus on the zero-drift price dynamics Z_t and its log-price process X_t defined in Eq (12).

2.4 Martingale property under MMA and Inverse Measures

We will collect important results related to the martingale property of the price process and its moments for log-normal SV model with quadratic drift and some other popular SV models. We show that, if return-volatility correlation is positive, the MMA measure does not exist for the log-normal SV with linear drift (and for SABR model with zero drift) and for the Exp-OU SV model. While Heston SV model always produces martingale dynamics under the MMA measure, the model may have non-stationary distribution of the volatility under the inverse measure.

We emphasize that the loss of martingale property directly leads to so-called strong bubble, because discounted price process becomes a strict local martingale. As a consequence, vanilla call option price will not be a convex function of the underlying price and Black-Scholes equation might have multiple solutions, see Cox and Hobson (2005), Jarrow, Protter and Shimbo (2010) and Herdegen and Schweizer (2016).

2.4.1 Log-normal SV model

Theorem 2.2. [Log-normal SV model with quadratic drift] Under model dynamics (9), the price processes Z_t and R_t in Eq (11) we have following properties.

1. The process Z_t is a martingale under the MMA measure \mathbb{Q} iff $\kappa_2 \geq \beta$.
2. The process R_t is a martingale under the inverse measure $\tilde{\mathbb{Q}}$ iff $\kappa_2 \geq 2\beta$.
3. When $u \geq 1$, $\mathbb{E}[(Z_T)^u]$ is finite if $\kappa_2 > \beta u + \vartheta \sqrt{u^2 - u}$ or $\kappa_2 = \beta u + \vartheta \sqrt{u^2 - u}$, $\kappa_1 \geq \kappa_2 \theta$; $\mathbb{E}[(Z_T)^u]$ is infinite if $\kappa_2 < \beta u + \vartheta \sqrt{u^2 - u}$.
When $u \leq 0$, $\mathbb{E}[(Z_T)^u]$ is finite if $\kappa_2 - 2\beta > -\beta u + \vartheta \sqrt{u^2 - u}$ or $\kappa_2 - 2\beta = -\beta u + \vartheta \sqrt{u^2 - u}$, $\kappa_1 \geq \kappa_2 \theta$; $\mathbb{E}[(Z_T)^u]$ is infinite if $\kappa_2 - 2\beta < -\beta u + \vartheta \sqrt{u^2 - u}$.
4. When $h \geq 1$, $\tilde{\mathbb{E}}[(R_T)^h]$ is finite if $\kappa_2 > \beta(h+1) + \vartheta \sqrt{h^2 - h}$ or $\kappa_2 = \beta(h+1) + \vartheta \sqrt{h^2 - h}$, $\kappa_1 \geq \kappa_2 \theta$; $\tilde{\mathbb{E}}[(R_T)^h]$ is infinite if $\kappa_2 < \beta(h+1) + \vartheta \sqrt{h^2 - h}$.
When $h \leq 0$, $\tilde{\mathbb{E}}[(R_T)^h]$ is finite if $\kappa_2 - \beta > -\beta h + \vartheta \sqrt{h^2 - h}$ or $\kappa_2 - \beta = -\beta h + \vartheta \sqrt{h^2 - h}$, $\kappa_1 \geq \kappa_2 \theta$; $\tilde{\mathbb{E}}[(R_T)^h]$ is infinite if $\kappa_2 - \beta < -\beta h + \vartheta \sqrt{h^2 - h}$.

Here, \mathbb{E} and $\tilde{\mathbb{E}}$ denote the expectation under \mathbb{Q} and $\tilde{\mathbb{Q}}$, respectively.

Proof. See Appendix A.1. □

Corollary 2.2. [Log-normal SV model with linear drift] For dynamics (9) with $\kappa_2 = 0$ we obtain.

1. The process Z_t is martingale under \mathbb{Q} iff $\beta \leq 0$.
2. The process R_t is martingale under $\tilde{\mathbb{Q}}$ iff $\beta \leq 0$.
3. When $u \geq 1$, $\mathbb{E}[(Z_T)^u]$ is finite iff $\beta u \leq -\vartheta \sqrt{u^2 - u}$.
When $u \leq 0$, $\mathbb{E}[(Z_T)^u]$ is finite iff $\beta(2-u) \leq -\vartheta \sqrt{u^2 - u}$.
4. When $h \geq 1$, $\tilde{\mathbb{E}}[(R_T)^h]$ is finite iff $\beta(h+1) \leq -\vartheta \sqrt{h^2 - h}$.
When $h \leq 0$, $\tilde{\mathbb{E}}[(R_T)^h]$ is finite iff $\beta(1-h) \leq -\vartheta \sqrt{h^2 - h}$.

Proof. Follows by setting $\kappa_2 = 0$ everywhere in Theorem 2.2. □

In Subplot (B) of Figure 2, we illustrate admissible regions for the log-normal SV model with quadratic drift. We observe that Z_T and R_T are martingales for broad range of parameters. As long as parameter κ_2 is larger than $\max\{\beta, 0\}$ and $\max\{2\beta, 0\}$, the MMA and the inverse measures, respectively, exist. For comparison, we also illustrate corresponding admissible regions when $\kappa_2 = 0$ in Subplot (A). We see that, in the log-normal SV model with linear drift, Z_T and R_T are martingales only if $\beta \leq 0$, so that return-volatility correlation must be negative.

2.4.2 Heston model

We consider Heston SV model model for the zero-drift price process Z_t and its inverse $R_t = Z_t^{-1}$

$$\begin{aligned} dZ_t &= \sqrt{V_t} Z_t dW_t^{(S)}, \quad Z_0 = Z, \\ dV_t &= \kappa(\theta - V_t) dt + \vartheta \sqrt{V_t} dW_t^{(V)}, \quad V_0 = v. \end{aligned} \tag{15}$$

where $W^{(S)}$ and $W^{(V)}$ are Brownian motions with the correlation parameter ρ .

Proposition 2.1. We have the following properties for Heston dynamics (15).

1. The process Z_t is always \mathbb{Q} -martingale.

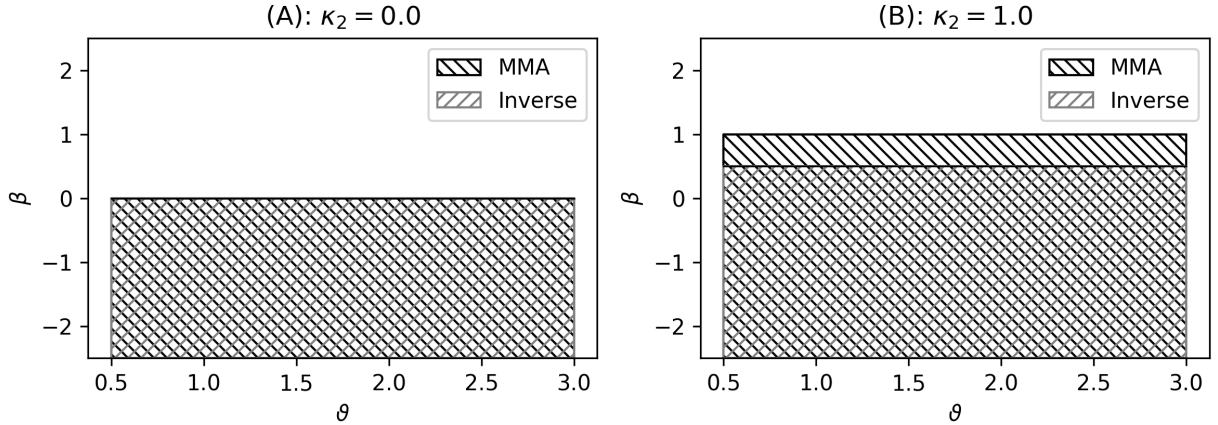


Figure 2: Subplot (A) shows the admissible region of model parameters (β, ϑ) for the martingale property of Z_T under the MMA measure \mathbb{Q} and of R_T under the inverse measure $\tilde{\mathbb{Q}}$ in the log-normal SV model with linear drift with $\kappa_2 = 0$. Subplot B shows the admissible region for the log-normal SV model with the quadratic drift with $\kappa_2 = 1$. Both measures \mathbb{Q} and $\tilde{\mathbb{Q}}$ are martingale in the area with overlapping hatches.

2. The process R_t is always $\tilde{\mathbb{Q}}$ -martingale.

3. $\mathbb{E}[(Z_T)^m]$ is finite for all $T > 0$, if $\rho \leq -\sqrt{\frac{m-1}{m}} + \frac{\kappa}{m\vartheta}$. If $\rho > -\sqrt{\frac{m-1}{m}} + \frac{\kappa}{m\vartheta}$, then $\mathbb{E}[S_T^m]$ is finite for all $T < T^*$, T^* is a blow-up time of $A(t)$, where $A(t)$ solves Riccati ODE

$$A(t)' = \frac{\vartheta}{2}(A(t))^2 + (\rho\vartheta m - \kappa)A(t) + \frac{m^2 - m}{2}, \quad A(0) = 0.$$

Furthermore, $\mathbb{E}[(Z_T)^m] = +\infty$ for all $T > T^*$ if $\rho > -\sqrt{\frac{m-1}{m}} + \frac{\kappa}{m\vartheta}$.

4. $\tilde{\mathbb{E}}[(R_T)^m]$ is finite for all $T > 0$, if $\rho \leq -1 + \frac{\kappa}{\vartheta(m-1)}$. If $\rho > -1 + \frac{\kappa}{\vartheta(m-1)}$, then $\tilde{\mathbb{E}}[(R_T)^m]$ is finite for all $T < T^*$, T^* is a blow-up time of $A(t)$, where $A(t)$ solves Riccati ODE

$$A(t)' = \frac{\vartheta}{2}(A(t))^2 + (\rho\vartheta(m-1) - \kappa)A(t) + \frac{m^2 - m}{2}, \quad A(0) = 0.$$

Furthermore, $\tilde{\mathbb{E}}[(R_T)^m] = +\infty$ for all $T > T^*$ if $\rho \leq -1 + \frac{\kappa}{\vartheta(m-1)}$.

Proof. See Appendix A.2. □

We conclude that, while Heston model produces martingale dynamics under both \mathbb{Q} and $\tilde{\mathbb{Q}}$, the model has a restriction for mean-reversion κ , $\kappa > \rho\vartheta$, to ensure that the stationary distribution of the variance exists under $\tilde{\mathbb{Q}}$. Under \mathbb{Q} , Feller condition is $2\kappa\vartheta > \vartheta^2$ which ensures that variance cannot hit zero. In Subplot (A) of Figure 3, we show the admissible regions using these conditions.

2.4.3 Exponential Ornstein-Uhlenbeck (OU) model

We consider Exponential OU (Exp-OU) SV model for the zero-drift price process Z_t and $R_t = Z_t^{-1}$

$$\begin{aligned} dZ_t &= Z_t e^{Y_t} dW_t^{(Z)}, \quad Z_0 = Z, \\ dY_t &= \kappa(\theta - Y_t)dt + \vartheta dW_t^{(Y)}, \quad Y_0 = \ln \sigma \end{aligned} \tag{16}$$

where $W^{(Z)}$ and $W^{(Y)}$ are Brownian motions with the correlation parameters ρ .

Proposition 2.2. For Exp-OU model (16) we have following properties.

1. The process Z_t is martingale iff $\rho \leq 0$.

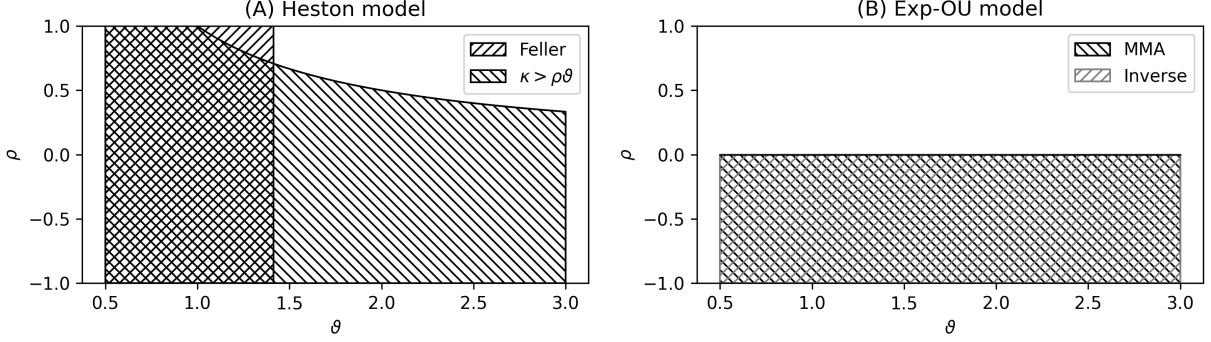


Figure 3: Subplot (A) shows the admissible region for parameters (ρ, ϑ) of Heston model where Feller condition is satisfied and the stationary distribution exists under the inverse measure using $\kappa = 1$, $\theta = 1$. Subplot (B) shows the admissible region parameters (ρ, ϑ) of Exp-OU SV model for the martingale property under the MMA and inverse measures using $\kappa = 1$, $\theta = 1$. Both conditions are satisfied in the area with overlapping hatches.

2. The process R_t is martingale iff $\rho \leq 0$.
3. When $u \geq 1$, $\mathbb{E}[(Z_T)^u]$ is finite iff $\rho u \leq -\sqrt{u^2 - u}$.
When $u \leq 0$, $\mathbb{E}[(Z_T)^u]$ is finite iff $\rho(2 - u) \leq -\sqrt{u^2 - u}$.
4. When $h \geq 1$, $\tilde{\mathbb{E}}[(R_T)^h]$ is finite iff $\rho(h + 1) \leq -\sqrt{h^2 - h}$.
When $h \leq 0$, $\tilde{\mathbb{E}}[(R_T)^h]$ is finite iff $\rho(1 - h) \leq -\sqrt{h^2 - h}$.

Proof. See Appendix A.3 □

We conclude that, under Exp-OU SV model, both the MMA and the inverse measures lack the martingale property when return-volatility correlation ρ is positive. In Subplot (B) of Figure 3, we illustrate the admissible regions for Exp-OU SV model. We note that OU SV model of Stein-Stein (1991) shares the same properties in (2.2) so that it cannot be applied for assets with positive return-volatility correlation (Lipton-Sepp (2008) show that Stein-Stein model is a viable SV model despite its volatility process is not sign-constraint).

3 Log-normal Volatility Process

3.1 Quadratic Drift

We establish important properties related to the regularity of the volatility process. We consider the SDE of volatility process in model dynamics (9) represented as follows

$$\begin{aligned} d\sigma_t &= \mu(\sigma_t)dt + v(\sigma_t)dW_t^{(*)}, \quad \sigma_0 = \sigma, \\ \mu(\sigma) &= (\kappa_1 + \kappa_2\sigma)(\theta - \sigma), \quad v(\sigma) = \vartheta\sigma, \end{aligned} \tag{17}$$

where $W_t^{(*)}$ is a standard Brownian motion and ϑ is the total volatility of volatility.

We notice that the process σ_t is not a polynomial diffusion, see Filipović and Larsson (2016), Lemma 2.2, because the drift coefficient is a second-order polynomial in σ_t . In Subplot (A) of Figure 4, we illustrate the three specifications of the mean-reversion drift. The first case with $\kappa_2 = 0$ corresponds to the linear drift in the current volatility σ_t . The second case with $\kappa_2 = \kappa_1/\theta$ corresponds to the pure quadratic drift $\kappa_1(\theta - \sigma_t^2/\theta)$ (we refer to Section 7.2 for the discussion of why we apply this specification for practical implementation of the model). The third case correspond to the quadratic case. In Subplot (B), we show the drift relative to the linear case. We see that, when the volatility is high, by increasing κ_2 , negative drift increases in the magnitude. Thus, the volatility reverts faster to the mean level when starting with high values.

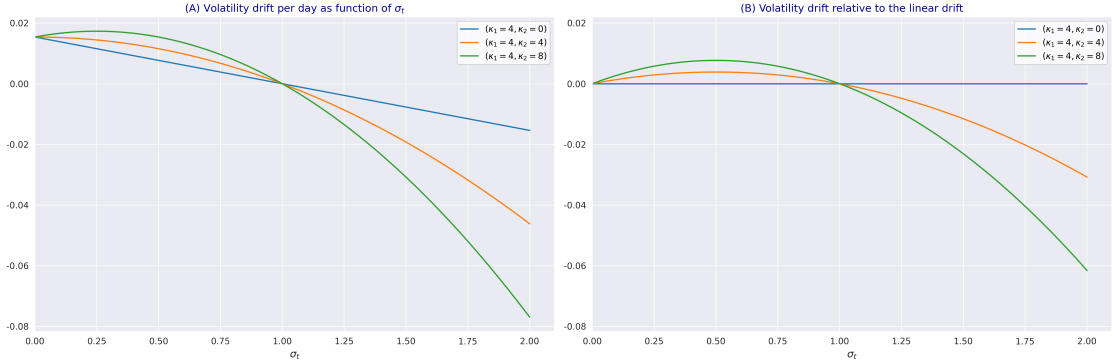


Figure 4: Subplot (A) displays the drift of the volatility process in Eq (17) as function of σ_t using $\theta = 1.0$. The case $(\kappa_1 = 4, \kappa_2 = 0)$ corresponds to the linear mean-reversion; the case $(\kappa_1 = 4, \kappa_2 = 4)$ (and more generally the case with $\kappa_2 = \kappa_1/\theta$) corresponds to the pure quadratic drift; the case $(\kappa_1 = 4, \kappa_2 = 8)$ corresponds to the quadratic drift. Subplot (B) shows the drifts relative to the linear drift.

3.2 Regularity

We note that SDE (17) has super-linearly growing drift, hence standard results for the uniqueness of strong solution are no longer applicable, see Section 5 of Karatzas and Shreve (1991) for details. We will establish the existence of the strong solution in Theorem 3.2. We first provide a boundary classification for the volatility process, and show that the log-normal volatility in SDE (17) cannot reach zero or explode to infinity, which are important properties of the volatility dynamics.

Theorem 3.1. *Boundary points $\{0, +\infty\}$ are unattainable for σ_t in SDE (17).*

Proof. See Appendix A.4. \square

Theorem 3.2. *We assume that*

$$\kappa_1 \geq 0, \kappa_2 \geq 0, \theta > 0, \vartheta \geq 0. \quad (18)$$

Then SDE (17) has unique strong solution.

Proof. See Appendix A.5. \square

Proposition 3.1. *Assuming that $\kappa_1\theta > 0$, we have the following for every $p \in \mathbb{R}$, such that $|p| \geq 1$, and for any T , $T > 0$*

$$\mathbb{E} \left[\sup_{t \in [0, T]} \sigma_t^p \right] < \infty.$$

Proof. See Appendix A.6. \square

We consider the quadratic variance (QV) I_t with $dI_t = d\sigma_t^2 dt$.

Proposition 3.2. *We assume that model parameters $\kappa_1, \kappa_2, \theta, \vartheta$ satisfy Eq (18) and $\kappa_1\theta > 0$. Then the QV is well-defined under the MMA measure and $\mathbb{E}[(I_t)^p] < \infty$ for any p , $|p| \geq 1$. If $\kappa_2 \geq \beta$, then the QV is well-defined under the inverse measure and $\tilde{\mathbb{E}}[(I_t)^p] < \infty$ for any p , $|p| \geq 1$.*

Proof. As $\mathbb{E}[(I_t)^p] = \mathbb{E} \left[\left(\int_0^t \sigma_s \right)^p \right] \leq t^p \mathbb{E} \left[\sup_{s \in [0, t]} \sigma_s^p \right] < \infty$, the first statement follows from Proposition 3.1. The second statement follows using dynamics of the volatility under $\tilde{\mathbb{Q}}$, see (47) \square

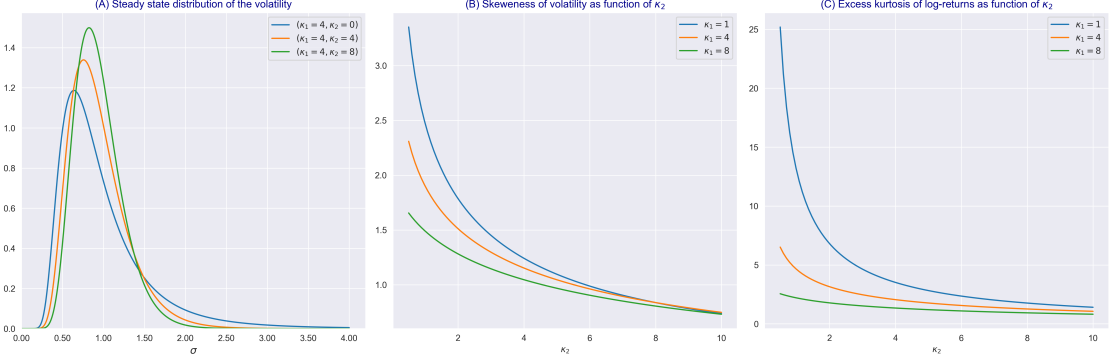


Figure 5: Subplot (A) shows the steady state PDF of the volatility computed using Eq (20) with fixed $\kappa_1 = 4$ and $\kappa_2 = \{0, 4, 8\}$. Subplot (B) and (C) show the skeweness of the volatility computed using Eq (21) and the excess kurtosis of the unconditional returns distribution computed using Eq (26), respectively, both as functions of κ_2 , for the three choices of $\kappa_1 = 1, 4, 8$. Other model parameters are fixed to $\theta = 1$ and $\vartheta = 1.5$.

3.3 Steady-state distribution of the volatility

The steady state density $G(\sigma)$ for the volatility process σ_t in SDE (17) solves the following ODE

$$\frac{1}{2}\vartheta^2 \frac{\partial^2}{\partial\sigma^2} (\sigma^2 G) - \frac{\partial}{\partial\sigma} ((\kappa_1 + \kappa_2\sigma)(\theta - \sigma)G) = 0. \quad (19)$$

The solution is given by the Generalized Inverse Gaussian distribution (see [Jørgensen \(1982\)](#))

$$G(\sigma) = c\sigma^{\eta-1} \exp\left\{-\left(\frac{q}{\sigma} + b\sigma\right)\right\}, \quad \sigma > 0, \quad (20)$$

$$q = 2\frac{\kappa_1\theta}{\vartheta^2}, \quad b = 2\frac{\kappa_2}{\vartheta^2}, \quad \eta = 2\frac{\kappa_2\theta - \kappa_1}{\vartheta^2} - 1, \quad c(b) = \frac{(b/q)^{\eta/2}}{2K_\eta(2\sqrt{qb})}.$$

where $b > 0$, $q \geq 0$, $\eta \in \mathbb{R}$ and K_η is a modified Bessel function of the second kind. For $\kappa_2 = 0$ we use $c(0) = q^{-\eta}\Gamma(-\eta)$, where $\Gamma(x)$ is the gamma function, and the steady state PDF is the inverse gamma function. The r -th moment $m(r)$ associated to the density in Eq (20) is given by

$$m(r) = \begin{cases} \left(\frac{q}{b}\right)^{r/2} \frac{K_{\eta+r}(2\sqrt{qb})}{K_\eta(2\sqrt{qb})} & b > 0, \quad r \in \mathbb{R}_+; \\ q^r \frac{\Gamma(-\eta-r)}{\Gamma(-\eta)} & b = 0, \quad r < -\eta; \\ \infty & b = 0, \quad r \geq -\eta. \end{cases} \quad (21)$$

We see that when $\kappa_2 = 0$, the volatility moments exist only to the order r less than $r < 1 + 2\kappa_1/\vartheta^2$.

In Subplot (A) of Figure 5, we show the steady state density for the set of the three model parameters as in Figure 4. The linear model with $\kappa_2 = 0$ implies the heavy right tail for the distribution of the volatility. In Subplot (B), we show the skewness of the volatility as function of κ_2 . As κ_2 increases, the skewness of the volatility declines.

3.3.1 Unconditional Distribution of Returns

We make an interesting connection between the skewness of the volatility process and the kurtosis of returns distribution. Following Chapter 9 in [Barndorff-Nielsen and Shiryaev \(2015\)](#), we assume that the distribution of returns over period δt is Gaussian conditional on σ

$$q(x | \sigma) = \frac{1}{\sqrt{2\pi\sigma^2\delta t}} \exp\left(-\frac{x^2}{2\sigma\sqrt{\delta t}}\right). \quad (22)$$

The unconditional distribution of returns under the steady-state distribution of the volatility is

$$p(x) = \int_0^\infty q(x | \sigma) G(\sigma) d\sigma. \quad (23)$$

The above integral cannot be computed explicitly. Instead, we compute the central moments of returns under the unconditional distribution

$$m(n) = \int_{-\infty}^\infty x^n p(x) dx = \int_0^\infty \left[\int_{-\infty}^\infty x^n q(x | \sigma) dx \right] G(\sigma) d\sigma, \quad (24)$$

where we exchange the integration order. It is clear that for odd n , $m(n) = 0$. For the second and the fourth moments, we have

$$m(2) = \delta t \int_0^\infty \sigma^2 G(\sigma) d\sigma, \quad m(4) = 3(\delta t)^2 \int_0^\infty \sigma^4 G(\sigma) d\sigma. \quad (25)$$

We compute the excess kurtosis of the distribution using $k = 3m(4)/m^2(2) - 3$ with Eq (21)

$$k = \begin{cases} \frac{3K_{\eta+4}(2\sqrt{qb})K_\eta(2\sqrt{qb})}{(K_{\eta+2}(2\sqrt{qb}))^2} - 3 & \kappa_2 > 0; \\ 3\frac{q^2}{\eta^2} - 3 & \kappa_2 = 0, \kappa_1/\vartheta^2 > 3/2; \\ \infty & \kappa_2 = 0, \kappa_1/\vartheta^2 \leq 3/2. \end{cases} \quad (26)$$

It follows that the kurtosis of the unconditional distribution in Eq (26) is maximal when $b = 0$ ($\kappa_2 = 0$), and it is finite only if liner mean-reversion parameter κ_1 is higher than the total volatility of variance. The kurtosis declines when rate b (κ_2) increases. In Subplot (C) of Figure 5, we show the kurtosis for the three choices of $\kappa_1 = 1, 4, 8$. We see that for the each choice, the parameter κ_2 can be thought as a dampening parameter to reduce both the skewness of the steady-state PDF of the volatility and the kurtosis of the unconditional PDF of returns.

3.4 Mean-adjusted Volatility Process

For further development, we introduce the mean-adjusted volatility process defined by

$$Y_t = \sigma_t - \theta, \quad (27)$$

with the domain of Y_t being $(-\theta, \infty)$. The dynamics of Y_t using SDE (9) become

$$dY_t = (-\kappa Y_t - \kappa_2 Y_t^2) dt + \beta (Y_t + \theta) dW_t^{(0)} + \varepsilon (Y_t + \theta) dW_t^{(1)}, \quad Y_0 = \sigma_0 - \theta, \quad (28)$$

where $\kappa = \kappa_1 + \kappa_2 \theta$. The marginal dynamics of Y_t using SDE (17) are

$$dY_t = (-\kappa Y_t - \kappa_2 Y_t^2) dt + \vartheta (Y_t + \theta) dW_t^{(*)}, \quad Y_0 = \sigma_0 - \theta, \quad (29)$$

where $W_t^{(*)}$ is a standard Brownian motion.

3.5 Moments of Volatility Process

We consider the mean-adjusted process $Y_t = \sigma_t - \theta$ using the dynamics (29) and define its power function $m_t^{(n)}$, $m_t^{(n)} = Y_t^n$, and the m-th moment, $\bar{m}_t^{(n)}$, $n = 0, 1, 2, \dots$, as follows

$$\bar{m}_t^{(n)}(\tau) = \mathbb{E}_t \left[m_\tau^{(n)} \right]. \quad (30)$$

By applying Itô's lemma for $m_t^{(n)}$ under the dynamics (29), we obtain

$$dm_t^{(n)} = (-\kappa Y_t - \kappa_2 Y_t^2) n Y_t^{n-1} dt + c(n) (Y_t + \theta)^2 Y_t^{n-2} dt + \vartheta (Y_t + \theta) n Y_t^{n-1} dW_t^{(*)}, \quad (31)$$

with $m_0^{(n)} = Y_0^n$ and $c(n) = \frac{1}{2}\vartheta^2 n(n-1)$. We notice a pattern of the powers of n which allows for a recursive solution as follows.

Proposition 3.3. [Moments of Volatility Process] The solution to moments in Eq (30), can be presented as a matrix equation for an infinite-dimensional vector

$$\partial_\tau M^{(0,\infty)}(\tau) = \Lambda^{(0,\infty)} M^{(0,\infty)}(\tau), \quad (32)$$

where ∂_τ is the derivative w.r.t. τ and

$$M^{(0,\infty)}(\tau) = (\bar{m}^{(0)}, \bar{m}^{(1)}, \bar{m}^{(2)}, \bar{m}^{(3)}, \bar{m}^{(4)}, \dots)^T, \quad M^{(0,\infty)}(0) = (1, Y_0, Y_0^2, Y_0^3, Y_0^4, \dots)^T$$

$$\Lambda^{(0,\infty)} = \begin{pmatrix} 0 & 0 & 0 & 0 & 0 & 0 & \dots \\ 0 & -\kappa & -\kappa_2 & 0 & 0 & 0 & \dots \\ c(2)\theta^2 & 2c(2)\theta & (c(2)-2\kappa) & -2\kappa_2 & 0 & 0 & \dots \\ 0 & c(3)\theta^2 & 2c(3)\theta & (c(3)-3\kappa) & -3\kappa_2 & 0 & \dots \\ 0 & 0 & c(4)\theta^2 & 2c(4)\theta & (c(4)-4\kappa) & -4\kappa_2 & \dots \\ \dots & & & & & & \end{pmatrix}.$$

An approximate solution to ODE system (32) is obtained using a truncation by fixing the number of terms to k^* and using a finite dimensional vector of m -th moments, $m = 1, \dots, k^*$

$$\partial_\tau M^{(1,k^*)} = \Lambda^{(1,k^*)} M^{(1,k^*)} + C^{(1,k^*)}, \quad (33)$$

$$M^{(1,k^*)}(0) = (Y_0, Y_0^2, \dots, Y_0^{k^*})^T, \quad C^{(1,k^*)} = (0, c(2)\theta^2, 0, 0, \dots, -k^*\kappa_2 Y_0^{k^*+1})^T$$

$$\Lambda^{(1,k^*)} = \begin{pmatrix} -\kappa & -\kappa_2 & 0 & 0 & 0 & \dots \\ 2c(2)\theta & (c(2)-2\kappa) & -2\kappa_2 & 0 & 0 & \dots \\ c(3)\theta^2 & 2c(3)\theta & (c(3)-3\kappa) & -3\kappa_2 & 0 & \dots \\ 0 & c(4)\theta^2 & 2c(4)\theta & (c(4)-4\kappa) & -4\kappa_2 & \dots \\ \dots & 0 & 0 & c(k^*)\theta^2 & 2c(k^*)\theta & (c(k^*)-k^*\kappa) \\ \dots & & & & & \end{pmatrix}.$$

The analytic solution to ODE (33) is given by

$$M^{(1,k^*)}(\tau) = \expm\{\Lambda^{(1,k^*)}t\} \cdot M^{(1,k^*)}(0) + (\Lambda^{(1,k^*)})^{-1} \cdot (\expm\{\Lambda^{(1,k^*)}t\} - I^{(k^*)}) \cdot C^{(1,k^*)}, \quad (34)$$

where $\expm()$ is the matrix exponent, \cdot and $^{-1}$ are the matrix product and inverse, respectively, and $I^{(k^*)}$ is $k^* \times k^*$ identity matrix.

Proof. See Appendix A.8. □

In Figure 6, we plot first four moments of the volatility process computed using Eq (34) with truncation order $k^* = 4$ (Subplot A) and $k^* = 8$ (B). For comparison, we show estimates and 95% confidence intervals obtained by MC simulations. We see that the low-order truncation with $k^* = 4$ is consistent with MC estimates for the first and second moments. The high-order truncation with $k^* = 8$ is consistent with the first four moments compared to MC estimates.

Remark. We note that if $\kappa_2 = 0$, the system (33) becomes lower tridiagonal so that it can be solved exactly for all moments up to k^* by the sequential integration from $n = 1$ to $n = k^*$.

3.5.1 Expected Quadratic Variance (QV)

The expected value of the QV is an important quantity for option pricing. This expected value equals to the model-based fair value of the continuous-time variance swap, which can be used for model calibration. We define the annualized expected QV as follows

$$\widehat{I}_\tau = \frac{1}{\tau} \mathbb{E}_t \left[\int_0^\tau \sigma_t^2 dt \right] = \frac{1}{\tau} \mathbb{E}_t \left[\int_0^\tau (Y_t + \theta)^2 dt \right], \quad I_0 = I. \quad (35)$$

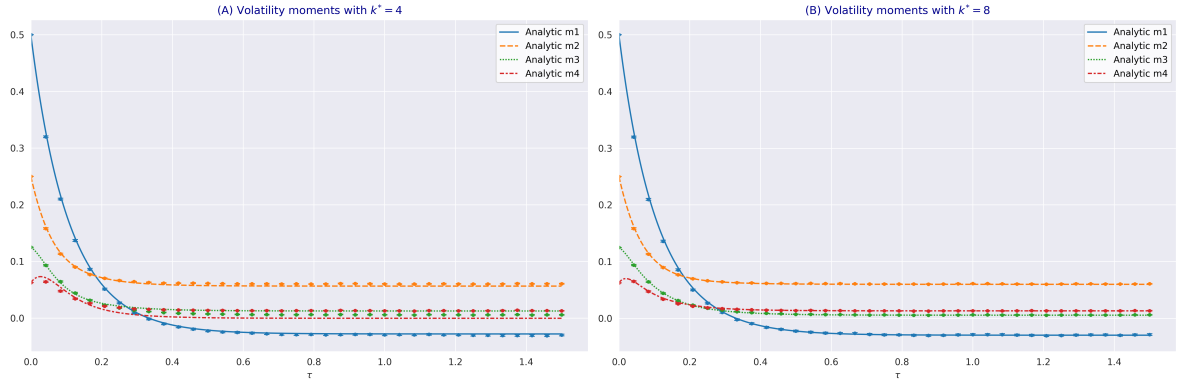


Figure 6: The first four moments of mean-adjusted volatility computed using Eq (34) with the truncation order $k^* = 4$ (Subplot A) and $k^* = 8$ (Subplot B) as functions of τ . The model parameters $\sigma_0 = 1.5$, $\theta = 1.0$, $\kappa_1 = \kappa_2 = 4$, $\vartheta = 1.5$. Dots and error bars denote the estimate and 95% confidence interval, respectively, computed using MC simulations of model dynamics using scheme in Eq (40) with number of path equal 100,000 and daily time steps.

Corollary 3.1 (Analytic solution). *The expected value of the QV using k^* -th order truncation is*

$$\widehat{I}_\tau = \frac{1}{\tau} \int_0^\tau \left(\overline{m}^{(2)}(\tau') + 2\theta \overline{m}^{(1)}(\tau') \right) d\tau' + \theta^2 = \frac{1}{\tau} \left(\widehat{\overline{m}}^{(2)}(\tau) + 2\theta \widehat{\overline{m}}^{(1)}(\tau) \right) + \theta^2 + O(k^*), \quad (36)$$

where $\widehat{\overline{m}}^{(1)}$ and $\widehat{\overline{m}}^{(2)}$ are the first and second elements in vector $\widehat{M}^{(1,k^*)}(\tau)$ computed using Eq (37), and $O(k^*)$ is the truncation error. The integrated moments of the volatility with the k^* -order truncation are computed by

$$\begin{aligned} \widehat{M}^{(1,k^*)}(\tau) \equiv & \int_0^\tau M^{(1,k^*)}(\tau) = \left(\Lambda^{(1,k^*)} \right)^{-1} \cdot \left(\text{expm} \left\{ \Lambda^{(1,k^*)} t \right\} - I \right) \cdot M^{(1,k^*)}(0) \\ & + \left(\Lambda^{(1,k^*)} \right)^{-1} \cdot \left(\left(\Lambda^{(1,k^*)} \right)^{-1} \cdot \left(\text{expm} \left\{ \Lambda^{(1,k^*)} t \right\} - I \right) - \tau I \right) \cdot C^{(1,k^*)}. \end{aligned} \quad (37)$$

The approximation term $O(k^*)$ includes only the truncation error $O(k^*)$, because Eq (37) is computed analytically using matrix exponentiation.

In Figure 7, we show the computation of the expected QV using Eq (36) with comparisons to the estimate (dot) and 95% confidence interval obtained by MC simulations. The truncation-based analytic solution is consistent with MC estimates.

3.6 Monte Carlo Discretization

We consider the SDE (17) for the volatility process σ_t . We introduce the log-volatility process $L_t = \ln \sigma_t$ and obtain the following dynamics for L_t using Itô's formula

$$\begin{aligned} dL_t &= \mu(L_t) dt + \vartheta dW_t^{(*)}, \quad L_0 = \ln \sigma_0, \\ \mu(L) &= (-\kappa_1 + \kappa_2 \theta) + \left(\kappa_1 \theta - \frac{1}{2} \vartheta^2 \right) e^{-L} - \kappa_2 e^L. \end{aligned} \quad (38)$$

We consider a time horizon $T > 0$ and an equidistant time grid $t_k = k\Delta$, $\Delta = \frac{T}{n}$, $0 \leq k \leq n$. Backward Euler-Maruyama (BEM) scheme for L_t is defined by

$$\hat{L}_{t_{k+1}} = \hat{L}_{t_k} + \mu \left(\hat{L}_{t_{k+1}} \right) (t_{k+1} - t_k) + \vartheta \left(W_{t_{k+1}}^{(*)} - W_{t_k}^{(*)} \right). \quad (39)$$

BEM scheme (also known as drift implicit Euler-Maruyama scheme) is based on Lamperti transform where original SDE (17) is transformed into an SDE (38) with constant diffusion coefficient with

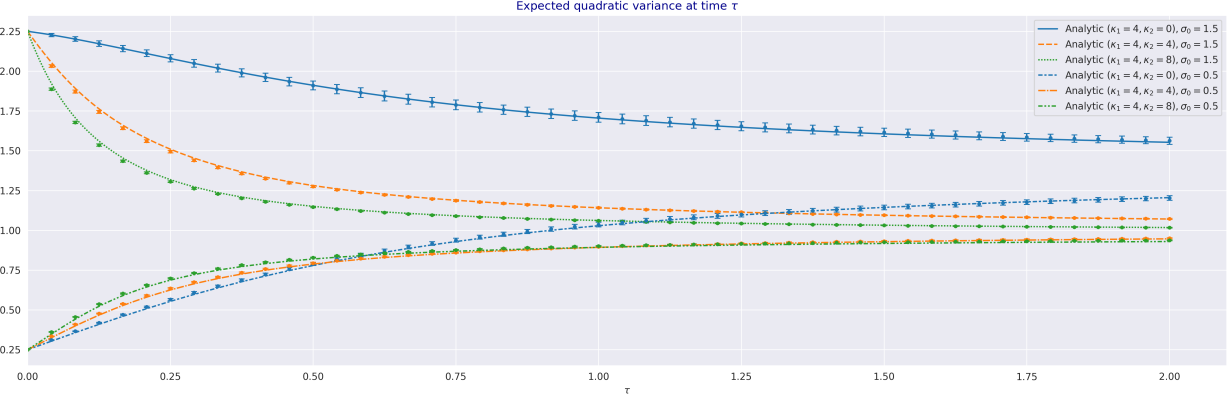


Figure 7: The expected QV computed using Eq (36) with $k^* = 4$. The top and bottom 3 lines correspond to $\sigma_0 = 1.5$ and $\sigma_0 = 0.5$, respectively. The dot and the error bars denote the estimate and 95% confidence interval computed using MC simulations of model dynamics (28) with scheme in SDE (40) with number of path equal 100,000 and daily time steps. The model cases of mean-reversion correspond to those in Figure 5 with other model parameters set to $\theta = 1.0$, $\vartheta = 1.5$.

non-linearity in the diffusion coefficient shifted into the drift of the process. We refer to [Neuenkirch and Szpruch \(2014\)](#) and [Alfonsi \(2013\)](#) for further details; [Chassagneux-Jacquier-Mihaylov \(2016\)](#) study Euler-Maruyama explicit scheme for SDEs with non-Lipschitz coefficients.

We prove that SDE (39) has a unique solution in $L_{t_{k+1}}$ in order to make BEM scheme well-defined. Although BEM scheme in Eq (39) cannot be solved analytically in $\hat{L}_{t_{k+1}}$, we still can solve Eq (39) numerically due to the smoothness and monotonicity of function G , see Proposition A.2, using a few iterations of Newton algorithm.

Theorem 3.3. *Backward Euler-Maruyama scheme for log-volatility process L_t in SDE (38) has a strong convergence rate of 1.*

Proof. See Appendix A.7. □

Corollary 3.2. *Monte Carlo discretization scheme of the model dynamics (9) under the MMA measure using log-price X_t in SDE (12) is given by*

$$\begin{aligned} X_{t_{k+1}} &= X_{t_k} - \frac{1}{2}\sigma_{t_k}^2(t_{k+1} - t_k) + \sigma_{t_k} \left(W_{t_{k+1}}^{(0)} - W_{t_k}^{(0)} \right), \quad X_{t_0} = \ln(S_0), \\ L_{t_{k+1}} &= L_{t_k} + \mu(L_{t_k})(t_{k+1} - t_k) + \beta \left(W_{t_{k+1}}^{(0)} - W_{t_k}^{(0)} \right) + \varepsilon \left(W_{t_{k+1}}^{(1)} - W_{t_k}^{(1)} \right), \quad L_{t_0} = \ln(\sigma_0) \quad (40) \\ I_{t_{k+1}} &= I_{t_k} + \sigma_{t_k}^2(t_{k+1} - t_k), \quad I_{t_0} = I_0, \\ \sigma_{t_{k+1}} &= \exp(L_{t_{k+1}}), \end{aligned}$$

where $W_{t_k}^{(0)}$ and $W_{t_k}^{(1)}$ are independent Brownian motions. The scheme (40) has the convergence rate of 1 in the log-volatility and of 1/2 in the log-price.

We note that the first two dynamics are defined on $(-\infty, +\infty)$, which does not require extra handling of boundary conditions, in contrast to some affine models for the variance process.

4 Martingale Dynamics under MMA and Inverse Measures

We derive conditions that ensure joint arbitrage-free valuation of options with vanilla and inverse payoffs using generic SV dynamics (41) under the MMA and inverse measures. These conditions identify the domain for model parameters that ensure the existence of the MMA and inverse martingale measures as defined in Corollary 2.1.

4.1 Martingale Property

In this section we consider a generic SV model for the price Z_t and volatility σ_t with dynamics specified under the MMA measure \mathbb{Q}

$$\begin{aligned} dZ_t &= Z_t \sigma_t dW_t^{(0)}, \\ d\sigma_t &= \mu(\sigma_t) dt + \beta v(\sigma_t) dW_t^{(0)} + \varepsilon v(\sigma_t) dW_t^{(1)}. \end{aligned} \quad (41)$$

To derive for restrictions of model parameters of specific SV models that we consider in Section 2.4, we need to ensure the following properties:

1. the martingale property for the drift-adjusted price Z_t and its inverse $R_t = (Z_t)^{-1}$, $0 \leq t \leq T$ under the MMA measure \mathbb{Q} and the inverse measure $\tilde{\mathbb{Q}}$;
2. the existence of higher-order moment $\mathbb{E}[(Z_T)^m]$ under the MMA measure \mathbb{Q} and negative moment $\mathbb{E}[(Z_T)^{-m}]$ under the inverse measure $\tilde{\mathbb{Q}}$ for $m > 1$.

To investigate the martingale property of Z_t under \mathbb{Q} , we refer to Theorem A.2 that relates it to the explosion of the volatility process under $\tilde{\mathbb{Q}}$. If price process Z_t is not a proper martingale, the model value of a call option fails to be a proper martingale as well. However, the put-call parity must hold regardless of the martingale property of S_t to preclude arbitrage.

Lemma 4.1. *Put-call parity for vanilla call option, $C(t, S, K)$, and put option, $P(t, S, K)$,*

$$C(t, S, K) - P(t, S, K) = S - Ke^{-\bar{r}(T)} \quad (42)$$

holds irrespective whether price dynamics are martingale under MMA measure \mathbb{Q} .

Put-call parity for inverse call option, $\tilde{C}(t, S, K)$, and inverse put option, $\tilde{P}(t, S, K)$,

$$\tilde{C}(t, S, K) - \tilde{P}(t, S, K) = 1 - S^{-1}Ke^{-\bar{r}(T)} \quad (43)$$

holds irrespective whether price dynamics are martingale under inverse measure $\tilde{\mathbb{Q}}$.

Proof. See Appendix A.9. □

In Section 2.4 we provide the key results for martingale properties of specific SV models:

1. Theorem 2.2 for Log-normal SV model dynamics (9);
2. Proposition 2.1 for Heston dynamics (15);
3. Proposition 2.2 for Exp-OU SV model dynamics (16).

4.2 Log-normal SV Dynamics under MMA and Inverse Measures

We now establish necessary results for the log-normal SV model (9). First we define the model dynamics (9) under the inverse measure $\tilde{\mathbb{Q}}$. As a by-product, we show that in SDE (44) the quadratic term is important to preserve the functional specification of volatility drift under $\tilde{\mathbb{Q}}$.

Lemma 4.2. *The volatility process in SDE (9) is driven under the inverse measure $\tilde{\mathbb{Q}}$ by*

$$d\sigma_t = (\kappa_1 \theta - (\kappa_1 - \kappa_2 \theta) \sigma_t - (\kappa_2 - \beta) \sigma_t^2) dt + \beta \sigma_t d\tilde{W}_t^{(0)} + \varepsilon \sigma_t d\tilde{W}_t^{(1)}. \quad (44)$$

Using the zero-drift stochastic driver Z_t , $Z_t = e^{-\int_0^t r(t') dt'} S_t$, in Eq (11), the MMA measure \mathbb{Q} and the inverse measure $\tilde{\mathbb{Q}}$ are related by the density process by

$$\Lambda_t = \mathbb{E}_t \left[d\tilde{\mathbb{Q}}/d\mathbb{Q} \right] = Z_t/Z_0. \quad (45)$$

Proof. We introduce $R_t = Z_t^{-1}$. Applying Itô's lemma, R_t satisfies

$$dR_t = \sigma_t^2 R_t dt - \sigma_t R_t dW_t^{(0)} = -\sigma_t R_t (dW_t^{(0)} - \sigma_t dt). \quad (46)$$

Using Girsanov's theorem, we switch to the inverse measure $\tilde{\mathbb{Q}}$ by using uncorrelated Brownian motions $\tilde{W}_t^{(0)}$ and $\tilde{W}_t^{(1)}$ defined by $\tilde{W}_t^{(0)} = W_t^{(0)} - \int_0^t \sigma_s ds$, $\tilde{W}_t^{(1)} = W_t^{(1)}$. As a result, the dynamics of volatility process σ_t under $\tilde{\mathbb{Q}}$ become

$$d\sigma_t = (\kappa_1 + \kappa_2 \sigma_t) (\theta - \sigma_t) dt + \beta \sigma_t \left(d\tilde{W}_t^{(0)} + \sigma_t dt \right) + \varepsilon \sigma_t d\tilde{W}_t^{(1)} \quad (47)$$

and Eq (44) follows. It is important to note that measures $\tilde{\mathbb{Q}}$ and \mathbb{Q} are related by the density $\Lambda_t = \mathbb{E}_t [d\tilde{\mathbb{Q}}/d\mathbb{Q}]$ specified by

$$d\Lambda_t / \Lambda_t = \sigma_t dW_t, \quad \Lambda(0) = 1 \quad \Rightarrow \quad \Lambda_t = \exp \left(\int_0^t \sigma_s dW_s - \frac{1}{2} \int_0^t \sigma_s^2 ds \right) = Z_t/Z_0. \quad (48)$$

□

We now derive sufficient conditions for the equivalence of measures $\mathbb{Q} \sim \tilde{\mathbb{Q}}$ which is required for the application of Girsanov theorem in the proof of Theorem 4.1.

Theorem 4.1. *Measures \mathbb{Q} and $\tilde{\mathbb{Q}}$ are equivalent if and only if $\kappa_2 \geq \beta$.*

Proof. By Lemma 4.2, the density $\mathbb{E}_t [d\tilde{\mathbb{Q}}/d\mathbb{Q}] = Z_t/Z_0$. Therefore, the martingale property for Z_t under \mathbb{Q} guarantees equivalence $\mathbb{Q} \sim \tilde{\mathbb{Q}}$. Using Theorem 2.2 1) concludes the proof. □

Remark. *The density process (45) can be derived directly from the relationship (6) between the measures \mathbb{Q} and $\tilde{\mathbb{Q}}$. Here we follow rather different approach and characterize $\tilde{\mathbb{Q}}$ as a measure under which inverse process R_t becomes driftless.*

Thus, the dynamics of the mean-adjusted volatility process $Y_t = \sigma_t - \theta$, defined in Eq (28) under the MMA measure, are driven under the inverse measure by

$$\begin{aligned} dY_t &= \left(\tilde{\lambda} - \tilde{\kappa} Y_t - \tilde{\kappa}_2 Y_t^2 \right) dt + \vartheta (Y_t + \theta) d\tilde{W}_t^{(*)}, \quad Y_0 = \sigma_0 - \theta, \\ \tilde{\lambda} &= \beta \theta^2, \quad \tilde{\kappa} = \kappa_1 - \kappa_2 \theta + 2(\kappa_2 - \beta)\theta, \quad \tilde{\kappa}_2 = \kappa_2 - \beta, \end{aligned} \quad (49)$$

where $\tilde{W}_t^{(*)}$ is a standard Brownian motion under the inverse measure.

We finally summarize the joint dynamics of transformed state variable using log-normal SV model dynamics (9) under measures \mathbb{Q} and $\tilde{\mathbb{Q}}$ as follows.

Corollary 4.1 (Dynamics under the MMA measure \mathbb{Q}). *The joint dynamics of log-price X_t , the mean-adjusted volatility process Y_t , and the QV I_t under the MMA measure \mathbb{Q} are driven by*

$$\begin{aligned} dX_t &= -\frac{1}{2} (Y_t + \theta)^2 dt + (Y_t + \theta) dW_t^{(0)}, \quad X_0 = X, \\ dY_t &= (-\kappa Y_t - \kappa_2 Y_t^2) dt + \beta (Y_t + \theta) dW_t^{(0)} + \varepsilon (Y_t + \theta) dW_t^{(1)}, \quad Y_0 = \sigma_0 - \theta, \\ dI_t &= (Y_t + \theta)^2 dt, \quad I_0 = I. \end{aligned} \quad (50)$$

Corollary 4.2 (Dynamics under the inverse measure $\tilde{\mathbb{Q}}$). *The joint dynamics of log-price X_t , the mean-adjusted volatility process Y_t , and the QV I_t under the inverse measure $\tilde{\mathbb{Q}}$ are driven by*

$$\begin{aligned} dX_t &= \frac{1}{2} (Y_t + \theta)^2 dt + (Y_t + \theta) d\tilde{W}_t^{(0)}, \quad X_0 = X, \\ dY_t &= \left(\tilde{\lambda} - \tilde{\kappa} Y_t - \tilde{\kappa}_2 Y_t^2 \right) dt + \beta (Y_t + \theta) d\tilde{W}_t^{(0)} + \varepsilon (Y_t + \theta) d\tilde{W}_t^{(1)}, \quad Y_0 = \sigma_0 - \theta, \\ dI_t &= (Y_t + \theta)^2 dt, \quad I_0 = I. \end{aligned} \quad (51)$$

5 Affine Expansion of Moment Generating Function

We consider the valuation problem of a derivative security with the payoff function $u(X, I)$ settled at maturity time T using the log-price process X_t defined in Eq (12). We denote the current time by t , and introduce the time to maturity variable $\tau = T - t$. We denote the undiscounted value function of this derivative security by $U(\tau, X, I, Y)$.

To solve the general valuation problem under both the MMA measure \mathbb{Q} and the inverse measure $\tilde{\mathbb{Q}}$, we parametrise the value function using binary parameter p , $p \in \{1, -1\}$, respectively, as follows

$$U(\tau, X, I, Y; p) = \begin{cases} \mathbb{E}[u(X_T, I_T) | \mathcal{F}_t] = \mathbb{E}[u(X_T, I_T) | X_t = X, I_t = I, Y_t = Y], & p = 1 \\ \tilde{\mathbb{E}}[u(X_T, I_T) | \mathcal{F}_t] = \tilde{\mathbb{E}}[u(X_T, I_T) | X_t = X, I_t = I, Y_t = Y], & p = -1. \end{cases} \quad (52)$$

where the expectation \mathbb{E} under the MMA measure \mathbb{Q} is computed using dynamics (50) and the expectation $\tilde{\mathbb{E}}$ under the inverse measure $\tilde{\mathbb{Q}}$ is computed using dynamics (51). We use the fact that the dynamics are Markovian under the both measures.

Theorem 5.1. *The value function $U(\tau, X, I, Y; p)$ solves the following PDE on the domain $[0, T] \times \mathbb{R} \times \mathbb{R}_+ \times (-\theta, \infty)$*

$$\begin{aligned} -U_\tau + (\mathcal{L}^{(Y; p)} + \mathcal{L}^{(X; p)} + \mathcal{L}^{(I; p)}) U &= 0, \\ U(0, X, I, Y) &= u(X, I), \end{aligned} \quad (53)$$

where diffusive operators $\mathcal{L}^{(Y; p)}$, $\mathcal{L}^{(X; p)}$ and $\mathcal{L}^{(I; p)}$ are defined as follows

$$\begin{aligned} \mathcal{L}^{(Y; p)} U &= \frac{1}{2} \vartheta^2 (Y + \theta)^2 U_{YY} + (\lambda^{(p)} - \kappa^{(p)} Y - \kappa_2^{(p)} Y^2) U_Y, \\ \mathcal{L}^{(X; p)} U &= (Y + \theta)^2 \left[\frac{1}{2} (U_{XX} - p U_X) + \beta U_{XY} \right], \\ \mathcal{L}^{(I; p)} U &= (Y + \theta)^2 U_I, \\ \kappa^{(p)} &= \kappa_1 - \kappa_2 \theta + 2\kappa_2^{(p)} \theta, \quad \lambda^{(p)} = (\kappa_2 - \kappa_2^{(p)}) \theta^2, \quad \kappa_2^{(p)} = \begin{cases} \kappa_2, & p = 1, \\ \kappa_2 - \beta, & p = -1. \end{cases} \end{aligned} \quad (54)$$

Proof. See Appendix A.10. We note that the classic Feynman-Kac formula (see for an example Section A.17 in Musiela and Rutkowski (2009)) cannot be applied directly to Eq (52) because the model dynamics (50) and (51) do not satisfy the linear growth conditions. \square

5.1 Moment Generating Function

We introduce the moment generating function (MGF) of the three model variables: the log-price X_t , the QV I_t , and the volatility driver $Y_t = \sigma_t - \theta$. We extend our analysis with the transform variable in the volatility process Y_t to show that our solution method works for all the three state variables in the model. We denote the MGF by $G(\tau, X, I, Y; \Phi, \Psi, \Theta; p)$ using respective complex-valued transform variables $\Phi, \Psi, \Theta \in \mathbb{C}$

$$G(\tau, X, I, Y; \Phi, \Psi, \Theta; p) = \begin{cases} \mathbb{E}[e^{-\Phi X_\tau - \Psi I_\tau - \Theta Y_\tau} | X_0 = X, I_0 = I, Y_0 = Y], & p = 1 \\ \tilde{\mathbb{E}}[e^{-\Phi X_\tau - \Psi I_\tau - \Theta Y_\tau} | X_0 = X, I_0 = I, Y_0 = Y], & p = -1. \end{cases} \quad (55)$$

Using model dynamics (50) under the MMA measure and model dynamics (51) under the inverse measure, respectively, the MGF solves the following PDE on the domain $[0, T] \times \mathbb{R} \times \mathbb{R}_+ \times (-\theta, \infty)$

$$\begin{aligned} -G_\tau + (\mathcal{L}^{(Y; p)} + \mathcal{L}^{(X; p)} + \mathcal{L}^{(I; p)}) G &= 0, \\ G(0, X, I, Y; \Phi, \Psi, \Theta; p) &= e^{-\Phi X - \Psi I - \Theta Y}, \end{aligned} \quad (56)$$

with operators defined in (54). For further development, we establish a sufficient condition for the existence of the MGF for the three state variables.

Theorem 5.2. Given the transform variable $\Phi = \Phi_R + i\Phi_I \in \mathbb{C}$, the MGF of the log-price X_τ

$$G(\tau, X; \Phi; p = 1) = \mathbb{E}[e^{-\Phi X_\tau} | X_0 = X]$$

exists for $\Phi_R \in (-1, 0)$, if Z_τ is a martingale under the MMA measure. By Theorem 2.2 1), the necessary condition is $\kappa_2 \geq \beta$.

Similarly, the MGF of the log-price X_τ

$$G(\tau, X; \Phi; p = -1) = \tilde{\mathbb{E}}[e^{-\Phi X_\tau} | X_0 = X]$$

exists for $\Phi_R \in (0, 1)$ if R_τ is a martingale under inverse measure. By Theorem 2.2 2), the necessary condition is $\kappa_2 \geq 2\beta$.

Proof. See Appendix A.11. \square

Theorem 5.3. Given the transform variable $\Psi = \Psi_R + i\Psi_I \in \mathbb{C}$, the MGF of the QV I_τ

$$G(\tau, I; \Psi; p = 1) = \mathbb{E}[e^{-\Psi I_\tau}]$$

exists for $\Psi_R < 0$ if $\kappa_2 > \vartheta\sqrt{-2\Psi_R}$.

Proof. See Appendix A.12. \square

Theorem 5.4. Given the transform variable $\Theta = \Theta_R + i\Theta_I \in \mathbb{C}$, the MGF of the mean-adjusted volatility variable Y_τ

$$G(\tau, Y; \Theta; p) = \begin{cases} \mathbb{E}[e^{-\Theta Y_\tau} | Y_0 = Y], & p = 1, \\ \tilde{\mathbb{E}}[e^{-\Theta Y_\tau} | Y_0 = Y], & p = -1 \end{cases}$$

exists for $\Theta_R < 0$, if

$$\kappa_2 > \frac{\vartheta^2}{2}|\Theta_R|, \quad p = 1; \quad \kappa_2 - \beta > \frac{\vartheta^2}{2}|\Theta_R|, \quad p = -1. \quad (57)$$

Proof. See Appendix A.13. \square

5.2 Affine Expansion

5.2.1 General consideration

Given that coefficients in PDE (56) are non-affine in state variable Y , the PDE cannot be solved by assuming an exponential affine-solution with a finite number of coefficients. Instead, we can show that the solution to the PDE (56) can be represented by an exponential-affine ansatz $E^{[\infty]}$ using an infinite dimensional vector $\mathbf{A}(\tau) = \{A^{(k)}(\tau; \Phi, \Psi, \Theta; p)\}$, $k = 0, 1, \dots, \infty$, as

$$E^{[\infty]}(\tau, X, I, Y; \Phi, \Psi, \Theta; p) = \exp \left\{ -\Phi X - \Psi I + \sum_{k=0}^{\infty} A^{(k)}(\tau; \Phi, \Psi, \Theta; p) Y^k \right\}, \quad (58)$$

where vector function $\mathbf{A}(\tau)$ solve an infinite-dimensional system of quadratic ODEs:

$$A_\tau^{(k)} = \mathbf{A}^\top M^{(k)} \mathbf{A} + (L^{(k)})^\top \mathbf{A} + H^{(k)}, \quad k = 0, 1, \dots, \infty, \quad (59)$$

where $M^{(k)}$, $L^{(k)}$ and $H^{(k)}$ are infinite dimensional (very) sparse matrices and vector, respectively.

We note the similarity between the current ansatz (58) for problem (56) and the problem of computing the moments of the volatility process addressed in Proposition 3.3. In Proposition 3.3, we first represent the recursive solution to the moments as an infinite dimensional vector in Eq (32). We then obtain an approximate solution by a truncation of infinite series and specifying a boundary condition to reduce the problem to a finite-dimensional vector (33), which can be solved using analytical methods. Here we follow this insight for solving PDE (56) and term our (truncated) solution as the affine expansion with a given order.

5.2.2 First-order Expansion

Theorem 5.5. [First-order affine expansion] The MGF in Eq (55) can be decomposed as follows

$$G(\tau, X, I, Y; \Phi, \Psi, \Theta; p) = E^{[1]}(\tau, X, I, Y; \Phi, \Psi, \Theta; p) + R^{[1]}(\tau, X, I, Y; \Phi, \Psi, \Theta; p), \quad (60)$$

where $E^{[1]}$ is the leading first-order term and $R^{[1]}$ is the remainder term. The leading term $E^{[1]}$ is given by the exponential-affine form

$$E^{[1]}(\tau, X, I, Y; \Phi, \Psi, \Theta; p) = \exp \left\{ -\Phi X - \Psi I + \sum_{k=0}^2 A^{(k)}(\tau; \Phi, \Psi, \Theta; p) Y^k \right\}, \quad (61)$$

where vector function $\mathbf{A}(\tau) = \{A^{(k)}(\tau; \Phi, \Psi, \Theta; p)\}$, $k = 0, 1, 2$, solve the quadratic differential system of ODEs as a function of τ :

$$\begin{aligned} A_\tau^{(k)} &= \mathbf{A}^\top M^{(k)} \mathbf{A} + \left(L^{(k)}(p) \right)^\top \mathbf{A} + H^{(k)}(p), \\ M^{(k)} &= \left\{ \begin{pmatrix} 0 & 0 & 0 \\ 0 & \frac{\theta^2 \vartheta^2}{2} & 0 \\ 0 & 0 & 0 \end{pmatrix}, \begin{pmatrix} 0 & 0 & 0 \\ 0 & \theta \vartheta^2 & \theta^2 \vartheta^2 \\ 0 & \theta^2 \vartheta^2 & 0 \end{pmatrix}, \begin{pmatrix} 0 & 0 & 0 \\ 0 & \frac{\vartheta^2}{2} & 2\theta \vartheta^2 \\ 0 & 2\theta \vartheta^2 & 2\theta^2 \vartheta^2 \end{pmatrix} \right\}, \\ L^{(k)}(p) &= \left\{ \begin{pmatrix} 0 \\ \lambda^{(p)} - \theta^2 \beta \Phi \\ \theta^2 \vartheta^2 \end{pmatrix}, \begin{pmatrix} 0 \\ -\kappa^{(p)} - 2\theta \beta \Phi \\ 2(\lambda^{(p)} + \theta \vartheta^2 - \theta^2 \beta \Phi) \end{pmatrix}, \begin{pmatrix} 0 \\ -\beta \Phi - \kappa_2^{(p)} \\ \vartheta - 2\kappa^{(p)} - 4\theta \beta \Phi \end{pmatrix} \right\}, \\ H^{(k)}(p) &= \left\{ \frac{1}{2} \theta^2 (\Phi^2 + p\Phi - 2\Psi), \theta (\Phi^2 + p\Phi - 2\Psi), \frac{1}{2} (\Phi^2 + p\Phi - 2\Psi) \right\} \end{aligned} \quad (62)$$

with the initial condition $\mathbf{A}(0) = (0, -\Theta, 0)^\top$.

The remainder term $R^{[1]}$ solves the following PDE (omitting arguments):

$$\begin{aligned} -R_\tau^{[1]} + \left(\mathcal{L}^{(Y; p)} + \mathcal{L}^{(X; p)} + \mathcal{L}^{(I; p)} \right) R^{[1]} &= -F^{[1]}(Y, A^{(1)}, A^{(2)}) E^{[1]}(\tau, X, I, Y; \Phi, \Psi, \Theta; p) \\ R^{[1]}(0, X, I, Y; \Phi, \Psi; p) &= 0, \end{aligned} \quad (63)$$

with operators $\mathcal{L}^{(Y)}$, $\mathcal{L}^{(X)}$, $\mathcal{L}^{(I)}$ defined in Eq (54) and residual function $F^{[1]}$

$$\begin{aligned} F^{[1]}(Y, A^{(1)}, A^{(2)}) &= \sum_{n=3}^4 C^{(n)}(\tau; A^{(1)}, A^{(2)}) Y^n, \\ C^{(3)}(\tau) &= 2A^{(2)} \left(\vartheta^2 \left(2\theta A^{(2)} + A^{(1)} \right) - \beta \Phi - \kappa_2 \right), \\ C^{(4)}(\tau) &= 2\vartheta^2 (A^{(2)})^2. \end{aligned} \quad (64)$$

Proof. We assume a solution using the leading term $E^{[1]}(\tau, X, I, Y; \Phi, \Psi, \Theta; p)$ in decomposition (61) and substitute it into the PDE (56). To obtain the ODEs (62) for $A^{(k)}$, we match terms with Y^k , $k = 0, 1, 2$. To obtain the PDE for the remainder term $R^{[1]}(\tau, X, I, Y; \Phi, \Psi, \Theta; p)$, we substitute the decomposition (61) into the PDE (56) and account for higher powers of Y^k , $k = 0, 1, 2$. Finally, initial conditions for ODEs (62) and PDE (63) are set to reproduce conditions of Eq (56). \square

Proposition 5.1. We take $\Psi = \Theta = 0$ and $\Re \Phi = -p/2$, $p \in \{-1, 1\}$. Assuming that hypotheses 5.7, 5.7, 5.7 listed in Theorem 5.7 hold, the continuous solution $\mathbf{A}(\tau)$ in Eq (62) exists on $[0, +\infty)$.

Proof. See Theorem 5.7. \square

In Figure 8, we show the real and imaginary parts of ODE solutions $\mathbf{A}(\tau)$ and the first-order leading term $E^{[1]}$. We see that functions $A^{(1)}$ and $A^{(2)}$ quickly reach an equilibrium point, while $A^{(0)}$ is the non-stationary part which contributes to the leading term $E^{[1]}$.

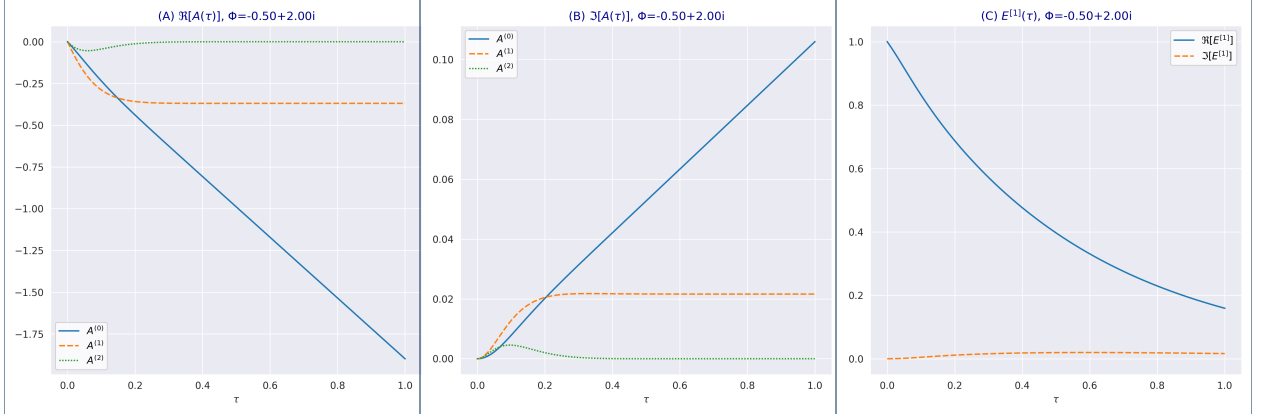


Figure 8: The solution of ODEs of the first order expansion in Eq (62) as function of τ for $\Phi = -0.5 + 2i$. We use the model parameters calibrated to Bitcoin options data and reported in Table 1. Subplot (A) shows the real part of the solution, (B) shows the imaginary part of the solution, (C) shows the the real and imaginary parts of the exponential term $E^{[1]}$ in Eq (61).

Corollary 5.1. [Estimate of the first-order remainder term]. *We obtain the following estimate for the remainder term $R^{[1]}$ in Eq (63)*

$$\left| R^{[1]}(\tau, X, I, Y; \Phi, \Psi, \Theta; p) \right| \leq \sum_{n=3}^4 C^{(4)}(\tau^*) \times M_\sigma^{(n)}(\tau^*), \quad (65)$$

where $M_\sigma^{(n)}(\tau)$ is the n -th central moment of the volatility defined by:

$$M_\sigma^{(n)}(\tau) = \mathbb{E}[(\sigma(\tau) - \theta)^n]. \quad (66)$$

Proof. See Appendix A.14. \square

Corollary 5.2. [First-order affine approximation for the MGF (55)] is obtained using the leading term $E^{[1]}$ in Eq (60)

$$G(\tau, X, I, Y; \Phi, \Psi, \Theta; p) = E^{[1]}(\tau, X, I, Y; \Phi, \Psi, \Theta; p), \quad (67)$$

where the approximation error arises from the truncation of the infinite dimensional anzats in (58) with the error magnitude estimated using (65).

In Figure 10, we illustrate that the first-order approximation (67) for the MGF produces valid and accurate PDFs for all three state variables.

5.2.3 Second-order Expansion

Theorem 5.6. [Second-order affine expansion] *The MGF in Eq (55) can be decomposed as follows*

$$G(\tau, X, I, Y; \Phi, \Psi, \Theta; p) = E^{[2]}(\tau, X, I, Y; \Phi, \Psi, \Theta; p) + R^{[2]}(\tau, X, I, Y; \Phi, \Psi, \Theta; p), \quad (68)$$

where $E^{[2]}$ is the leading term and $R^{[2]}$ is the remainder term.

The leading term $E^{[2]}(\tau, X, I, Y; \Phi, \Psi, \Theta; p)$ is given by the exponential-affine form

$$E^{[2]}(\tau, X, I, Y; \Phi, \Psi, \Theta; p) = \exp \left\{ -\Phi X - \Psi I + \sum_{k=0}^4 A^{(k)}(\tau; \Phi, \Psi, \Theta; p) Y^k \right\}, \quad (69)$$

where vector function $\mathbf{A}(\tau) = \{A^{(k)}(\tau; \Phi, \Psi, \Theta; p)\}$, $k = 0, \dots, 4$, solve the system the quadratic differential system of ODEs as a function of τ :

$$A_\tau^{(k)} = \mathbf{A}^\top M^{(k)} \mathbf{A} + \left(L^{(k)}(p) \right)^\top \mathbf{A} + H^{(k)}(p), \quad (70)$$

$$M^{(k)} = \left\{ \begin{pmatrix} 0 & 0 & 0 & 0 \\ 0 & \frac{\theta^2 \vartheta^2}{2} & 0 & 0 \\ 0 & 0 & 0 & 0 \\ 0 & 0 & 0 & 0 \\ 0 & 0 & 0 & 0 \end{pmatrix}, \begin{pmatrix} 0 & 0 & 0 & 0 \\ 0 & \theta \vartheta^2 & \theta^2 \vartheta^2 & 0 \\ 0 & \theta^2 \vartheta^2 & 0 & 0 \\ 0 & 0 & 0 & 0 \\ 0 & 0 & 0 & 0 \end{pmatrix}, \begin{pmatrix} 0 & 0 & 0 & 0 \\ 0 & \frac{\vartheta^2}{2} & 2\theta \vartheta^2 & \frac{3}{2}\theta^2 \vartheta^2 \\ 0 & 2\theta \vartheta^2 & 2\theta^2 \vartheta^2 & 0 \\ 0 & \frac{3}{2}\theta^2 \vartheta^2 & 0 & 0 \\ 0 & 0 & 0 & 0 \end{pmatrix}, \right. \\ \left. \begin{pmatrix} 0 & 0 & 0 & 0 \\ 0 & 0 & \vartheta^2 & 3\theta \vartheta^2 \\ 0 & \vartheta^2 & 4\theta \vartheta^2 & 3\theta^2 \vartheta^2 \\ 0 & 3\theta \vartheta^2 & 3\theta^2 \vartheta^2 & 0 \\ 0 & 2\theta^2 \vartheta^2 & 0 & 0 \end{pmatrix}, \begin{pmatrix} 0 & 0 & 0 & 0 \\ 0 & 0 & 0 & \frac{3}{2}\vartheta^2 \\ 0 & 0 & 2\vartheta^2 & 6\theta \vartheta^2 \\ 0 & \frac{3}{2}\vartheta^2 & 6\theta \vartheta^2 & \frac{9}{2}\theta^2 \vartheta^2 \\ 0 & 4\theta \vartheta^2 & 4\theta^2 \vartheta^2 & 0 \end{pmatrix} \right\}, \\ L^{(k)}(p) = \left\{ \begin{pmatrix} 0 \\ \lambda^{(p)} - \theta^2 \beta \Phi \\ \theta^2 \vartheta^2 \\ 0 \\ 0 \end{pmatrix}, \begin{pmatrix} 0 \\ -\kappa^{(p)} - 2\theta \beta \Phi \\ 2(\lambda^{(p)} + \theta \vartheta^2 - \theta^2 \beta \Phi) \\ 3\theta^2 \vartheta^2 \\ 0 \end{pmatrix}, \begin{pmatrix} 0 \\ -\beta \Phi - \kappa_2^{(p)} \\ \vartheta^2 - 2\kappa^{(p)} - 4\theta \beta \Phi \\ 3(2q \vartheta^2 + \lambda^{(p)} - \theta^2 \beta \Phi) \\ 6\theta^2 \vartheta^2 \end{pmatrix}, \right. \\ \left. \begin{pmatrix} 0 \\ 0 \\ -2(\beta \Phi + \kappa_2^{(p)}) \\ 3(\vartheta^2 - \kappa^{(p)} - 2\theta \beta \Phi) \\ 4(3\theta \vartheta^2 + \lambda^{(p)} - \theta^2 \beta \Phi) \end{pmatrix}, \begin{pmatrix} 0 \\ 0 \\ 0 \\ -3(\beta \Phi + \kappa_2^{(p)}) \\ 2(3\vartheta^2 - 2\kappa^{(p)} - 4\theta \beta \Phi) \end{pmatrix} \right\}, \\ H^{(k)}(p) = \left\{ \frac{1}{2} \theta^2 (\Phi^2 + p\Phi - 2\Psi), \theta (\Phi^2 + p\Phi - 2\Psi), \frac{1}{2} (\Phi^2 + p\Phi - 2\Psi), 0, 0 \right\}, \end{math>$$

with initial condition $\mathbf{A}(0) = (0, -\Theta, 0, 0, 0)^\top$.

The remainder term $R^{[2]}$ solves the following PDE (omitting arguments)

$$\begin{aligned} -R_\tau^{[2]} + (\mathcal{L}^{(Y; p)} + \mathcal{L}^{(X; p)} + \mathcal{L}^{(I; p)}) R^{[2]} &= -F^{[2]}(Y, A^{(1)}, A^{(2)}, A^{(3)}, A^{(4)}) E^{[2]} \\ R^{[2]}(0, X, I, Y; \Phi, \Psi, \Theta; p) &= 0, \end{aligned} \tag{71}$$

with operators $\mathcal{L}^{(Y)}$, $\mathcal{L}^{(X)}$, $\mathcal{L}^{(I)}$ defined in Eq (54) and residual function $F^{[2]}$ is given by:

$$F^{[2]}(\tau, Y; A^{(1)}, A^{(2)}, A^{(3)}, A^{(4)}) = \sum_{k=5}^8 C^{(k)}(\tau; A^{(1)}, A^{(2)}, A^{(3)}, A^{(4)}) Y^k \tag{72}$$

$$\begin{aligned} C^{(5)}(\tau) &= 3\vartheta^2 A^{(3)} \left(3\theta A^{(3)} + 2A^{(2)} \right) + 4A^{(4)} \left(\vartheta^2 \left(3\theta^2 A^{(3)} + 4\theta A^{(2)} + A^{(1)} \right) - \kappa_2 \right), \\ C^{(6)}(\tau) &= \frac{1}{2} \vartheta^2 \left(16\theta^2 (A^{(4)})^2 + 16A^{(4)} \left(3\theta A^{(3)} + A^{(2)} \right) + 9(A^{(3)})^2 \right), \\ C^{(7)}(\tau) &= 4\vartheta^2 A^{(4)} \left(4\theta A^{(4)} + 3A^{(3)} \right), \quad C^{(8)}(\tau) = 8\vartheta^2 \left(A^{(4)} \right)^2. \end{aligned}$$

Proof. The proof follows by analogy to the first-order expansion in Theorem 5.5. \square

Remark. We emphasize that sparse matrices quadratic term matrices $M^{(k)}$ do not depend on the measure parameter p , while the linear $L^{(k)}(p)$ and homogenous term $H^{(k)}(p)$ for both the first and the second order ODEs (62) and (70).

Proposition 5.2. We take $\Psi = \Theta = 0$ and $\Re \Phi = -p/2$, $p \in \{-1, 1\}$. Assuming that hypotheses 5.7, 5.7, 5.7 listed in Theorem 5.7 hold, the continuous solution $\mathbf{A}(\tau)$ in Eq (70) exists on $[0, +\infty)$.

Proof. See Theorem 5.7. \square

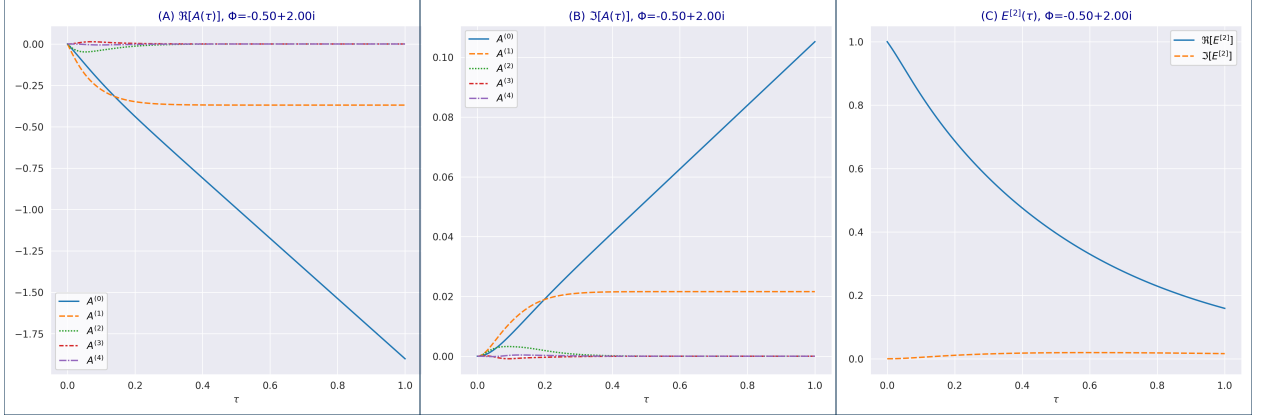


Figure 9: The solution of ODEs in Eq (70) as function of τ for $\Phi = -0.5 + 2i$. We use the model parameters calibrated to Bitcoin options data and reported in Table 1. Subplot (A) shows the real part of the solution, (B) shows the imaginary part of the solution, (C) shows the the real and imaginary parts of the exponential term $E^{[2]}$ in Eq(69).

In Figure 9, we show the real and imaginary parts of $\mathbf{A}(\tau)$ for the second-order expansion and the leading term $E^{[2]}$. We see that, similarly to the first order expansion illustrated in Figure 8, functions $A^{(1)}, A^{(2)}, A^{(3)}, A^{(4)}$ quickly reach an equilibrium point, while $A^{(0)}$ is the non-stationary part which contributes to the leading term $E^{[2]}$. By comparing the small order terms $A^{(0)}, A^{(1)}, A^{(2)}$ between the first and the second expansions, we notice no visible difference, which suggest that the expansion is rather recursive and higher order terms make insignificant contribution to the low order terms. We also notice that terms $A^{(3)}$ and $A^{(4)}$ are very small in magnitude compared to the first three terms, which suggest that higher order term only provide a small marginal contribution.

Corollary 5.3. [Estimate of the second-order remainder term]. *We obtain the following estimate for the remainder term $R^{[2]}$ which solves Eq (71)*

$$\left| R^{[2]}(\tau, X, I, Y; \Phi, \Psi, \Theta; p) \right| \leq \sum_{n=5}^8 C_n(\tau^*) \times M_\sigma^{(n)}(\tau^*), \quad (73)$$

where $M_\sigma^{(n)}$ is the n -th central moment of the volatility defined by (66).

Proof. See Appendix A.14. □

Corollary 5.4. [Second-order affine approximation for the MGF (55)] is obtained using the leading term $E^{[2]}$ in Eq (69)

$$G(\tau, X, I, Y; \Phi, \Psi, \Theta; p) = E^{[2]}(\tau, X, I, Y; \Phi, \Psi, \Theta; p), \quad (74)$$

where the approximation error arises from the truncation of the infinite dimensional affine anzats in (58) with the error magnitude estimated using (73).

In Figure 10, we illustrate that the second-order approximation (74) for the MGF produces valid and accurate PDFs for all three state variables.

5.2.4 Solution of Quadratic System of ODEs

It is established that the global existence problem for the solution of quadratic differential systems is non-trivial, see Coppel (1966), Dickson and Perko (1970), Jacobson (1977), Baris, Baris and Ruchlewicz (2008) among others. Although it can help with the global existence of solutions of the quadratic differential systems, when matrices of the quadratic terms are negative definite, the matrices of quadratic terms in Eq (62) and (70) are indefinite as its eigenvalues are of both signs. Hence, we can provide a result for global existence that is only conditional by nature.

We focus on important case of option valuation on underlying assets with $\Re\Phi = -p/2$, $p \in \{-1, 1\}$, and $\Psi = \Theta = 0$. [Dickson and Perko \(1970\)](#) show that complex-valued solution of quadratic ODEs such as $\mathbf{A}(\tau; \Phi)$ of Eq (62) or (70) has maximal interval of existence $[0, \tau_+(\Phi; \mathbf{A}))$, where $\tau_+(\Phi; \mathbf{A})$ denotes its *blow-up time*. We make following hypotheses.

Theorem 5.7. *Assume following conditions are satisfied:*

1. $\tau_+(\Phi; \Re\mathbf{A}) \geq \tau_+(\Re\Phi; \mathbf{A})$, $\Phi \in \mathbb{C}$, i.e. real part of $\mathbf{A}(\tau; \Phi)$ cannot blow up before $\mathbf{A}(\tau; \Re\Phi)$.
 2. $\sum_{k=0}^{2m} A_k(\tau; \Phi; p) Y^k \rightarrow +\infty$ as $\tau \uparrow \tau_+(\Phi)$, $\Phi \in \mathbb{R}$, i.e. leading term of the affine expansion does not vanish as we approach blow-up time when transform variable Φ is real.
 3. $\lim_{\tau \uparrow \tau_+(\Phi)} R^{[n]}(\tau; \Phi) > -\infty$, $\Phi \in \mathbb{R}$, i.e. remainder term is uniformly bounded from below.
- If MGF in Eq (56) is finite $G(\tau_0; X, I, Y; \Re\Phi, \Psi = 0, \Theta = 0) < \infty$ then continuous solution $A(\tau; \Phi, \Psi = 0, \Theta = 0)$ of Eq (62) and of Eq (70) exists on $[0, \tau_0)$.

Proof. See [A.16](#). □

By Theorem 5.7, we obtain that continuous solution $\mathbf{A}(\tau)$ for the first- and second-order affine expansions in (61) and (69), respectively, exists on $[0, +\infty)$ if three hypotheses 5.7, 5.7, 5.7 hold.

5.3 Properties of Affine Expansions

We now consider the key properties of the affine expansion of the MGF. For brevity, we focus on the properties of the second-order expansion, which is our key development. For the first order expansion, martingale conditions stated in Proposition 5.3 hold, and the consistency with the expected values (but not with variances) of three state variables is also ascertained.

Proposition 5.3. [Martingale conditions] Assuming that hypotheses 5.7, 5.7, 5.7 in Theorem 5.7 hold, the second-order leading affine term in (68) satisfies the martingale conditions for log-return X_τ

$$E^{[2]}(\tau, X, I, Y; \Phi = 0, \Psi = 0, \Theta = 0; p) = 1, \quad (75)$$

$$\mathbb{E}[e^{X_\tau}] \equiv E^{[2]}(\tau, X = X_0, I = 0, Y; \Phi = -1, \Psi = 0, \Theta = 0; p = 1) = e^{X_0}, \quad (76)$$

$$\tilde{\mathbb{E}}[e^{-X_\tau}] \equiv E^{[2]}(\tau, X = X_0, I = 0, Y; \Phi = 1, \Psi = 0, \Theta = 0; p = -1) = e^{-X_0},$$

Proof. For $\Phi = \Psi = \Theta = 0$, we obtain $H^{(p)} \equiv 0$ in (70). Given zero initial conditions, $A^{(k)}(\tau; \Phi = 0, \Psi = 0, \Theta = 0; p) \equiv 0$ due to the uniqueness of the solution. Similarly, for $\Phi = -1$ and $\Theta = \Psi = 0$, we obtain that $H^{(1)} \equiv 0$, hence $A^{(k)}(\tau; \Phi = -1, \Psi = 0, \Theta = 0; p = 1) \equiv 0$. Likewise, for $\Phi = 1$ and $\Psi = 0$ we obtain that $H^{(-1)} \equiv 0$, hence $A^{(k)}(\tau; \Phi = 1, \Psi = 0, \Theta = 0; p = -1) \equiv 0$. □

Proposition 5.4. [Volatility moments] The second-order leading affine term in (69) is consistent with the expected value and the variance of the volatility process for $\kappa_2 = 0$.

Proposition 5.5. [Log-price moments] The second-order leading affine term in (69) is consistent with the expected value and the variance of the log-price process for $\kappa_2 = 0$.

Proposition 5.6. [QV moments] The second-order leading affine term in (69) is consistent with the expected value and the variance of the QV process for $\kappa_2 = 0$.

Proof. See [A.15.1](#) and [A.15.2](#) for 5.4 and 5.5. Proof of (5.6) is obtained by analogy to [A.15.2](#). □

Remark. In 3.5 we note that for $\kappa_2 = 0$ the system of volatility moments (33) is solved exactly, otherwise the solution is approximate. Thus, we cannot generalize above statements for $\kappa_2 > 0$. However, it is our hypothesis that moments obtained using (69) correspond to moments computed with (33) using truncation order $k^* = 4$ and that truncation error as function of κ_2 is very small.

In Figure 10, we show PDFs computed using the inversion of first-order solution $E^{[1]}$ in Eq (61) and second-order solution $E^{[2]}$ in Eq (69) for three state variables in model dynamics (50). The blue histogram is computed using MC simulations of joint model dynamics. We see that both first- and second-order expansions produce valid PDFs and match consistently histograms produced by the MC simulations. The first-order expansion may not be very accurate for the volatility process because it is not consistent with the variance. The second-order expansion is consistent with variances of state variables and accurately matches PDFs computed using MC simulations.

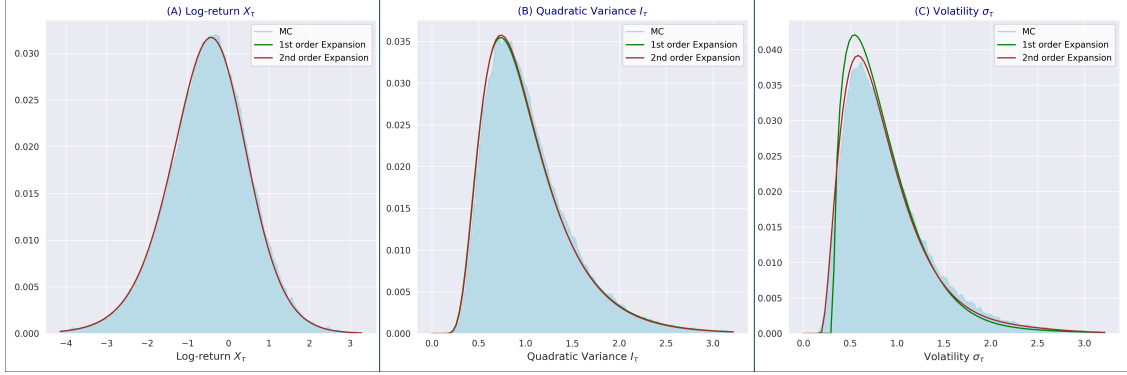


Figure 10: PDFs computed using the inversion of the first order expansion term $E^{[1]}$ in Eq (61) and the second-order expansion term $E^{[2]}$ in Eq (69) for the state variables under the MMA measure: Subplots (A), (B), (C) show PDFs of log-return X_τ , of QV I_τ , of volatility $\sigma_\tau = Y_\tau + \theta$, respectively. We use the model parameters for Bitcoin options reported in Table (1) with $\tau = 1.0$. The blue histogram is computed using realizations from MC simulations of joint model dynamics (9) using scheme in Eq (40) with the number of path equal 400,000 and daily time steps.

6 Option Valuation

We apply the zero-drift log-price process X_t in (12) and expressions (13) and (14) for spot and futures prices, respectively, for option valuations on both spot and futures underlyings. We denote by P_T the price process of either spot or futures asset as follows

$$P_T = e^{\bar{\mu}(T)} e^{X_T}, \quad X_0 = S_0, \quad (77)$$

where $\bar{\mu}(T) = \bar{r}(0, T)$ for spot price and $\bar{\mu}(T) = \bar{r}(0, T) - \bar{q}(0, T)$ for futures price.

As concluded in (5.2) and (5.4), we apply the affine expansion given by either the first order in Eq (61) or the second order in Eq (69) as analytic solutions to the MGF under the dynamics (12). Given that the MFG is available analytically, we then apply Lewis – Lipton approach for valuation of vanilla options using Fourier transform, see Lewis (2000), Lipton (2001), Lipton (2002).

6.1 Vanilla Calls and Puts

Using Eq (77), we represent the put and call payoff functions using capped payoffs as

$$\begin{aligned} c(P_T, K) &= \max \{P_T - K, 0\} = P_T - \min \{P_T, K\} = P_T - \min \left\{e^{\bar{\mu}(T)+X_T}, K\right\}, \\ p(P_T, K) &= \max \{K - P_T, 0\} = K - \min \{P_T, K\} = K - \min \left\{e^{\bar{\mu}(T)+X_T}, K\right\}. \end{aligned} \quad (78)$$

Accordingly, we need to evaluate option on the capped payoff under the MMA measure

$$U(\tau, X) = e^{-\bar{r}(T)} \mathbb{E} \left[\min \left\{ e^{\bar{\mu}(T)+X_T}, K \right\} \middle| \mathcal{F}_t \right] \quad (79)$$

Proposition 6.1. *The valuation formula for capped payoff is given by*

$$U(\tau, X) = \frac{e^{-\bar{r}(T)} K}{\pi} \Re \left[\int_0^\infty e^{-(iy-1/2)X^*} \frac{1}{y^2 + 1/4} E^{[m]}(\tau, Y; \Phi = iy - 1/2, \Psi = 0, \Theta = 0; p = 1) dy \right], \quad (80)$$

where $X^* = \ln(S_0/K) + \bar{\mu}(T)$ is log-moneyness, $E^{[1]}$ and $E^{[2]}$ are given in Eq (61) and Eq (69), respectively.

Proof. See Appendix A.17. \square

As a result, calls and puts on spot and futures underlyings are valued using Eqs (78) and (79)

$$C(\tau, P, K) = e^{-\bar{r}(T)+\bar{\mu}(T)}S - U(\tau, X), \quad P(\tau, P, K) = e^{-\bar{r}(T)}K - U(\tau, X). \quad (81)$$

Given the futures price $f_0(T)$ in Eq (14), the value of futures call option is

$$c(\tau, F, K) = e^{-\bar{r}(T)}f_0(T) - U(\tau, X). \quad (82)$$

with log-moneyness $X^* = \ln(f_0(T)/K)$. Thus, given a set of futures prices quoted in the market, we can evaluate options on this set of futures without need to compute the convenience yield explicitly.

We emphasize that in valuation equations (81) we implicitly assume that the price process $Z_t = \exp(X_t)$, $t \in (0, T]$, is \mathbb{Q} -martingale under the MMA measure, otherwise formulas (81) are not valid, see Theorem A.3. For that we assume a restriction $\kappa_2 \geq \beta$, see Theorem 2.2 1.).

6.2 Inverse Calls and Puts

Using generic price process of underlying spot and futures given in Eq (77), we represent the payoffs of inverse calls and puts by

$$\begin{aligned} \tilde{c}(P_T, K) &= \frac{1}{P_T} \max \{P_T - K, 0\} = 1 - \frac{1}{P_T} \min \{P_T, K\} = 1 - e^{-X_T-\bar{\mu}(T)} \min \left\{ e^{\bar{\mu}(T)+X_T}, K \right\} \\ \tilde{p}(P_T, K) &= \frac{1}{P_T} \max \{K - P_T, 0\} = \frac{K}{P_T} - \frac{1}{P_T} \min \{P_T, K\} = \frac{K}{P_T} - e^{-X_T-\bar{\mu}(T)} \min \left\{ e^{\bar{\mu}(T)+X_T}, K \right\}. \end{aligned}$$

As a result, we need to evaluate option on the inverse capped payoff under the inverse measure

$$\tilde{U}(\tau, X) = \tilde{\mathbb{E}} \left[e^{-X_T-\bar{\mu}(T)} \min \left\{ e^{\bar{\mu}(T)+X_T}, K \right\} \middle| \mathcal{F}_t \right]. \quad (83)$$

Proposition 6.2. *The valuation formula (179) for the inverse capped payoff then becomes*

$$\tilde{U}(\tau, X) = \frac{1}{\pi} \int_0^\infty e^{-(iy+1/2)X^*} \frac{1}{y^2 + 1/4} E^{[m]}(\tau, Y; \Phi = iy + 1/2, \Psi = 0, \Theta = 0, p = -1) dy, \quad (84)$$

where $X^* = \ln(S_0/K) + \bar{\mu}(T)$ is log-moneyness, $E^{[1]}$ and $E^{[2]}$ are given in Eq (61) and Eq (69), respectively.

Proof. See Appendix A.18. \square

As a result, calls and puts are valued using capped payoff (83)

$$\tilde{c}(\tau, P, K) = 1 - \tilde{U}(\tau, X), \quad \tilde{p}(\tau, P, K) = Ke^{-X-\bar{\mu}(T)} - \tilde{U}(\tau, X). \quad (85)$$

Hereby, we need to compute

$$f(\tau, X) = \tilde{\mathbb{E}} \left[\frac{1}{P_T} \middle| \mathcal{F}_t \right] = \tilde{\mathbb{E}} \left[e^{-X_T-\bar{\mu}(T)} \middle| \mathcal{F}_t \right] = e^{-\bar{\mu}(T)} e^{-X}, \quad (86)$$

with the last equality following from Eq (76).

Given the term structure of futures prices $f_0(T)$ in Eq (14), the put option on the future is

$$p(\tau, F, K) = \frac{K}{f_0(T)} - \tilde{U}(\tau, X), \quad (87)$$

with log-moneyness $X^* = \ln(f_0(T)/K)$. We emphasize that Eq (85) holds only if the MMA measure \mathbb{Q} and inverse measure $\tilde{\mathbb{Q}}$ are equivalent, which requires restriction $\kappa_2 \geq \beta$ by Theorem 4.1. In addition, we assume that the inverse process $R_t = \exp(-X_t)$, $t \in (0, T]$, is a proper $\tilde{\mathbb{Q}}$ martingale, so that Eq (86) is valid by Theorem A.3. For this we need $\kappa_2 \geq 2\beta$ by Theorem 2.2 2).

6.3 Options on Quadratic Variance

We consider a call options on QV with the payoff function

$$u(I) = \frac{1}{T} \max\{I(T) - TK, 0\}, \quad (88)$$

where K is the strike in terms of annualized variance.

Proposition 6.3. *The value of the call option on the QV under the MMA measure \mathbb{Q} is given by*

$$\begin{aligned} U(\tau, X, Y, I) &= e^{-\bar{r}(T)} \mathbb{E}[u(I_T) | \mathcal{F}_t] \\ &= \frac{e^{-\bar{r}(T)}}{T} \frac{1}{\pi} \int_0^{+\infty} \Re \left[\hat{u}(\Psi) E^{[m]}(\tau, Y; \Phi = 0, \Psi; \Theta = 0; p = 1) \right] d\Psi, \\ \hat{u}(\Psi) &= \frac{e^{-\Psi I}}{\Psi^2} e^{\Psi T K}, \end{aligned} \quad (89)$$

provided $\Re[\Psi] < 0$, with $E^{[1]}$ and $E^{[2]}$ given in Eq (61) and Eq (69), respectively.

Proof. See A.19. \square

Sepp (2008) derives transforms $\hat{u}(\Psi)$ for typical payoff on the QV including puts and calls on the square root of the QV.

Assuming that the inverse measure $\tilde{\mathbb{Q}}$ is a martingale measure for generic spot and futures underlying P_t defined in Eq (77), the inverse option on the QV equals

$$\tilde{U}(\tau, X, Y, I) = \tilde{\mathbb{E}} \left[\frac{u(I_T)}{P_T} \middle| \mathcal{F}_t \right]. \quad (90)$$

where the expectation on the right-hand side is taken under $\tilde{\mathbb{Q}}$. Similarly to Eq (6), values $\tilde{U}(\tau, X, Y, I)$ and $U(\tau, X, Y, I)$ in (90) and (89), respectively, are related by:

$$U(\tau, X, Y, I) = P_t \tilde{U}(\tau, X, Y, I).$$

Proposition 6.4. *The value of the call option on the QV under the inverse measure $\tilde{\mathbb{Q}}$ is*

$$\tilde{U}(\tau, X, Y, I) = \frac{e^{-\bar{r}(T)}}{T} \frac{1}{\pi} \int_0^{+\infty} \Re \left[\hat{u}(\Psi) e^{X - \bar{\mu}(T)} E^{[m]}(\tau, Y; \Phi = 1, \Psi, \Theta = 0; p = 1) \right] d\Psi, \quad (91)$$

provided $\Re[\Psi] < 0$, with $E^{[m]}$ and $\hat{u}(\Psi)$ defined as in Eq (89).

Proof. See Appendix A.20. \square

7 Model Implementation and Calibration to Options Data

7.1 Implementation and Computational Cost

For practical applications, either for model calibration or options valuation, we need to compute call and put option prices on a grid, also called as option chain, of several maturities and strikes. For brevity, we assume a homogeneous grid with M maturities and J strikes. For the implementation, we apply the affine expansion given by either the first order in Eq (61) or the second order in Eq (69) as the analytic solution to the MGF.

1) We fix the space grid with size P (typically, $P \approx 500$) of the transform variable Φ for the log-price log-price. We solve the system of ODEs numerically for either the first-order expansion Eq (61) or for the second-order expansion Eq (69) in time grid up to the last maturity time. The time grid includes all maturities in the chain with the size of intermediate grids adopted optimally by an ODE solver. The computational cost of this step is

$$\mathcal{C}^{(1)} = \mathcal{O}(P \times N_{\max}), \quad (92)$$

Table 1: Estimated model parameters of the beta SV model (9) calibrated to options data.

Param	VIX	-3x Nasdaq	Bitcoin	Gold	S&P500
$\hat{\sigma}_0$	0.9767	0.9114	0.8327	0.1505	0.227
$\hat{\theta}$	0.5641	0.9390	1.0139	0.1994	0.2616
$\hat{\kappa}_1$	4.9067	4.9544	4.8609	2.2062	4.9325
$\hat{\kappa}_2$	8.6985	5.2762	4.7940	11.063	18.855
$\hat{\beta}$	2.3425	1.3215	0.1988	0.1547	-1.8123
$\hat{\varepsilon}$	1.0163	0.9964	2.3694	2.8011	0.9832

where N_{\max} is the number of time steps for ODE solver (typically we have one step per one-two weeks) and \mathcal{O} is the number of arithmetic (or elementary) operations.

2) For each maturity we compute the MGF on the grid of Φ . We then compute values of capped payoffs for the MMA measure in Eq (80) or for the inverse measure in Eq (84) using Simpson rule for numerical integration. We then value all options in a given chain. The computational cost of this step is

$$\mathcal{C}^{(2)} = \mathcal{O}(J \times M \times P), \quad (93)$$

The main difference with an implementation of affine models is the first step for computing the MGF, which in affine models could be computed with cost close to $\mathcal{O}(P \times M)$ because the solution to the MGF is available analytically. The cost ratio between the implementation of the log-normal SV model and an affine SV model compares favorably when the number of maturities becomes large with M close to N_{\max} , and when the number of strikes J becomes larger.

7.2 Model Calibration

By model calibration we estimate six model parameters from market implied volatilities: $\sigma_0, \theta, \kappa_1, \kappa_2, \beta, \varepsilon$. Parameter values are bounded to the following domains $\sigma_0, \theta \in [0.01, 2.0]$, $\kappa_1 \in [0.5, 10.0]$, $\beta \in [-3.0, 3.0]$, $\varepsilon \in [0.1, 5.0]$. For stability, we implement the following constraints.

1) We set $\kappa_2 = \kappa_1/\theta$ to reduce the number of calibrated parameters. In our extensive tests, we found that keeping κ_2 as a free parameter does not significantly improve the quality of model fit to market data. This specification result in pure quadratic drift of the volatility Eq (17).

2a) We set the constraint $\kappa_2 \geq \beta$ so that by Theorem 2.2 the dynamics under the MMA measure are martingale.

2b) For cryptocurrency options, instead of **2a)** we use stronger constraint $\kappa_2 \geq 2\beta$ so that by Theorem 2.2 the dynamics under the inverse measure are martingale.

We use scipy implementation of Sequential Least Squares Programming (SLSQP) algorithm to minimized squared differences between model implied volatilities and market implied volatilities, constrained, which are weighted by corresponding Black-Scholes vegas.

We illustrate the model calibration to the assets with the positive implied volatility skews shown in Figure 1, and we add the S&P 500 index with the significant negative return-volatility correlation for the comparison⁴. For all assets, we use implied option skews for most liquid options with maturity of 2 weeks, 1 month, 2 and 6 months. We use the four most liquid market slices and the range of strike that includes puts and calls with deltas in the range $(-0.05, -0.5)$ and $[0.5, 0.05]$, respectively. For options on the VIX and ETFs, we use the market data from 15-July-2022. For Bitcoin, we use the market data observed on Deribit option exchange on 21-Oct-2021.

In Table 1 we display the calibrated model parameters of the dynamics (9). In Figure 11, we show the quality of model fit for Bitcoin options. The quality of model fit is similar for other assets. We see that the calibrated model for Bitcoin options is able to capture the market implied skew very well across most liquid maturities with only 5 parameters. The average mean squared

⁴The data and implementation of model calibration to assets in Table 1 is provided in paper's Github project <https://github.com/ArturSepp/StochVolModels>

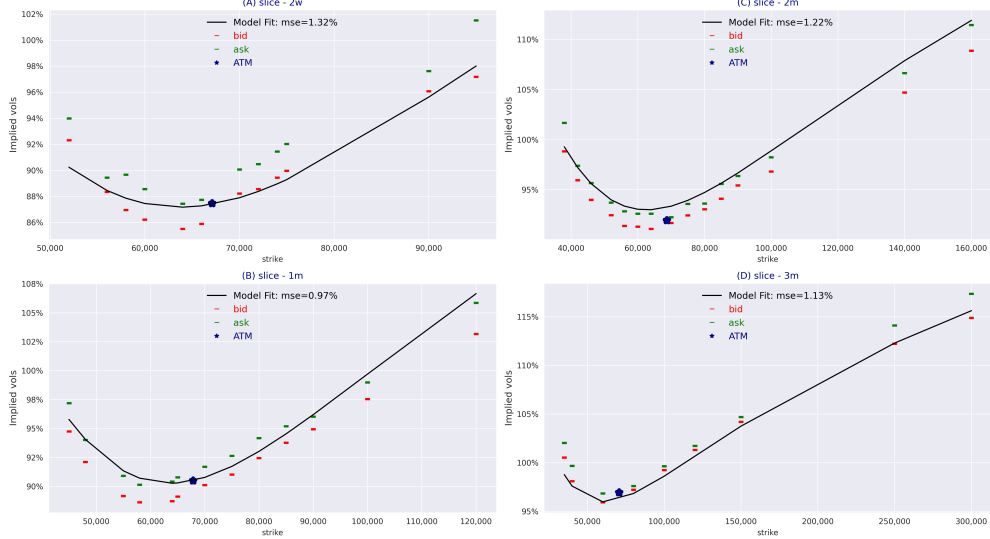


Figure 11: Quality of model fit to Bitcoin options on 21-Oct-2021 reported in Table 1 using the four most liquid slices: 2 weeks (Subplot A), 1 month (B), 2 months (C), and 3 months (D). Continuous black line is model implied volatilities computed using the second-order affine expansion in Eq (81) and (85). Bid and ask displays the market bid and ask quotes, the ATM is the at-the-money mid-point volatility. Model implied volatility is displayed using the continuous black line. MSE is the mean squared error between the model and the mid of market bid-ask volatilities.

error (MSE) is about 1% in implied volatilities, which is mostly within bid-ask spread. Calibration to ATM region can be further improved using a term structure of the mean volatility θ . In a practical setting, the SV model dynamics can be augmented with a local volatility (Lipton (2002)) to accurately fit the implied volatility surface.

We see that the estimated volatility β is positive for all assets with positive implied volatility skews. For VIX options, the estimate of β is very large. Thus, as we discussed in Section 2.4, the conventional SV models may not be arbitrage-free for the valuation of options on the VIX and other assets with positive return-volatility correlation.

7.2.1 Comparison of valuation under MMA and Inverse measures for Bitcoin Options

Since Bitcoin options which are traded on the Deribit exchange have inverse payoffs, it is important that there is no-arbitrage between the MMA and the inverse measures. In Figure (12), we compare the model implied volatilities computed from prices of vanilla and inverse options valued under the MMA and inverse measures, respectively, with the second-order affine expansion and model parameters reported in Table 1. As benchmark, we use the MC simulation of the model dynamics (9) using scheme in Eq (40) with the number of paths equal 400,000 and daily time steps. We show the 95% confidence interval of MC estimates as dashed lines like to bid/ask lines.

We observe that option values computed using the second order affine expansion under the MMA and inverse measures are very close to each other with the differences being within the numerical accuracy of an ODE solver and Fourier inversion (of order 1e-4). The difference in terms of implied volatilities does not exceed 1e-4.

In Figure 13, we show model prices of call options on the QV computed using the second-order affine expansion under the MMA and inverse measures, and the comparison with MC estimates. We also observe that the solution under the both measures are accurate with each other and agree with MC simulations. Interestingly, we observe that the implied volatility skew of options on the QV is upward sloping, which is observed in market data of options on the QV and of listed options on the VIX, as we show in Figure 1. It is known that Heston model, even augmented when with jumps, produces downward sloping skews on options on the QV (see for an example Drimus (2012)

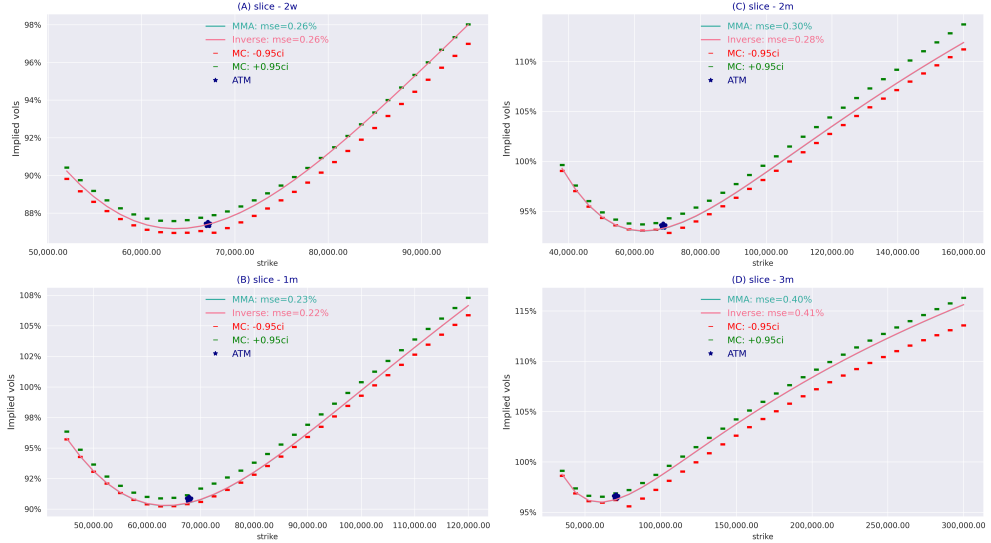


Figure 12: Implied volatilities of Bitcoin options, with model reported in Table 1, for the slices used in model calibration for the uniform range of strikes using the valuation under the MMA measure (MMA) and the inverse measure (Inverse). Continuous black line is model implied volatilities computed using the second-order affine expansion in Eq (81) and (85). Dashed lines labeled by $MC - 0.95ci$ and $MC + 0.95ci$ are MC 95% confidence intervals computed using scheme in Eq (40) with number of path equal 400,000 and daily time steps. MSE is the mean squared error between BSM volatilities inferred from model values and the MC estimates.

and Sepp (2012)). Thus, the log-normal SV model implies realistic patterns of implied volatility-of-volatility.

8 Conclusion

We have considered the log-normal SV model with the quadratic drift which plays an important role for the existence of martingale measures. We have applied this SV model for modeling of implied volatility surfaces of assets with positive return-volatility correlation. We have derived admissible bounds of model parameters for the existence of both the money market account measure and the inverse measures.

Since the log-normal SV model is not affine, there is no analytical solution available for this model. To circumvent this, we have developed an affine expansion approach under which the joint moment generating function (MGF) of three state variables (log-price, the quadratic variance (QV), and the volatility) is decomposed into a leading term, which is given by an exponential-affine form, and a residual term, whose estimate depends on the higher order moments of the volatility process. We have proved that the second-order leading term is consistent with the expected values and the second moments of the state variables. We have applied Fourier inversion techniques for valuation of vanilla and inverse options on spot and futures underlying. By comparison of model values computed using our method with estimates obtained from Monte Carlo simulations, we have shown that the second-order leading term is very accurate for option valuation. We have demonstrated that our model fits implied volatilities of assets with positive return-volatility correlation.

We also show that Monte-Carlo simulation of the log-normal SV model with quadratic drift is robust. We derive backward Euler-Maruyama scheme for discretization of the log-volatility process and show that it has a strong convergence rate of 1.

As an extension of the framework we shall consider the applications to the rough SV models proposed by Gatheral et al (2018) using log-normal volatility. We shall also apply the developed

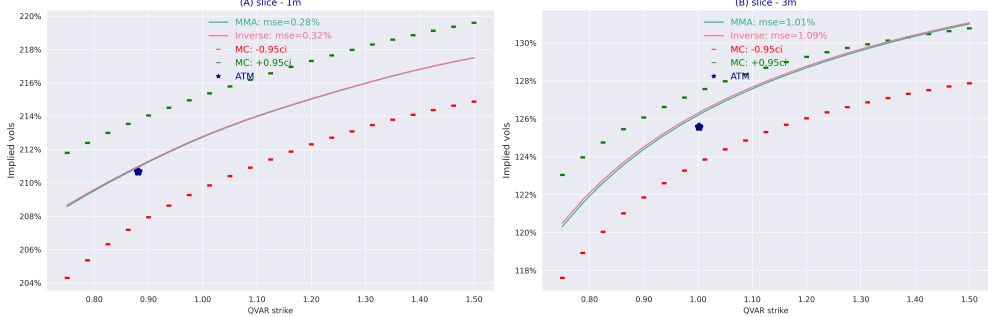


Figure 13: Implied volatilities of call options on Quadratic Variance of Bitcoin, with model reported in Table 1, for maturities of 1 month (Subplot A) and 3 months (B) using the valuation under the MMA measure (MMA) and the inverse measure (Inverse). BSM volatilities are implied from model prices using expected QV $\hat{I}_\tau = \{0.88, 1.00\}$ computed using Eq (36). Continuous black line is model implied volatilities computed using the second-order affine expansion in Eq (89) and (91). Dashed lines labeled by $MC - 0.95ci$ and $MC + 0.95ci$ are MC 95% confidence intervals computed using scheme in Eq (40) with number of path equal 400,000 and daily time steps. MSE is the mean squared error between BSM volatilities inferred from model values and the MC estimates.

solution for valuation of interest rate and credit derivatives⁵.

A Proofs

A.1 Proof of Theorem 2.2

1. Although the theorem can be proved by applying results in [Lions and Musiela \(2007\)](#) and [Carr and Willems \(2019\)](#), we provide an alternative proof using Theorem A.2 because our same arguments are applicable for other class of SV models discussed in Section 2.3. Theorem A.2 shows that Z_t is \mathbb{Q} -martingale if and only if the process

$$d\sigma_t = ((\kappa_0 + \kappa_1 \sigma_t)(\theta - \sigma_t) + \beta \sigma_t^2) dt + \vartheta \sigma_t d\tilde{W}_t^{(*)}$$

has unique strong solution under $\tilde{\mathbb{Q}}$. Using Theorem 3.2, we immediately obtain that the uniqueness holds iff $\kappa_2 \geq \beta$.

2. According to Lemma 4.2, the dynamics of $\{\sigma_t, R_t\}$ under $\tilde{\mathbb{Q}}$ is

$$\begin{aligned} d\sigma_t &= ((\kappa_1 + \kappa_2 \sigma_t)(\theta - \sigma_t) + \beta \sigma_t^2) dt + \beta \sigma_t d\tilde{W}_t^{(0)} + \varepsilon \sigma_t d\tilde{W}_t^{(1)}, \\ dR_t &= (-\sigma_t) R_t d\tilde{W}_t^{(0)}. \end{aligned} \quad (94)$$

Using Theorem 2.4 (i), (ii) of [Lions and Musiela \(2007\)](#) we see that R_t is a martingale if

$$\limsup_{\xi \uparrow +\infty} (\beta \xi^2 + (\kappa_1 + \kappa_2 \xi)(\theta - \xi) + \beta \xi^2) \xi^{-1} < \infty,$$

which holds if $\kappa_2 \geq 2\beta$. And R_t is not a martingale if for some smooth, positive, increasing function φ we have

$$\liminf_{\xi \uparrow +\infty} (\beta \xi^2 + (\kappa_1 + \kappa_2 \xi)(\theta - \xi) + \beta \xi^2) \varphi(\xi)^{-1} > 0, \quad (95)$$

where $\int_\varepsilon^{+\infty} \varphi(\xi)^{-1} d\xi < \infty$, $\varepsilon > 0$. Choosing $\varphi(\xi) = \xi^2$, we see that (95) holds if $\kappa < 2\beta$.

3. Case $u \geq 1$ follows immediately from Theorem 2.5, 2.6 of [Lions and Musiela \(2007\)](#), see also [Carr and Willems \(2019\)](#). Let $u \leq 0$. We can rewrite as follows

$$\mathbb{E} Z_T^u = \mathbb{E} R_T^{-u} = \tilde{\mathbb{E}} \left[R_T^{-u} \frac{R_T}{R_0} \right] = \frac{1}{R_0} \tilde{\mathbb{E}} \left[R_T^h \right], \quad h = -u + 1. \quad (96)$$

⁵For an example, [Pan & Singleton \(2008\)](#) find that the single factor default model following a log-normal process captures most of the variation in the term structures of CDS spreads for sovereign credits.

Here we assume that $\kappa_2 \geq \beta$ which ensures equivalence $\mathbb{Q} \sim \tilde{\mathbb{Q}}$. Hence $\mathbb{E} Z_T^u$ is finite if $\tilde{\mathbb{E}} [R_T^h]$ is finite, which according to case (2.) holds if

$$\kappa_2 - \beta > \beta h + \vartheta \sqrt{h^2 - h} \quad \text{or} \quad \kappa_2 - \beta = \beta h + \vartheta \sqrt{h^2 - h}, \quad \kappa_1 \geq \kappa_2 \theta. \quad (97)$$

Result follows immediately by setting $h = -u + 1$ in conditions (97).

4. Using relationship (96), the result follows from case (iii).

A.2 Proof of Proposition 2.1

First, we need a generic boundary classification for the CIR process.

Lemma A.1. *Assume that variance process V_t follows CIR dynamics (15). Then boundary point $+\infty$ is*

1. attractive for $\kappa < 0$
2. not attractive for $\kappa \geq 0$
3. not attainable for all $\kappa \in \mathbb{R}$

Proof. Follows from Feller boundary classification criteria, see Karatzas and Shreve (1991), Karlin and Taylor (1981) and Proposition 2.5 of Andersen and Piterbarg (2007). Note we are not restricting mean reversion speed κ to be positive here, i.e. κ can be negative. We omit technical details. \square

Using proof of Lemma 4.2, we see that the dynamics of $\{V_t, R_t\}$ under $\tilde{\mathbb{Q}}$ is

$$\begin{aligned} dV_t &= (\kappa(\theta - V_t) + \rho\vartheta V_t) dt + \vartheta \sqrt{V_t} d\tilde{W}_t^{(S)}, \\ dR_t &= R_t \left(-\sqrt{V_t} \right) d\tilde{W}_t^{(V)}. \end{aligned} \quad (98)$$

1. By Theorem A.2, S_t is \mathbb{Q} -martingale iff the variance process under $\tilde{\mathbb{Q}}$ in SDE (98) does not explode in finite time. Using Lemma A.1, we conclude that point $+\infty$ is unattainable for the variance process in (98), hence it does not explode in finite time.

2. As seen in (98), V_t is still a CIR process under $\tilde{\mathbb{Q}}$, however, with different mean reversion speed κ and level $\kappa\theta/(\kappa - \rho\vartheta)$, respectively. Repeated application of Lemma A.1 concludes the proof.

3. See Theorem 3.2 (vi), 3.3 (iv) in Lions and Musiela (2007).
4. Follows from the dynamics of $\{V_t, R_t\}$ under $\tilde{\mathbb{Q}}$ in (98) and Theorem 3.2 (vi), 3.3 (iv) of Lions and Musiela (2007).

A.3 Proof of Proposition 2.2

Applying Itô's lemma to $\sigma_t 0 \exp(Y_t)$ in SDE (16), we have

$$d\sigma_t = \sigma_t \kappa (\theta + \vartheta^2/(2k) - \ln \sigma_t) dt + \beta \sigma_t dW_t^{(0)} + \varepsilon \sigma_t dW_t^{(1)}, \quad \sigma_0 = \sigma, \quad (99)$$

where $\beta = \rho\vartheta$, $\varepsilon = \sqrt{1 - \rho^2}\vartheta$ and $W^{(0)}$, $W^{(1)}$ are independent Wiener processes. Note that the volatility has a non-linear mean reversion due to the presence of logarithmic term in the drift.

As the difference between model (16) and log-normal SV model with linear drift is in presence of non-linear drift in σ_t , we proceed exactly as in the proof of Proposition 2.2. By Proposition 2.2, the constraints on model parameters that ensure martingale property of Z_t or finiteness of moments in exp-OU model are identical to the one in SV model with linear drift.

A.4 Proof of Theorem 3.1

We consider the interval (l, r) and define the scale function and its density, denoted by $S(x)$ and $s(x)$, respectively, as follows (see, for example, Chapter IV.15 in [Borodin \(2017\)](#))

$$s(x) = \exp \left\{ - \int_c^x \frac{2\mu(\sigma)}{v(\sigma)^2} d\sigma \right\}, \quad S(x) = \int_c^x s(y) dy, \quad (100)$$

where $x \in (l, r)$ and c is an arbitrary but fixed interior point of (l, r) . We also define the speed function and its density, denoted by $M(x)$ and $m(x)$, respectively, as follows

$$m(x) = \frac{2}{v(x)^2} \exp \left\{ \int_c^x \frac{2\mu(\sigma)}{v(\sigma)^2} d\sigma \right\}, \quad x \in (l, r), \quad M(x) = \int_c^x m(y) dy. \quad (101)$$

Choosing c such that the integral $\int_c^x \frac{2\mu(\sigma)}{v(\sigma)^2} d\sigma$ vanishes and setting $\eta = 2 \frac{\kappa_1 - \kappa_2 \theta}{\vartheta^2}$, we have

$$s(x) = x^\eta \exp \left\{ \frac{2\kappa_1 \theta}{\vartheta^2} \frac{1}{x} + \frac{2\kappa_2}{\vartheta^2} x \right\}, \quad m(x) = \frac{2}{\vartheta^2} x^{-\eta-2} \exp \left\{ - \frac{2\kappa_1 \theta}{\vartheta^2} \frac{1}{x} - \frac{2\kappa_2}{\vartheta^2} x \right\} \quad (102)$$

Using

$$\begin{aligned} S(x) &= \int_c^x s(y) dy \leq \int_c^x y^\eta \exp \left\{ \frac{2\kappa_1 \theta}{\vartheta^2} \frac{1}{y} \right\} dy, \quad x \downarrow 0+, \\ S(x) &\geq \int_c^x s(y) dy \geq \int_c^x y^\eta \exp \left\{ \frac{2\kappa_2}{\vartheta^2} y \right\} dy, \quad x \uparrow +\infty, \end{aligned} \quad (103)$$

we find that

$$S(0+) = \lim_{x \downarrow 0+} S(x) = -\infty, \quad S(+\infty) = \lim_{x \uparrow +\infty} S(x) = +\infty. \quad (104)$$

Consequently, boundaries $l = 0$, $r = +\infty$ are not attractive.

We define $\Sigma(l)$, $\Sigma(r)$ and show that the boundary $r = +\infty$ is unattainable

$$\Sigma(l) := \iint_{l < z < y < x} s(z)m(y)dzdy, \quad \Sigma(r) := \iint_{x < y < z < r} s(z)m(y)dzdy \quad (105)$$

$$\begin{aligned} \Sigma(r) &= \int_x^r \left(\int_y^r s(z) dz \right) m(y) dy = \int_x^r \left(\int_x^y m(z) dz \right) s(y) dy = \\ &= \int_x^r \left(\int_x^y \frac{2}{\vartheta^2} z^{-\eta-2} \exp \left\{ - \frac{2\kappa_1 \theta}{\vartheta^2} \frac{1}{z} - \frac{2\kappa_2}{\vartheta^2} z \right\} dz \right) y^\eta \exp \left\{ \frac{2\kappa_1 \theta}{\vartheta^2} \frac{1}{y} + \frac{2\kappa_2}{\vartheta^2} y \right\} dy \end{aligned} \quad (106)$$

We note that the right hand side of (106) is finite if and only if

$$\widehat{\Sigma}(r) := \int_x^r \left(\int_x^y z^{-\eta-2} \exp \left\{ - \frac{2\kappa_2}{\vartheta^2} z \right\} dz \right) y^\eta \exp \left\{ \frac{2\kappa_2}{\vartheta^2} y \right\} dy \quad (107)$$

is finite. We split inner integral into two integrals, over $[x, +\infty)$ and $[y, +\infty)$

$$\int_x^y z^{-\eta-2} \exp \left\{ - \frac{2\kappa_2}{\vartheta^2} z \right\} dz = \int_x^{+\infty} \cdots dz - \int_y^{+\infty} \cdots dz = I_1 - I_2 \quad (108)$$

we see that I_1 is finite for all $\kappa_1, \kappa_2 > 0$. Then, using asymptotic expansion of incomplete gamma function (see formula 6.5.32 in [Abramowitz and Stegun \(1972\)](#)), we have for $y \rightarrow +\infty$

$$I_2 = \int_y^{+\infty} z^{-\eta-2} \exp \left\{ - \frac{2\kappa_2}{\vartheta^2} z \right\} dz = \left(\frac{2\kappa_2}{\vartheta^2} \right)^{-1} y^{-\eta-2} \exp \left\{ - \frac{2\kappa_2}{\vartheta^2} y \right\} \left(1 + O \left(\frac{1}{y} \right) \right). \quad (109)$$

Substituting asymptotic expansion (109) into (108) and (107), we have

$$\widehat{\Sigma}(r) = I_1 \int_x^r y^\eta \exp \left\{ \frac{2\kappa_2}{\vartheta^2} y \right\} dy - \left(\frac{2\kappa_2}{\vartheta^2} \right)^{-1} \int_x^r y^{-2} dy + O \left(\int_x^r y^{-3} dy \right), \quad y \rightarrow +\infty \quad (110)$$

We conclude that $\widehat{\Sigma}(+\infty) = +\infty$. Hence, boundary $r = +\infty$ is unattainable. Next, we show that boundary $l = 0$ is unattainable as well. By definition of $\Sigma(l)$

$$\begin{aligned} \Sigma(l) &= \int_l^x \left(\int_l^y s(z) dz \right) m(y) dy = \int_l^x \left(\int_y^x m(z) dz \right) s(y) dy = \\ &= \int_l^x \left(\int_y^x \frac{2}{\vartheta^2} z^{-\eta-2} \exp \left\{ - \frac{2\kappa_1 \theta}{\vartheta^2} \frac{1}{z} - \frac{2\kappa_2}{\vartheta^2} z \right\} dz \right) y^\eta \exp \left\{ \frac{2\kappa_1 \theta}{\vartheta^2} \frac{1}{y} + \frac{2\kappa_2}{\vartheta^2} y \right\} dy \end{aligned} \quad (111)$$

We make an reciprocal transformation $\{z \rightarrow 1/z, y \rightarrow 1/y\}$ in (111)

$$\Sigma(l) = \int_{1/x}^{1/l} \left(\int_{1/x}^y \frac{2}{\vartheta^2} z^\eta \exp \left\{ -\frac{2\kappa_1\theta}{\vartheta^2} z - \frac{2\kappa_2}{\vartheta^2} \frac{1}{z} \right\} dz \right) y^{-\eta-2} \exp \left\{ \frac{2\kappa_1\theta}{\vartheta^2} y + \frac{2\kappa_2}{\vartheta^2} \frac{1}{y} \right\} dy. \quad (112)$$

The right hand side of (112) is finite if and only if

$$\widehat{\Sigma}(l) := \int_{1/x}^{1/l} \left(\int_{1/x}^y z^\eta \exp \left\{ -\frac{2\kappa_1\theta}{\vartheta^2} z \right\} dz \right) y^{-\eta-2} \exp \left\{ \frac{2\kappa_1\theta}{\vartheta^2} y \right\} dy \quad (113)$$

is finite. Splitting inner integral into two integrals, over $[1/x, +\infty)$ and $[y, +\infty)$, respectively

$$\int_{1/x}^y z^\eta \exp \left\{ -\frac{2\kappa_1\theta}{\vartheta^2} z \right\} dz = \int_{1/x}^{+\infty} \cdots dz - \int_y^{+\infty} \cdots dz = I_1 - I_2 \quad (114)$$

we see that I_1 is finite for all $\kappa_1, \kappa_2 > 0$. As before, using asymptotic expansion of incomplete gamma function (see formula 6.5.32 in [Abramowitz and Stegun \(1972\)](#)), we have

$$\begin{aligned} I_2 &= \int_y^{+\infty} z^\eta \exp \left\{ -\frac{2\kappa_1\theta}{\vartheta^2} z \right\} dz = \left(\frac{\vartheta^2}{2\kappa_1\theta} \right)^{\eta+1} \int_{\frac{2\kappa_1\theta}{\vartheta^2} y}^{+\infty} u^\eta e^{-u} du = \\ &= \left(\frac{\vartheta^2}{2\kappa_1\theta} \right) y^\eta \exp \left\{ -\frac{2\kappa_1\theta}{\vartheta^2} y \right\} \left(1 + O \left(\frac{1}{y} \right) \right), y \rightarrow +\infty. \end{aligned} \quad (115)$$

Substituting expansion (115) into (114) and (113), we have for $y \rightarrow +\infty$

$$\widehat{\Sigma}(l) = I_1 \int_{1/x}^{1/l} y^{-\eta-2} \exp \left\{ \frac{2\kappa_1\theta}{\vartheta^2} y \right\} dy - \left(\frac{\vartheta^2}{2\kappa_1\theta} \right) \int_{1/x}^{1/l} y^{-2} dy + O \left(\int_{1/x}^{1/l} y^{-3} dy \right). \quad (116)$$

We conclude that $\widehat{\Sigma}(+\infty) = +\infty$. Hence, boundary $l = 0$ is unattainable.

A.5 Proof of Theorem 3.2

We consider general SDE with monotonic coefficients. We will refer to following theorem that guarantees the existence and uniqueness of its solutions.

Theorem A.1. *Let $a_t(x) : [0, T] \times \mathbb{R} \rightarrow \mathbb{R}$, $b_t(x) : [0, T] \times \mathbb{R} \rightarrow \mathbb{R}$ be functions, continuous in x , satisfying following conditions:*

1. $\int_0^T \sup_{|x| \leq R} (|a_t(x)| + |b_t(x)|^2) dt < \infty$ for any $T \geq 0$, $R \geq 0$,
2. for every $x, y, z \in \mathbb{R}$ such that $|x| \leq R, |y| \leq R, |z| \leq R$ following conditions hold:

(a) (monotonicity condition):

$$2(x-y)(a_t(x)-a_t(y)) + (b_t(x)-b_t(y))^2 \leq K_t(R)(x-y)^2 \quad (117)$$

(b) (growth condition): $2za_t(z) + (b_t(z))^2 \leq K_t(1)(1+z)^2$.

where function $K_t(R) : [0, T] \times \mathbb{R}_+ \rightarrow \mathbb{R}_+$ satisfies $\int_0^t K_s(R) ds < \infty$ for any $T \geq 0$, $R \geq 0$.

Then there exists unique solution of the SDE

$$x_t = x_0 + \int_0^t a_s(x_s) ds + \int_0^t b_s(x_s) dW_s, \quad t \leq T. \quad (118)$$

Proof. We refer to [Gyöngy and Krylov \(1980\)](#). \square

We now show that SDE (17), where $\kappa_1, \kappa_2, \theta, \nu$ satisfy (18), does indeed satisfy conditions 1-3 of Theorem A.1. We emphasize that positivity of the process demonstrated in Theorem 3.1 is extremely important. As in our case $a_t(x) = (\kappa_1 + \kappa_2 x)(\theta - x)$, $b_t(x) = \vartheta x$, we get

$$\begin{aligned} &2(x-y)(a_t(x)-a_t(y)) + (b_t(x)-b_t(y))^2 = \\ &= (\vartheta^2 - 2(\kappa_1 - \kappa_2\theta))(x-y)^2 - 2\kappa_2(x+y)(x-y)^2 \leq (\vartheta^2 - 2(\kappa_1 - \kappa_2\theta) + 2\kappa_2R)(x-y)^2 \end{aligned}$$

when $|x| \leq R, |y| \leq R$. As for any $R > 0$ we have $\int_0^t [\vartheta^2 - 2(\kappa_1 - \kappa_2\theta) + 2\kappa_2R] ds < \infty$, we conclude that monotonicity condition 2a is satisfied. As to the growth condition, we have

$$2za_t(z) + b_t(z)^2 = 2z[(\kappa_1 + \kappa_2z)(\theta - z)] + \vartheta^2z^2 = 2\kappa_1\theta z + [\vartheta^2 - 2(\kappa_1 - \kappa_2\theta)]z^2 - 2\kappa_2z^3 \quad (119)$$

Using that zero is unattainable boundary and simple inequalities $z \leq 1 + z^2, z^3 < 0$ valid for $z > 0$, we can estimate the right hand side of (119) as follows

$$2\kappa_1\theta(z^2 + 1) + [\vartheta^2 - 2(\kappa_1 - \kappa_2\theta)]z^2 \leq 2\kappa_1\theta + [2\kappa_1\theta + \vartheta^2 - 2(\kappa_1 - \kappa_2\theta)]z^2.$$

We conclude that the growth condition 2b is also satisfied. The final result follows from Theorem A.1

A.6 Proof of Proposition 3.1

To prove proposition 3.1, we need slightly weaker result.

Proposition A.1. *We assume $\kappa_1\theta > 0$. Then, for every $|p| \geq 1$: $\sup_{t \in [0, T]} \mathbb{E}\sigma_t^p < \infty$ for any $T > 0$.*

Proof. We consider cases $p \geq 1, p \leq -1$: When $p \geq 1$, applying Itô's lemma to σ_t^p we have

$$\mathbb{E}\sigma_t^p \leq \sigma_0^p + t \sup_{\sigma \in (0, +\infty)} \left[p\sigma^{p-1}(\kappa_1 + \kappa_2\sigma)(\theta - \sigma) + \frac{\vartheta^2}{2}p(p-1)\sigma^p \right]. \quad (120)$$

We consider function $F(\sigma) = p\sigma^{p-1}(\kappa_1 + \kappa_2\sigma)(\theta - \sigma) + \frac{\vartheta^2}{2}p(p-1)\sigma^p$. First, we assume $\sigma \in [1, +\infty)$. We observe that its derivative:

$$F'(\sigma) = p(p-1)\kappa_1\theta\sigma^{p-2} + p^2 \left(\kappa_2\theta - \kappa_1 + \frac{\vartheta^2}{2}(p-1) \right) \sigma^{p-1} - p(p+1)\kappa_2\sigma^p$$

is continuous and satisfies $F'(\sigma) = -p(p+1)\kappa_2\sigma^p(1+o(1))$ as $\sigma \rightarrow +\infty$. Hence $F'(\sigma) < 0$ for sufficiently large σ , therefore $F(\sigma) \leq K_1$ for all $\sigma \in [1, +\infty)$, where $K_1 = K_1(p)$.

For $\sigma \in (0, 1)$, as $p \geq 1$, $F(\sigma)$ is bounded by some constant $K_2 = K_2(p)$. Choosing $K = \max(K_1, K_2)$, we conclude that $\sup_{\sigma \in (0, +\infty)} F(\sigma) \leq K$. Thus, $\mathbb{E}\sigma_t^p \leq \sigma_0^p + Kt$ in Eq (120).

We take $p \leq -1$ and denote $q = -p, q \geq 1$. Similarly to previous case, we consider

$$F(\sigma) = p\sigma^{p-1}(\kappa_1 + \kappa_2\sigma)(\theta - \sigma) + \frac{\vartheta^2}{2}p(p-1)\sigma^p$$

Let $\sigma \in (0, 1)$. Applying $z = \frac{1}{\sigma}, z \in (1, +\infty)$, we have $F(\sigma) = F_2(z)$, where

$$F_2 = -q\kappa_1\theta z^{q+1} + q \left(-\kappa_2\theta + \kappa_1 - \frac{\vartheta^2}{2}(q+1) \right) z^q + q\kappa_2\sigma^{q-1}.$$

F_2 is continuous and satisfies $F'_2 = -q(q+1)\kappa_1\theta z^q(1+o(1))$ as $z \rightarrow +\infty$. Hence, as $\kappa_1\theta > 0$, we see that $F(\sigma) \leq K_1$ for all $\sigma \in (0, 1)$, where $K_1 = K_1(p)$.

When $\sigma \in [1, +\infty)$, we observe that $F(\sigma)$ is bounded, therefore $F(\sigma) \leq K_2, K_2 = K_2(p)$. Thus, $\sup_{\sigma \in (0, +\infty)} F(\sigma) \leq K, K = \max(K_1, K_2)$, which implies $\mathbb{E}\sigma_t^p \leq \sigma_0^p + Kt$ in Eq (120). \square

Now similarly to the proof of Proposition A.1, we apply Itô's formula to σ_t^p

$$\sigma_t^p = \sigma_0^p + \int_0^t \sigma_u^{p-1} \left((\kappa_1 + \kappa_2\sigma_u)(\theta - \sigma_u) + \frac{\vartheta^2}{2}p(p-1)\sigma_u^p \right) dt + p\vartheta \int_0^t \sigma_u^p dW_u^{(*)}.$$

We obtain

$$\mathbb{E} \sup_{t \in [0, T]} \sigma_t^p \leq \sigma_0^p + \mathbb{E} \sup_{t \in [0, T]} \int_0^t \left| p\sigma_u^{p-1}(\kappa_1 + \kappa_2\sigma_u)(\theta - \sigma_u) + \frac{\vartheta^2}{2}p(p-1)\sigma_u^p \right| dt + p\vartheta \mathbb{E} \left[\sup_{t \in [0, T]} \int_0^t \sigma_u^p dW_u^{(*)} \right].$$

Using Burkholder-Davis-Gundy inequality and Proposition A.1, we establish

$$\mathbb{E} \left[\sup_{t \in [0, T]} \int_0^t \sigma_u^p dW_u^{(*)} \right] \leq C \mathbb{E} \left(\int_0^T \sigma_t^p dt \right)^{1/2} \leq C \left(\int_0^T \mathbb{E}\sigma_t^{2p} dt \right)^{1/2}.$$

A.7 Proof of Theorem 3.3

Proposition A.2. *Le us introduce $G(l) := l - \mu(l)\Delta$. Then, for every $c \in \mathbb{R}$, the equation $G(l) = c$ has a unique solution in $l \in \mathbb{R}$.*

Proof. As $G(l)$ is continuous, $G'(l) > 0$ and $\lim_{l \rightarrow \pm\infty} G(l) = \pm\infty$, result immediately follows. \square

The proof of the Theorem is based on estimate A.3, which can be found in Alfonsi (2013).

Proposition A.3. *Let $p \geq 1$ and assume that*

$$\mathbb{E} \left[\int_0^T \left| \mu'(L_u) \mu(L_u) + \frac{\vartheta^2}{2} \mu''(L_u) \right| du \right]^p + \mathbb{E} \left[\int_0^T \mu'(L_u)^2 du \right]^{p/2} < \infty. \quad (121)$$

Then, there exists a constant $K_p > 0$ such that $(\mathbb{E} \sup_{t \in [0, T]} |\hat{L}_t - L_t|^p)^{1/p} \leq K_p \Delta$.

Instead of (121), we prove slightly stronger estimate (122). The latter follows from the combination of Hölder inequality and Proposition 3.1. We omit straightforward details:

$$\mathbb{E} \sup_{u \in [0, T]} \left| \mu'(L_u) \mu(L_u) + \frac{\vartheta^2}{2} \mu''(L_u) \right|^p + \mathbb{E} \sup_{u \in [0, T]} |\mu'(L_u)|^p < \infty. \quad (122)$$

A.8 Proof to Proposition 3.3

We first present Eq (31) as follows

$$\begin{aligned} dm_t^{(n)} &= (-n\kappa Y_t^n - n\kappa_2 Y_t^{n+1}) dt + c(n) (Y_t^n + 2\theta Y_t^{n-1} + \theta^2 Y_t^{n-2}) dt + \vartheta (Y_t + \theta) Y_t^{n-1} dW_t^{(*)} \\ &= [c(n)\theta^2 Y_t^{n-2} + 2c(n)\theta Y_t^{n-1} + (c(n) - n\kappa) Y_t^n - n\kappa_2 Y_t^{n+1}] dt + \vartheta (Y_t + \theta) m Y_t^{n-1} dW_t^{(*)}. \end{aligned}$$

Thus, the expected moment $\bar{m}_\tau^{(n)}$ solves recursive equation (omitting subscript t)

$$\partial_\tau \bar{m}^{(n)} = c(n)\theta^2 \bar{m}^{(n-2)} + 2c(n)\theta \bar{m}^{(n-1)} + (c(n) - n\kappa) \bar{m}^{(n)} + (2\theta c(n) - n\kappa_2) \bar{m}^{(n+1)}. \quad (123)$$

Using the fact that $\bar{m}^{(0)} = 1$ and $c(1) = 0$ we can present Eq (123) for $n = 0, 1, \dots$ as a matrix equation for infinite-dimensional column vector in Eq (32). Clearly, that under regularity conditions (real part of eigenvectors of $\Lambda^{(0, \infty)}$ negative), we must have $\lim_{k \rightarrow \infty} \partial_\tau \bar{m}^{(k)} = 0$. Thus, to make a finite-dimensional approximation of Eq (32), we fix k^* and assume

$$\partial_\tau \bar{m}^{(k^*+1)} = 0 \Rightarrow \bar{m}^{(k^*+1)} = Y_0^{k^*+1}. \quad (124)$$

Thus, by substituting fixed values for $\bar{m}^{(0)}$ and $\bar{m}^{(k^*+1)}$, we present (32) for finite-dimensional vector of m -th moments, $m = 1, \dots, k^*$, in Eq (33). Solution in Eq (34) is obtained by integration.

A.9 Proof of Lemma 4.1

First we need the following auxiliary results for general SV model dynamics in (41) under MMA measure \mathbb{Q} .

Theorem A.2. *Assume that the volatility process in (41) has a unique strong solution under \mathbb{Q} . Then Z_t is \mathbb{Q} -martingale if and only if $\tilde{\mathbb{Q}}_{exp}(\sigma_t, +\infty) = 0$, where $\tilde{\mathbb{Q}}_{exp}(\sigma_t, \tau) = 0$ is the probability of explosion before T , starting at σ_t , $\tau = T - t$, in the volatility process σ_t under $\tilde{\mathbb{Q}}$: $d\sigma_t = (\mu(\sigma_t) + \beta v(\sigma_t))dt + \vartheta v(\sigma_t) d\tilde{W}_t^{(*)}$, where $\tilde{W}_t^{(*)}$ is a Brownian motion under $\tilde{\mathbb{Q}}$.*

Proof. We refer to Theorem 9.2 in Lewis (2000) and to Sin (1998). \square

Borrowing the notations introduced later in Section 6, we state the theorem that gives the formula for vanilla option prices when price process Z_t is not a proper martingale.

Theorem A.3. We consider the zero-drift price process Z_t and the volatility process σ_t in Eq (41) under the MMA measure $\tilde{\mathbb{Q}}$. We assume that σ_t in (41) has unique strong solution under $\tilde{\mathbb{Q}}$. Then the model values of vanilla call and put options and the forward on underlying S_t are given by

$$\begin{aligned} C(\tau, S, K) &= e^{-\bar{r}(T)} \mathbb{E} [\max\{S_T - K, 0\} | S_t = S] + S e^{\bar{\mu}(T) - \bar{r}(T)} \tilde{\mathbb{Q}}_{exp}(\sigma_t, \tau), \\ P(\tau, S, K) &= e^{-\bar{r}(T)} \mathbb{E} [\max\{K - S_T, 0\} | S_t = S], \\ F(\tau, S, K) &= e^{-\bar{r}(T)} \mathbb{E} [S_T - K | S_t = S] + S e^{\bar{\mu}(T) - \bar{r}(T)} \tilde{\mathbb{Q}}_{exp}(\sigma_t, \tau). \end{aligned} \quad (125)$$

Theorem A.4. We consider the inverse price process R_t and the volatility process σ_t under the inverse measure $\tilde{\mathbb{Q}}$. We assume that σ_t has unique strong solution under $\tilde{\mathbb{Q}}$. Then the model values of inverse call and put options and the forward on underlying S_t are given by

$$\begin{aligned} \tilde{C}(\tau, S, K) &= \tilde{\mathbb{E}} [S_T^{-1} \max\{S_T - K, 0\} | S_t = S], \\ \tilde{P}(\tau, S, K) &= \tilde{\mathbb{E}} [S_T^{-1} \max\{K - S_T, 0\} | S_t = S] + K S_0^{-1} e^{\bar{\mu}(T) - \bar{r}(T)} \tilde{\mathbb{Q}}_{exp}(\sigma_t, \tau), \\ \tilde{F}(\tau, S, K) &= \tilde{\mathbb{E}} [S_T^{-1} (S_T - K) | S_t = S] = 1 - K S_0^{-1} e^{\bar{\mu}(T) - \bar{r}(T)} \tilde{\mathbb{Q}}_{exp}(\sigma_t, \tau). \end{aligned} \quad (126)$$

Proof of Theorems A.3, A.4. We refer to Theorem 9.3 in Lewis (2000). \square

Finally, the proof of Lemma 4.1 follows from (125), (126).

A.10 Proof of Theorem 5.1

First, we provide a version of Feynman-Kac formula in general multidimensional setting, building on results in Heath and Schweizer (2000). Let $T > 0$ be a fixed time horizon and D be a domain in \mathbb{R}^d . We consider Cauchy problem

$$\begin{aligned} \frac{\partial U}{\partial t} + \mathcal{L}U &= 0, \quad (t, x) \in Q, Q = (0, T) \times D, \\ U(T, x) &= \phi(x), \quad x \in D, \end{aligned} \quad (127)$$

where $b_t : D \rightarrow \mathbb{R}^d$, $a_t : D \rightarrow \mathbb{R}^{d \times d}$ are continuous functions and operator \mathcal{L} is defined by

$$\mathcal{L}U = \sum_{i=1}^d b_t^i(x) \frac{\partial U}{\partial x_i}(t, x) + \frac{1}{2} \sum_{i,k=1}^d a_t^{ik}(x) \frac{\partial^2 U}{\partial x_i \partial x_k}(t, x). \quad (128)$$

We assume that matrix (a_t^{ij}) is non-negative definite for every t . Under certain restrictions on the coefficients of operator \mathcal{L} and growth conditions on ϕ , it is possible to represent the solution of (127) by means of conditional expectation known as a Feynman–Kac formula. However, standard results require uniform ellipticity of the operator \mathcal{L} , see Friedman (1975), which does not satisfy in our case, as we see later. Consequently, the problem (127) becomes degenerate parabolic one. We consider the multi-dimensional SDE

$$dX_s = b_s(X_s)ds + \sigma_s(X_s)dW_s, \quad X_t = x \in D, \quad (129)$$

where $W = (W^{(1)}, \dots, W^{(d)})^\top$ is d -dimensional Brownian motion and $\sigma_t(x) = (\sigma_t^{ij}(x))$ denotes square root of matrix $a_t(x)$: $a_t^{ik}(x) = (\sigma_t(x)\sigma_t(x)^\top)^{ik}$. We assume that SDE (129) admits unique strong solution and define $U^* : [0, T] \times D \rightarrow [0, +\infty]$ by $U^*(\tau, x) = \mathbb{E}[\phi(X_T) | X_t = x]$ which is well-defined in $[0, +\infty]$ if X does not explode or leave domain D before T . We give sufficient conditions to ensure that U^* solves the problem (127).

Theorem A.5. Suppose that following conditions hold

1. Solution X of (129) neither explodes nor leaves D before T

$$\mathbb{P} \left(\sup_{t \leq s \leq T} |X_s| < \infty \right) = \mathbb{P}(X_s \in D, \forall s \in [t, T]) = 1.$$

2. $\phi(x)$ is bounded in D .

Let $U \in C(\overline{Q}) \cap C^2(Q)$ be the solution of problem (127). Then $U(t, x) = U^*(t, x)$ for any $(t, x) \in \overline{Q}$.

Proof. Consider sequence of bounded domains $\{D_n\}_{n=1}^\infty$ contained in D such that $\bigcup_{n=1}^\infty D_n = D$ and $D_n \subseteq \{x \in \mathbb{R}^d : \|x\| < n\}$. We fix $x \in D$ and find n such that $x \in D_n$. Let $\eta = \inf\{s \geq t : X_s \notin D\}$, $\eta_n = \inf\{s \geq t : X_s \notin D_n\}$ denote exits time from domains D and D_n . By Itô's formula:

$$u(\eta_n \wedge T, X_{\eta_n \wedge T}) = u(x) + \int_t^{\eta_n \wedge T} \left[\frac{\partial U}{\partial s} - \mathcal{L}U(s, X_s) \right] ds + \int_t^{\eta_n \wedge T} \frac{\partial U}{\partial x_i} \sigma_{ij}(X_s) dW_s^{(j)}$$

As domain D_n is bounded and $U \in C^2(Q)$, we have

$$\mathbb{E}^{t,x} \left[\int_t^{\eta_n \wedge T} \frac{\partial U}{\partial x_i} \sigma_{ij}(X_s) dW_s^{(j)} \right] = 0 \implies u(x) = \mathbb{E}^{t,x} [u(\eta_n \wedge T, X_{\eta_n \wedge T})] \quad (130)$$

$$\text{We will show that } \mathbb{P}^{t,x} [\tau_n \leq T] \leq c_1(1 + \|x\|^2)n^{-2}. \quad (131)$$

Using Markov inequality and estimate from Karatzas and Shreve (1991), p. 306, we have

$$\begin{aligned} \mathbb{P}^{t,x} [\tau_n \leq T] &\leq \mathbb{P}^{t,x} \left[\sup_{s \in [t,T]} \|X_s\| \geq n \right] \leq \mathbb{E}^{t,x} \left[\sup_{s \in [t,T]} |X_s|^2 \right] n^{-2} \\ \mathbb{E}^{t,x} \left[\sup_{s \in [t,T]} |X_s|^2 \right] &\leq c(1 + \|x\|^2). \end{aligned}$$

Inequality (131) then follows immediately. Thus, $\lim_{n \rightarrow +\infty} u(\eta_n \wedge T, X_{\eta_n \wedge T}) = g(X_T)$ a.s. It implies that $u(t, x)$ is bounded by the maximum principle. Finally, by the dominated convergence theorem:

$$\lim_{n \rightarrow +\infty} \mathbb{E}[u(\eta_n \wedge T, X_{\eta_n \wedge T})] = \mathbb{E}[g(X_T)]. \quad (132)$$

Combining (130) and (132) concluded the proof. \square

Now using the diffusive operators in the valuation PDE (53), we obtain that matrix a in Eq (128) equals

$$a = \begin{pmatrix} (Y_t + \theta)^2 & \beta(Y_t + \theta)^2 & 0 \\ \beta(Y_t + \theta)^2 & \vartheta^2(Y_t + \theta)^2 & 0 \\ 0 & 0 & 0 \end{pmatrix} \quad (133)$$

We can find that its eigenvalues equal

$$\lambda_1 = 0, \quad \lambda_{2,3} = \left(1 + \vartheta^2 \pm \sqrt{1 + 4\beta^2 - 2\vartheta^2 + \vartheta^4} \right) (Y_t + \theta)^2.$$

As $\beta < \vartheta$, we observe that $0 = \lambda_1 < \lambda_2 < \lambda_3$, hence matrix a is non-negative definite and its smallest eigenvalue is always zero.

We now set the domain D of state variables $\{X_t, Y_t, I_t\}$ in PDE (53) by $D = \mathbb{R} \times (-\theta, +\infty) \times \mathbb{R}_+$. As we showed in Theorem (3.1), under the MMA measure (50) and the inverse measure (51), the boundary points $\{0, +\infty\}$ are unattainable for the volatility process σ , hence solution $\{X_t, Y_t, I_t\}$ neither explodes nor leaves D before T . Thus, condition 1 of Theorem A.5 is satisfied. As boundedness condition 2 is satisfied by construction, the statement of Theorem (5.1) follows from Theorem A.5.

A.11 Proof of Theorem 5.2

As Z_T is \mathbb{Q} -martingale, the result immediately follows from Jensen's inequality, as the function $g(y) := y^{|\Phi_R|-1}$ is convex for $|\Phi_R| \in (0, 1)$. Result for the inverse measure follows analogously.

A.12 Proof of Theorem 5.3

We denote $K_t = e^{It}$ which satisfied SDE $dK_t = K_t dI_t = K_t \sigma_t^2 dt$ and set $p = -\Psi_R$. Feynman-Kac formula allows to recast the solution $U(\tau, \sigma, K) = \mathbb{E}(K_T^p | K_t = K, \sigma_t = \sigma)$ as the solution of the Cauchy problem

$$-\frac{\partial U}{\partial \tau} + \mathcal{L}^{(\sigma, K)} U = 0, \quad U(0, \sigma, K) = K, \quad (134)$$

where operator $\mathcal{L}^{(\sigma, K)}$ is defined by $\mathcal{L}^{(\sigma, K)} = (\kappa_1 + \kappa_2 \sigma)(\theta - \sigma) \frac{\partial}{\partial \sigma} + \frac{1}{2} \vartheta^2 \sigma^2 \frac{\partial^2}{\partial \sigma^2} + K \sigma^2 \frac{\partial}{\partial K}$. We build a supersolution $\bar{U}(\tau, \sigma, K)$ to (134) using ansatz $\bar{U} = K^p u(\tau, \sigma)$, $u(\tau, \sigma) = e^{a\sigma + b\tau}$. Inserting \bar{U} into (134), we obtain

$$-\frac{\partial \bar{U}}{\partial \tau} + \mathcal{L}^{(\sigma, K)} \bar{U} = -u K^p \left[-b + \kappa_1 \theta a + (\kappa_2 \theta - \kappa_1) a \sigma + \left(\frac{1}{2} \vartheta^2 a^2 + p - \kappa_2 a \right) \sigma^2 \right]. \quad (135)$$

We show there exists $a \geq 0$ such that

$$\lim_{\sigma \uparrow +\infty} -b + \kappa_1 \theta a + (\kappa_2 \theta - \kappa_1) a \sigma + \left(\frac{1}{2} \vartheta^2 a^2 - \kappa_2 a + p \right) \sigma^2 < +\infty. \quad (136)$$

We notice that inequality (136) holds if there exist $a > 0$ such that $\frac{1}{2} \vartheta^2 a^2 - \kappa_2 a + p < 0$. As latter defines a parabola in a , we can always find required positive a , if $\kappa_2 > \vartheta \sqrt{2p} = \vartheta \sqrt{-2\Psi_R}$.

A.13 Proof of Theorem 5.4

We set $c = -\Phi_R$ and consider

$$U(\tau, Y; c; p) := \begin{cases} \mathbb{E}[e^{cY_\tau} | Y_0 = Y], & p = 1 \\ \tilde{\mathbb{E}}[e^{cY_\tau} | Y_0 = Y], & p = -1. \end{cases} \quad (137)$$

Using Feynman-Kac formula we can rewrite $U(\tau, Y; c; p)$ as the solution of the Cauchy problem

$$-\frac{\partial U}{\partial \tau} + \mathcal{L}^{(Y; p)} U = 0, \quad U(0, Y; c; p) = e^{cY} \quad (138)$$

where operator $\mathcal{L}^{(Y; p)}$ is defined by (54). We build a supersolution $\bar{U}(\tau, Y; c; p)$ to (138) using ansatz $\bar{U} = e^{aY + b\tau}$, $a \geq c$, $b \geq 0$. Inserting \bar{U} into (138), we have

$$-\frac{\partial \bar{U}}{\partial \tau} + \mathcal{L}^{(Y; p)} \bar{U} = -\bar{U} \left[b - \left(\lambda^{(p)} - \kappa^{(p)} Y - \kappa_2^{(p)} Y^2 \right) b - \frac{1}{2} \vartheta^2 (Y + \theta)^2 b^2 \right] \quad (139)$$

where coefficients are defined in (54). We show there exists $a \geq c$ such that

$$\lim_{Y \uparrow +\infty} b - \left(\lambda^{(p)} - \kappa^{(p)} Y - \kappa_2^{(p)} Y^2 \right) a - \frac{1}{2} \vartheta^2 (Y + \theta)^2 a^2 < \infty.$$

We notice that last inequality is satisfied if there exist $a \geq c > 0$ such that $-\kappa_2^{(p)} a + \frac{1}{2} \vartheta^2 a^2 < 0$. Dividing by $a > 0$ we conclude that it is satisfied if $\kappa_2^{(p)} > \frac{\vartheta^2}{2} c$. Rewriting the last condition in terms of κ_2 , β using (54), we arrive at (57).

A.14 Proof of Proposition 5.3

The formal solution for the remainder term $R^{[2]}$ solving Problem (71) is obtained by applying the Feynman-Kac formula and is given by

$$R^{[2]}(\tau, X, I, Y; \Phi, \Psi) = \int_0^\tau \int_{-\infty}^\infty \int_0^\infty \int_{-\theta}^\infty \left[F^{[2]}(\tau - t, Y') E^{[2]}(\tau - t, X', I', Y'; \Phi, \Psi) \right] \times P(t, X, I, Y; X', I', Y') dt dX' dI' dY', \quad (140)$$

where $P(t, X, I, Y; X', I', Y')$ is the joint PDF of $X' = X(t)$, $I' = I(t)$ and $Y' = Y(t)$ conditional on X , I , and Y . The joint PDF P solves the PDE (53), subject to initial condition $P(0, X, I, Y; X', I', Y') = \delta(X' - X)\delta(I' - I)\delta(Y' - Y)$.

Using Eq (140), we obtain the following estimate

$$\begin{aligned}
|R^{[2]}(\tau, Y; \Phi, \Psi)| &\leq \int_0^\tau \int_{-\infty}^\infty \int_0^\infty \int_{-\theta}^\infty |E^{[2]}(\tau - t, X', I', Y'; \Phi, \Psi)| \\
&\quad \times |F^{[2]}(\tau - t, Y'; A^{(1)}, A^{(2)}, A^{(3)}, A^{(4)})P(t, X, I, Y; X', I', Y')| dt dX' dI' dY' \\
&\leq \int_0^\tau \int_{-\infty}^\infty \int_0^\infty \int_{-\theta}^\infty |F^{[2]}(\tau - t, Y')P(t, X, I, Y; X', I', Y')| dt dX' dI' dY' \\
&= \int_0^\tau \int_{-\infty}^\infty |F^{[2]}(\tau - t, Y')P(t, \cdot, \cdot, Y; \cdot, \cdot, Y')| dt dY'.
\end{aligned} \tag{141}$$

In the above, we used the bound on the MGF $|E^{[2]}(\tau - t, X', I', Y'; \Phi, \Psi)| \leq 1$ and we integrated out the log-return X and the QV I .

Next we substitute the polynomial function $F^{[2]}$ in Eq (72). We use the continuity of functions $A^{(k)}$, $k = 1, 2, 3, 4$, and apply the first mean value theorem for definite integrals to estimate the time integral. Finally, we approximate the expected value of the powers of the mean-adjusted volatility by its steady-state n -th order central moments $M_\sigma^{(n)}$ specified in Eq (66).

A.15 Proofs of Consistency of Moment for second-order Affine Expansion

We first state a lemma relating central moments of the random variable to derivatives of MGF.

Lemma A.2. *The MGF defined by the following equation*

$$G(\Phi) = \mathbb{E}[e^{-\Phi Z}] \tag{142}$$

where Z is a random variable with finite MGF has the following properties

$$\begin{aligned}
G(0) &= 1 \\
\partial_\Phi G(\Phi) \Big|_{\Phi=0} &\equiv G_\Phi(0) = -\mathbb{E}[Z], \\
\partial_\Phi^2 G(\Phi) \Big|_{\Phi=0} &\equiv G_{\Phi\Phi}(0) = \mathbb{E}[Z^2].
\end{aligned} \tag{143}$$

Corollary A.1. *Given that MGF assumes an exponential-affine form*

$$G(\Phi) = e^{f(\Phi)}, \tag{144}$$

with $f(0) = 0$, we have

$$f_\Phi(0) = -\mathbb{E}[Z], \quad f_{\Phi\Phi}(0) = \mathbb{Var}[Z]. \tag{145}$$

A.15.1 Proof of Proposition 5.4

We set $\Phi = \Psi = 0$ in second-order expansion in 5.4 and suppress arguments X, I, Φ, Ψ, p for brevity. We note that it is sufficient to prove that second-order leading term $E^{[2]}(\tau, Y; \Theta)$ is consistent with expected value and variance.

To prove consistency for the expected value, we consider $R^{[2]}(\tau, Y; \Theta)$ in (71). Differentiating it with respect to parameter Θ , we see that remainder term $R_\Theta^{[2]}$ solves following problem

$$-R_{\Theta, \tau}^{[2]} + \mathcal{L}^{(Y)} R_\Theta^{[2]} = -\sum_{k=5}^8 Y^k \left[C_\Theta^{(k)}(\tau; \Theta) E^{[2]} + C^{(k)}(\tau; \Theta) E_\Theta^{[2]} \right], \tag{146}$$

with $R_\Theta^{[2]}(0, Y; \Theta) = 0$ and where $C^{(k)}(\tau; \Theta)$ are given in (72). It We note that $A^{(k)}(\tau; \Theta)$ vanish at $\Theta = 0$, i.e.

$$A^{(k)}(\tau; \Theta) \Big|_{\Theta=0} = 0. \tag{147}$$

Calculating $C_\Theta^{(k)}(\tau; \Theta) \Big|_\Theta$ and taking into account conditions (147) at $\Theta = 0$, we find that

$$C_\Theta^{(k)}(\tau; \Theta) \Big|_{\Theta=0} = \begin{cases} -4\kappa_2 A_\Theta^{(4)}(\tau; \Theta) \Big|_{\Theta=0}, & k = 5, \\ 0, & k \geq 6 \end{cases} \tag{148}$$

Now, due to condition

$$C^{(k)}(\tau; \Theta) \Big|_{\Theta=0} \equiv 0 \quad (149)$$

we can simplify problem (146) at $\Theta = 0$ as follows

$$-R_{\Theta,\tau}^{[2]} + \mathcal{L}^{(Y)} R_{\Theta}^{[2]} = 4\kappa_2 A_{\Theta}^{(4)} Y^5, \quad R_{\Theta}^{[2]}(0, Y; \Theta) = 0, \quad (150)$$

As seen, $R_{\Theta}^{[2]}(\tau, Y; \Theta) \Big|_{\Theta=0} \equiv 0$ when $\kappa_2 = 0$. Hence, second order decomposition $E^{[2]}(\tau, Y; \Theta)$ is consistent with expected value of Y_t for $\kappa_2 = 0$.

To prove the consistency for variance, we first differentiate (70) with respect to parameter Θ and see that $A_{\Theta}^{(k)}(\tau, \Theta)$ solve the system of ODEs (151) at $\Theta = 0$ as a function of τ

$$\begin{aligned} A_{\Theta,\tau}^{(0)} &= \theta^2 \vartheta^2 A_{\Theta}^{(2)} + \lambda(p) A_{\Theta}^{(1)}, \\ A_{\Theta,\tau}^{(1)} &= -\kappa A_{\Theta}^{(1)} + 2(\theta \vartheta^2 + \lambda(p)) A_{\Theta}^{(2)} + 3\theta^2 \vartheta^2 A_{\Theta}^{(3)}, \\ A_{\Theta,\tau}^{(2)} &= -\kappa_2 A_{\Theta}^{(1)} + (\vartheta^2 - 2\kappa) A_{\Theta}^{(2)} + 6\theta \vartheta^2 A_{\Theta}^{(3)} + 3\lambda(p) A_{\Theta}^{(3)} + 6\theta A_{\Theta}^{(4)}, \\ A_{\Theta,\tau}^{(3)} &= -2\kappa_2 A_{\Theta}^{(2)} + 3(\vartheta^2 - \kappa) A_{\Theta}^{(4)} + 12\theta \vartheta^2 A_{\Theta}^{(4)} + 4\lambda(p) A_{\Theta}^{(4)}, \\ A_{\Theta,\tau}^{(4)} &= -3\kappa_2 A_{\Theta}^{(3)} + 2(3\vartheta^2 - 2\kappa) A_{\Theta}^{(4)}, \end{aligned} \quad (151)$$

with boundary condition:

$$A_{\Theta}^{(k)}(\tau; \Theta) \Big|_{\Theta=0} = \begin{cases} -1, & k = 1, \\ 0, & k \neq 1. \end{cases}$$

We can verify that last two functions in solution of (151) are zero

$$A^{(3)}(\tau; \Theta) \equiv A^{(4)}(\tau; \Theta) \equiv 0. \quad (152)$$

Now, taking the second derivative wrt parameter Θ in (71), we obtain for $R_{\Theta\Theta}^{[2]}$

$$-R_{\Theta\Theta,\tau}^{[2]} + \mathcal{L}^{(Y)} R_{\Theta\Theta}^{[2]} = -\sum_{k=5}^8 \left\{ Y^k \left[C_{\Theta\Theta}^{(k)}(\tau; \Theta) E^{[2]} + 2C_{\Theta}^{(k)}(\tau; \Theta) E_{\Theta}^{[2]} + C^{(k)}(\tau; \Theta) E_{\Theta\Theta}^{[2]} \right] \right\}, \quad (153)$$

$$R_{\Theta\Theta}^{[2]}(0, Y; \Theta) = 0.$$

Taking second derivative of $C^{(k)}(\tau; \Theta)$ in (72) with respect to parameter Θ , and taking into account boundary conditions (147) and (152) at $\Theta = 0$, we find that

$$C_{\Theta\Theta}^{(k)}(\tau; \Theta) \Big|_{\Theta=0} = \begin{cases} -4\kappa_2 A_{\Theta}^{(4)}(\tau; \Theta) \Big|_{\Theta=0}, & k = 5, \\ 0, & k \geq 6. \end{cases} \quad (154)$$

We note that following straightforward relationships are valid

$$E^{[2]}(\tau; \Theta) \Big|_{\Theta=0} = 1, \quad E_{\Theta}^{[2]}(\tau; \Theta) \Big|_{\Theta=0} = -Y. \quad (155)$$

Combining (154), (148), (149) and (155), we are able to simplify the problem (150) at $\Theta = 0$

$$-R_{\Theta\Theta,\tau}^{[2]} + \mathcal{L}^{(Y)} R_{\Theta\Theta}^{[2]} = 4\kappa_2 \left(Y^5 A_{\Theta\Theta}^{(4)} - 2Y^6 A_{\Theta}^{(4)} \right), \quad R_{\Theta\Theta}^{[2]}(0, Y; \Theta) = 0. \quad (156)$$

As a result, when $\kappa_2 = 0$, $R_{\Theta\Theta}^{[2]}(\tau, Y; \Theta) \Big|_{\Theta=0} \equiv 0$, hence $E^{[2]}(\tau; \Theta)$ is consistent with variance of Y_t .

A.15.2 Proof of Proposition 5.5

Similarly to the proof of Theorem 5.4 we set $\Theta = \Psi = 0$ in second-order expansion and omit remainig arguments for brevity. We note that it is sufficient to prove that second-order leading term $E^{[2]}(\tau, X; \Phi)$ is consistent with expected value and variance. To prove consistency for the

expected value, we consider the remainder term $R^{[2]}(\tau, X; \Phi)$ in (71). Differentiating it with respect to parameter Φ , we see that $R_{\Phi}^{[2]}$ solves following problem

$$\begin{aligned} -R_{\Phi,\tau}^{[2]} + \mathcal{L}^{(Y)} R_{\Phi}^{[2]} &= -\frac{\partial}{\partial \Phi} \left[\sum_{k=5}^8 C^{(k)}(\tau; \Phi) E^{[2]} Y^k \right] = \\ &= -\sum_{k=5}^8 Y^k \left[C_{\Phi}^{(k)}(\tau; \Phi) E^{[2]} + C^{(k)}(\tau; \Phi) E_{\Phi}^{[2]} \right], \quad R_{\Phi}^{[2]}(0, X; \Phi) = 0, \end{aligned} \quad (157)$$

where $C^{(k)}(\tau; \Phi)$ are given by (72). It is important to note that $A^{(k)}(\tau; \Phi)$ vanish at $\Phi = 0$:

$$A^{(k)}(\tau; \Phi) \Big|_{\Phi=0} = 0. \quad (158)$$

Differentiating $C^{(k)}(\tau; \Phi)$ with respect to parameter Φ and taking into account conditions (158) at $\Phi = 0$, we find that

$$C_{\Phi}^{(k)}(\tau; \Phi) \Big|_{\Phi=0} = \begin{cases} -4\kappa_2 A_{\Phi}^{(4)}(\tau; \Phi) \Big|_{\Phi=0}, & k = 5, \\ 0, & k \geq 6 \end{cases} \quad (159)$$

Now, due to condition:

$$C^{(k)}(\tau; \Phi) \Big|_{\Phi=0} \equiv 0, \quad (160)$$

we can simplify problem (157) at $\Phi = 0$ as follows

$$-R_{\Phi,\tau}^{[2]} + \mathcal{L}^{(Y)} R_{\Phi}^{[2]} = 4\kappa_2 A_{\Phi}^{(4)} Y^5, \quad R_{\Phi}^{[2]}(0, X; \Phi) = 0. \quad (161)$$

As seen, $R_{\Phi}^{[2]}(\tau, X; \Phi) \Big|_{\Phi=0} \equiv 0$ when $\kappa_2 = 0$. Hence, the second-order expansion term $E^{[2]}(\tau, X; \Phi)$ is consistent with the expected value of X_{τ} for $\kappa_2 = 0$.

To prove the consistency for variance, we first differentiate (70) with respect to parameter Φ and see that $A_{\Phi}^{(k)}(\tau, \Phi)$ solve the system of ODEs (162) at $\Phi = 0$ as a function of τ

$$\begin{aligned} A_{\Phi,\tau}^{(0)} &= \theta^2 \vartheta^2 A_{\Phi}^{(2)} + \lambda(p) A_{\Phi}^{(1)} + \frac{1}{2} \theta^2, \\ A_{\Phi,\tau}^{(1)} &= -\kappa A_{\Phi}^{(1)} + 2(\theta \vartheta^2 + \lambda(p)) A_{\Phi}^{(2)} + 3\theta^2 \vartheta^2 A_{\Phi}^{(3)} + \theta, \\ A_{\Phi,\tau}^{(2)} &= -\kappa_2 A_{\Phi}^{(1)} + (\vartheta^2 - 2\kappa) A_{\Phi}^{(2)} + 6\theta \vartheta^2 A_{\Phi}^{(3)} + 3\lambda(p) A_{\Phi}^{(3)} + 6\theta A_{\Phi}^{(4)} + \frac{1}{2}, \\ A_{\Phi,\tau}^{(3)} &= -2\kappa_2 A_{\Phi}^{(2)} + 3(\vartheta^2 - \kappa) A_{\Phi}^{(4)} + 12\theta \vartheta^2 A_{\Phi}^{(4)} + 4\lambda(p) A_{\Phi}^{(4)}, \\ A_{\Phi,\tau}^{(4)} &= -3\kappa_2 A_{\Phi}^{(3)} + 2(3\vartheta^2 - 2\kappa) A_{\Phi}^{(4)}, \end{aligned} \quad (162)$$

with boundary condition:

$$A_{\Phi}^{(k)}(\tau; \Phi) \Big|_{\Phi=0} = \begin{cases} -1, & k = 1, \\ 0, & k \neq 1. \end{cases} \quad (163)$$

We can verify that last two functions in solution of (162) are zero

$$A^{(3)}(\tau; \Phi) \equiv A^{(4)}(\tau; \Phi) \equiv 0. \quad (164)$$

Now, taking the second derivative in (71) wrt Φ , we obtain for $R_{\Phi\Phi}^{[2]}$

$$\begin{aligned} -R_{\Phi\Phi,\tau}^{[2]} + \mathcal{L}^{(Y)} R_{\Phi\Phi}^{[2]} &= -\frac{\partial^2}{\partial \Phi^2} \left[\sum_{k=5}^8 C^{(k)}(\tau; \Phi) E^{[2]} Y^k \right] = \\ &= -\sum_{k=5}^8 \left\{ Y^k \left[C_{\Phi\Phi}^{(k)}(\tau; \Phi) E^{[2]} + 2C_{\Phi}^{(k)}(\tau; \Phi) E_{\Phi}^{[2]} + C^{(k)}(\tau; \Phi) E_{\Phi\Phi}^{[2]} \right] \right\}, \\ R_{\Phi\Phi}^{[2]}(0, Y; \Phi) &= 0. \end{aligned} \quad (165)$$

Taking the second derivative of $C^{(k)}(\tau; \Phi)$ in (72) wrt Φ , and taking into account boundary conditions (158) and (164) at $\Phi = 0$, we find that

$$C_{\Phi\Phi}^{(k)}(\tau; \Phi)\Big|_{\Phi=0} = \begin{cases} -4\kappa_2 A_{\Phi}^{(4)}(\tau; \Phi)\Big|_{\Phi=0}, & k = 5, \\ 0, & k \geq 6 \end{cases} \quad (166)$$

We note that following straightforward relationships are valid:

$$E^{[2]}(\tau; \Phi)\Big|_{\Phi=0} = 1, \quad E_{\Phi}^{[2]}(\tau; \Phi)\Big|_{\Phi=0} = -Y. \quad (167)$$

Combining conditions (166), (159), (160) as well as (167), we are able to simplify the problem (161) at $\Phi = 0$ as follows

$$-R_{\Phi\Phi,\tau}^{[2]} + \mathcal{L}^{(Y)} R_{\Phi\Phi}^{[2]} = 4\kappa_2 \left(Y^5 A_{\Phi\Phi}^{(4)} - 2Y^6 A_{\Phi}^{(4)} \right), \quad R_{\Phi\Phi}^{[2]}(0, Y; \Phi) = 0. \quad (168)$$

Thus, when $\kappa_2 = 0$, $R_{\Phi\Phi}^{[2]}(\tau, Y; \Phi)\Big|_{\Phi=0} \equiv 0$, i.e. $E^{[2]}(\tau, Y; \Phi)$ is consistent with variance of X_t .

A.16 Proof of Theorem 5.7

Consider following system of d nonlinear ODEs

$$\partial_{\tau} A_i(\tau; \Gamma) = A(\tau; \Gamma)^{\top} M_i A(\tau; \Gamma) + L_i^{\top} A(\tau; \Gamma) + H_i, \quad A_i(0, u) = A_{i,0}, \quad (169)$$

for $i = 1, \dots, d$. We assume that $\Gamma \in \mathbb{C}^3$ and each matrix M_i is symmetric real-valued, whereas vectors L_i and H_i are allowed to be complex-valued. Hence solutions $A_i(\tau; \Gamma)$, $i = 1, \dots, d$ are complex-valued functions.

It is well-known that complex-valued solution $A(\tau; \Gamma)$ is defined on maximal interval of existence $[0, \tau_+(\Gamma; A))$ such that either $\tau_+(\Gamma; A) = +\infty$ or $\tau_+(\Gamma; A) < +\infty$ and $\|A(\tau; \Gamma)\| \rightarrow +\infty$ as $\tau \uparrow \tau_+(\Gamma; A)$.

We will combine d non-linear ODEs in (169) into single (non-linear) vector ODE

$$\partial_{\tau} A(\tau; \Gamma) = M(A(\tau; \Gamma)) + L A(\tau; \Gamma) + H, \quad A(0, u) = A_0, \quad (170)$$

where $M : \mathbb{R}^d \rightarrow \mathbb{R}^d$ is a vector-valued function of argument $A \in \mathbb{R}^d$. For convenience, we denote the right-hand side of (170) as follows

$$R(A) := M(A) + L A + H. \quad (171)$$

Lemma A.3. *There exists function g which is finite and non-negative such that for all $z \in \mathbb{C}^d$*

$$\Re \langle \bar{z}, R(z) \rangle \leq g(\Re(z)) (1 + \|z\|^2). \quad (172)$$

Proof. Obtained following Keller-Ressel and Mayerhofer (2015). \square

Lemma A.4. *There exist function g which is finite and non-negative such that*

$$\|A(\tau; \Gamma)\|^2 \leq \|A_0\|^2 + \|A_0\|^2 \int_0^t h(s) e^{\int_0^s h(r) dr} ds, \quad h(s) = g(\Re(A(\tau; \Gamma))) \quad (173)$$

Proof. The proof is essentially contained in Keller-Ressel and Mayerhofer (2015) and based on the application of Gronwall's inequality. \square

Lemma A.5. *Assume that following conditions are satisfied:*

1. $H_I = H_I(u) = (0, \dots, 0)^{\top} \in \mathbb{R}^d$ when Γ is a real vector;
2. $L_I = L_I(u)$ is zero $d \times d$ matrix when Γ is a real vector;
3. zero initial condition $A(0, \Gamma) = (0, \dots, 0)^{\top} \in \mathbb{R}^d$.

Then solution $A(\tau; \Gamma)$ of the system (170) remain real for real $\Gamma \in \mathbb{R}^d$.

Proof. The proof is available upon request. \square

We now consider the problem of continuity of solutions of quadratic differential systems arising in option valuation problem. It is important to highlight that linear $L(p)$ and free terms $H(p)$ satisfy assumptions of the Lemma (A.5) when we set $p = 1$ and restrict $\Re\Phi = -\frac{1}{2}$, $\Phi = \Psi = 0$ for pricing vanilla options under MMA measure. Same for the inverse options when we set $p = -1$ and restrict $\Re\Phi = \frac{1}{2}$, $\Phi = \Psi = 0$. We omit straightforward calculations.

Now, slightly abusing the notations, we use $\tau_+(\Phi; A)$ and $\tau_+(\Re\Phi; A_R)$ to denote blow-up times $\tau_+(\Gamma; A)$ and $\tau_+(\Re\Gamma; A_R)$ when $\Gamma = (\Phi, \Psi = 0, \Theta = 0)$ and $\Re\Gamma = (\Re\Phi, \Psi = 0, \Theta = 0)$, respectively.

Proof to Theorem 5.7. We assume first that $\Phi \in \mathbb{R}$. We denote

$$D(\tau) := \{\Phi \in \mathbb{R} : \tau < \tau_+(\Phi; A)\}, \quad M(\tau) := \{\Phi \in \mathbb{R} : G(\tau; X, I, Y; \Phi) < \infty\}.$$

We will argue by contradiction. Assume that solution $A(\tau; \Phi)$ blows up before τ_0 , i.e.

$$\tau_+(\Gamma; A) < \tau_0 \tag{174}$$

We set $\alpha^* := \sup\{\alpha \geq 0 : \alpha\Gamma \in D(\tau)\}$. Then assumption (174) implies that $\alpha^* < 1$. On the one hand,

$$G(\tau; X, I, Y; \alpha\Phi, \Psi = 0, \Theta = 0) \leq G(\tau; X, I, Y; \alpha\Phi, \Psi = 0, \Theta = 0)^\alpha < \infty \tag{175}$$

for all $\alpha < \alpha^* < 1$ due to Jensen inequality. On the other hand

$$\begin{aligned} G(\tau; X, I, Y; \alpha\Phi, \Psi = 0, \Theta = 0) &= \exp \left\{ -\alpha\Phi X + \sum_{k=0}^{2n} A_k(\tau; \alpha\Phi, \Psi = 0, \Theta = 0) Y^k \right\} \\ &\quad + R^{[2]}(\tau; X, I, Y; \alpha\Phi, \Psi = 0, \Theta = 0) \end{aligned}$$

Thus we obtain

$$\begin{aligned} \lim_{\alpha \uparrow \alpha^*} G(\tau; X, I, Y; \alpha\Phi, \Psi = 0, \Theta = 0) &= \lim_{\alpha \uparrow \alpha^*} \left[\exp \left\{ -\alpha\Phi X + \sum_{k=0}^{2n} A_k(\tau; \alpha\Phi, \Psi = 0, \Theta = 0) Y^k \right\} \right. \\ &\quad \left. + R^{[2]}(\tau; X, I, Y; \alpha\Phi, \Psi = 0, \Theta = 0) \right] = +\infty \end{aligned} \tag{176}$$

using assumptions 2 and 3. Comparing (175) and (176) we get a contradiction, so

$$\tau_+(\Phi; A) \geq \tau_0 \tag{177}$$

Now, we let $\Phi \in \mathbb{C}$ be complex. Due to assumption 5.7 and Lemma A.4, we have $\tau_+(\Phi; A) \geq \tau_+(\Phi; A_R) \geq \tau(\Re\Phi; A)$. Repeating the first part of the proof for $\Re\Phi$, leads to (177), i.e. $\tau_+(\Re\Phi; A) \geq \tau_0$. Hence, solution $A(\tau; \Phi, \Psi = 0, \Theta = 0)$ must remain continuous on $[0, \tau_0]$. \square

A.17 Proof of Proposition 6.1

Using the affine approximation, the density of X_τ is computed by the Fourier inversion

$$\begin{aligned} G(\tau, X, Y; X'; p = 1) &= \frac{1}{\pi} \Re \left[\int_0^\infty \exp \{ \Phi(X' - X) \} E^{[m]}(\tau, Y; \Phi, \Psi = 0; p = 1) d\Phi \right] \\ E^{[m]}(\tau, Y; \Phi, \Psi = 0; p = 1) &= \exp \left\{ \sum_{k=0}^{2m} A^{(k)}(\tau; \Phi, \Psi = 0; p = 1) Y^k \right\}. \end{aligned} \tag{178}$$

We have

$$U(\tau, X) = e^{-\bar{r}(T)} \Re \left[\int_{-\infty}^\infty \min \left\{ e^{\bar{\mu}(T) + X'}, K \right\} \left[\frac{1}{\pi} \int_0^\infty e^{\Phi(X' - X)} E^{[m]}(\tau, Y; \Phi, \Psi = 0; p = 1) d\Phi \right] dX' \right]$$

Assuming that the inner integrals are finite we exchange the integration order to obtain

$$U(\tau, X) = \frac{1}{\pi} e^{-\bar{r}(T)} \Re \left[\int_0^\infty \hat{u}(\Phi) E^{[m]}(\tau, Y; \Phi, \Psi = 0; p = 1) d\Phi \right], \tag{179}$$

where $\hat{u}(\Phi)$ is the transformed payoff function

$$\begin{aligned}\hat{u}(\Phi) &= e^{-\Phi X} \int_{-\infty}^{\infty} e^{\Phi X'} \min \left\{e^{X'+\bar{\mu}(T)}, K\right\} d X' \\ &= e^{-\Phi X} \left(e^{\bar{\mu}(T)} \frac{e^{(\Phi+1)k^*}}{\Phi+1} - e^{k^*+\bar{\mu}(T)} \frac{1}{\Phi} e^{\Phi k^*} \right) = e^{-\Phi X} \left(-e^{\bar{\mu}(T)} e^{(\Phi+1)k^*} \frac{1}{(\Phi+1)\Phi} \right) \\ &= -K e^{-\Phi(\ln(S/K)+\bar{\mu}(T))} \frac{1}{(\Phi+1)\Phi} = -K e^{-\Phi X^*} \frac{1}{(\Phi+1)\Phi}\end{aligned}\quad (180)$$

where $X^* = \ln(S/K) + \bar{\mu}(T)$ is the log-moneyness, $k^* = \ln K - \bar{\mu}(T)$ with the first integral being finite for $\Re[\Phi] > -1$ and the second integral being finite for $\Re[\Phi] < 0$. The integral (180) is finite for $-1 < \Re[\Phi] < 0$. Setting $\Phi = iy - 1/2$, we derive (80)

$$\hat{u}(\Phi = iy - 1/2) = -K e^{-(iy-1/2)x^*} \frac{1}{(1/2+iy)(-1/2+iy)} = K e^{-(iy-1/2)X^*} \frac{1}{y^2 + 1/4} \quad (181)$$

A.18 Proof of Proposition 6.2

Similarly to Eq (180), we compute the transform $\hat{u}(\Phi)$ of the inverse capped option

$$\begin{aligned}\hat{u}(\Phi) &= e^{-\Phi X} \int_{-\infty}^{\infty} e^{\Phi X'} e^{-X'-\bar{\mu}(T)} \min \left\{e^{X'+\bar{\mu}(T)}, K\right\} d X' \\ &= e^{-\Phi X} \left(\int_{-\infty}^{k^*} e^{\Phi X'} d X' + K \int_{k^*}^{\infty} e^{\Phi X'-X'-\bar{\mu}(T)} d X' \right) = -e^{-\Phi X^*} \frac{1}{\Phi(\Phi-1)},\end{aligned}\quad (182)$$

where $X^* = \ln(S/K) + \bar{\mu}(T)$ is the log-moneyness and $k^* = \ln K - \bar{\mu}(T)$, with the first integral being finite for $\Re[\Phi] > 0$ and the second integral being finite for $\Re[\Phi] < 1$. The integral (182) is finite for $0 < \Re[\Phi] < 1$. We set $\Phi = iy + 1/2$, then

$$\hat{u}(\Phi = iy + 1/2) = e^{-(iy+1/2)x^*} \frac{1}{y^2 + 1/4} \quad (183)$$

A.19 Proof of proposition 6.3

Consider an option on quadratic variance I_T with terminal payoff $u(I_T)$. Using Sepp (2008), we find that option value is given by Eq (89), where $\hat{u}(\Psi)$ is the transformed payoff function

$$\hat{u}(\Psi) = \int_0^{+\infty} u(I') e^{\Psi(I'-I)} d I'. \quad (184)$$

For a call option on QV with strike K , provided $\Re[\Psi] < 0$, Eq (184) becomes

$$\hat{u}(\Psi) = e^{-\Psi I} \int_0^{+\infty} u(I') e^{\Psi I'} d I' = e^{-\Psi I} \int_0^{+\infty} \max\{I' - TK, 0\} e^{\Psi I'} d I' = \frac{e^{-\Psi I}}{\Psi^2} e^{\Psi T K}. \quad (185)$$

A.20 Proof of proposition 6.4

Using affine approximation, we can compute the joint density of $\{X_\tau, I_\tau\}$ using inverse Fourier transform, leading to

$$\begin{aligned}P_{X,I}(\tau, X, Y, I; X', I') &= \frac{1}{4\pi^2} \Re \left[\int_{-\infty}^{+\infty} \int_{-\infty}^{+\infty} e^{\Phi(X'-X)+\Psi(I'-I)} E^{[m]}(\tau, Y; \Phi, \Psi) d\Phi d\Psi \right], \\ E^{[m]}(\tau, Y; \Phi, \Psi) &= \exp \left\{ \sum_{k=0}^{2m} A^{(k)}(\tau; \Phi, \Psi) Y^k \right\}.\end{aligned}$$

As a result, we obtain

$$\begin{aligned}\tilde{U}(\tau, X, Y, I) &= \frac{e^{-\bar{r}(T)}}{T} \Re \left[\int_{-\infty}^{+\infty} \int_0^{+\infty} e^{-X'-\bar{\mu}(T)} u(I') \times \right. \\ &\quad \times \left. \frac{1}{4\pi^2} \int_{-\infty}^{+\infty} \int_{-\infty}^{+\infty} e^{\Phi(X'-X)+\Psi(I'-I)} E^{[m]}(\tau, Y; \Phi, \Psi) d\Phi d\Psi \right] dX' dI'.\end{aligned}$$

Exchanging the integration order, we have

$$\tilde{U}(\tau, X, Y, I) = \frac{e^{-\bar{r}(T)}}{T} \frac{1}{4\pi^2} \int_{-\infty}^{+\infty} \int_{-\infty}^{+\infty} \Re \left[E^{[m]}(\tau, Y; \Phi, \Psi) \hat{u}(\Phi, \Psi) \right] d\Phi d\Psi, \quad (186)$$

where $\hat{u}(\Phi, \Psi)$ is the transformed payoff function

$$\begin{aligned} \hat{u}(\Phi, \Psi) &= e^{-\Phi X - \Psi I} \int_{-\infty}^{+\infty} \int_0^{+\infty} e^{-X' - \bar{\mu}(T)} u(I') e^{\Phi X' + \Psi I'} dX' dI' = \\ &= e^{-\Phi X - \Psi I} e^{-\bar{\mu}(T)} \int_{-\infty}^{+\infty} e^{(\Phi-1)X'} dX' \int_0^{+\infty} u(I') e^{\Psi I'} dI' = 2\pi e^{-\Phi X - \bar{\mu}(T)} \delta_0(\Phi - 1) \hat{u}(\Psi), \end{aligned} \quad (187)$$

where $\hat{u}(\Psi) = e^{-\Psi I} \int_0^{+\infty} u(I') e^{\Psi I'} dI'$, provided $\Re[\Psi] < 0$. Note that we integrated out the complex exponential in (187) using results of Sepp (2007). Thus, (186) becomes

$$\tilde{U}(\tau, X, Y, I) = \frac{e^{-\bar{r}(T)}}{T} \frac{1}{2\pi} \int_{-\infty}^{+\infty} \Re \left[e^{-X - \bar{\mu}(T)} E^{[m]}(\tau, Y; \Phi = 1, \Psi) \hat{u}(\Psi) \right] d\Psi. \quad (188)$$

B Acknowledgments

The authors are thankful to Vladimir Lucic for valuable insights and comments. We thank Alan Lewis, Johannes Muhle-Karbe, Blanka Horvath, Kalev Pärna and participants at Imperial College Finance and Stochastics Seminar, TU Munich Oberseminar, EAJ Conference 2022 in Tartu for discussion and comments.

C Disclosures

The views and opinions presented in this article are those of the authors alone.

References

- Abramowitz, M. and Stegun, I. A. (1972), *Handbook of mathematical functions with formulas, graphs, and mathematical tables*, Applied Mathematics Series, National Bureau of Standards.
- Ackerer, D. and Filipović, D. (2020), ‘Option pricing with orthogonal polynomial expansions’, *Mathematical Finance* **30**(1), 47–84.
- Alòs, E., Gatheral, J., Radoicic, R. (2020), ‘Exponentiation of conditional expectations under stochastic volatility’, *Quantitative Finance* **20**, 13–27.
- Alfonsi, A. (2013), ‘Strong order one convergence of a drift implicit euler scheme: Application to the cir process’, *Statistics & Probability Letters* **83**(2), 602–607.
- Andersen, L. B. and Piterbarg, V. V. (2007), ‘Moment explosions in stochastic volatility models’, *Finance and Stochastics* **11**(1), 29–50.
- Baris, J., Baris, P. and Ruchlewicz, B. (2008), ‘Blow-up solutions of quadratic differential systems’, *Journal of Mathematical Sciences* **149**(4), 1369–1375.
- Barndorff-Nielsen, O. E. and Shiryaev, A. N. (2015), *Change of time and change of measure*, Vol. 21, World Scientific Publishing Company.
- Bayer, C., Gatheral, J. and Karlsmark, M. (2013), ‘Fast ninomiya–victoir calibration of the double-mean-reverting model’, *Quantitative Finance* **13**(11), 1813–1829.
- Bakshi, G., Ju, J. and Ou-Yang, H. (2006), ‘Estimation of continuous-time models with an application to equity volatility dynamics’, *Journal of Financial Economics* **82**(1), 227–249.

- Bergomi, L. (2015), ‘Stochastic Volatility Modeling’, *CRC Press*.
- Bergomi, L. and Guyon, J. (2012), ‘Stochastic volatility’s orderly smiles’, *Risk Magazine* 117–123.
- Black, F. and Scholes, M. (1973), The pricing of options and corporate liabilities, *The Journal of Political Economy*, **81** 637-659
- Bormetti, G., Cazzola, V., Montagna, G. and Nicrosini, O. (2008), ‘The probability distribution of returns in the exponential Ornstein–Uhlenbeck model’, *Journal of Statistical Mechanics: Theory and Experiment* **2008**(11), P11013.
- Borodin, A. N. (2017), *Stochastic processes*, Springer.
- Bühler, H. (2006), Volatility markets: Consistent modeling, hedging and practical implementation, PhD thesis, TU Berlin.
- Carr, P. and Sun, J. (2007), ‘A new approach for option pricing under stochastic volatility’, *Review of Derivatives Research* **10**(2), 87–150.
- Carr, P. and Willems, S. (2019), ‘A lognormal type stochastic volatility model with quadratic drift’, *arXiv preprint arXiv:1908.07417* .
- Carr, P. and Wu, L. (2017), ‘Leverage effect, volatility feedback, and self-exciting market disruptions’, *Journal of Financial and Quantitative Analysis* **52**(5), 2119–2156.
- Chassagneux, J-F., Jacquier, A. & Mihaylov, I. (2016), ‘An explicit Euler scheme with strong rate of convergence for financial SDEs with non-Lipschitz coefficients’, *SIAM Journal on Financial Mathematics* **7**(1), 993–1021.
- Christoffersen, P., Jacobs, K. and Mimouni, K. (2010), ‘Models for s&p 500 dynamics: Evidence from realized volatility, daily returns and options prices’, *The Review of Financial Studies* **23**(9), 3141–3189.
- Coppel, W. (1966), ‘A survey of quadratic systems’, *Journal of Differential Equations* **2**(3), 293–304.
- Cox, A. M., & Hobson, D. G. (2005). Local martingales, bubbles and option prices. *Finance and Stochastics*, 9(4), 477-492.
- Cuchiero, C., Keller-Ressel, M. and Teichmann, J. (2012), ‘Polynomial processes and their applications to mathematical finance’, *Finance and Stochastics* **16**(4), 711–740.
- Delbaen, F. and Schachermayer, W. (1994), ‘A general version of the fundamental theorem of asset pricing’, *Math. Ann.* **300**, 436–520.
- Detemple, J. and Osakwe, C. (2000), ‘The valuation of volatility options’, *Review of Finance* **4**(1), 21–50.
- Dickson, R. and Perko, L. (1970), ‘Bounded quadratic systems in the plane’, *Journal of Differential Equations* **7**(2), 251–273.
- Drimus, G. G. (2012), ‘Options on realized variance in log-on models’, *Applied Mathematical Finance* **19**(5), 477–494.
- Drimus, G. G. (2012), ‘Options on Realized Variance by Transform Methods: A Non-Affine Stochastic Volatility Model’, *Quantitative Finance* **12**(11), 1679–1694.

- Duffie, D., Filipović, D. and Schachermayer, W. (2003), ‘Affine processes and applications in finance’, *The Annals of Applied Probability* **13**(3), 984–1053.
- Filipović, D. and Larsson, M. (2016), ‘Polynomial diffusions and applications in finance’, *Finance and Stochastics* **20**(4), 931–972.
- Filipovic, D. and Mayerhofer, E. (2009), ‘Affine diffusion processes: theory and applications’, *Advanced Financial Modelling* **8**, 1–40.
- Fouque, J.-P., Papanicolaou, G. and Sircar, K. R. (2000), ‘Mean-reverting stochastic volatility’, *International Journal of theoretical and applied finance* **3**(01), 101–142.
- Friedman, A. (1975), *Stochastic Differential Equations and Applications*, Vol. 1, Academic Press.
- Gatheral J., Jaisson, T. & Rosenbaum, M. (2018), ‘Volatility is rough’, *Quantitative Finance* **18**(6), 933–949.
- Gyöngy, I. and Krylov, N. V. (1980), ‘On stochastic equations with respect to semimartingales I.’, *Stochastics: An International Journal of Probability and Stochastic Processes* **4**(1), 1–21.
- Hagan, P. S., Kumar, D., Lesniewski, A. S. and Woodward, D. E. (2002), ‘Managing smile risk’, *The Best of Wilmott* **1**, 249–296.
- Heath, D. and Schweizer, M. (2000), ‘Martingales versus pdes in finance: an equivalence result with examples’, *Journal of Applied Probability* **37**(4), 947–957.
- Henry-Labordère, P. (2009), ‘Calibration of local stochastic volatility models to market smiles’, *Risk Magazine* 112–117.
- Herdegen, M., & Schweizer, M. (2018). Semi-efficient valuations and put-call parity. *Mathematical Finance*, **28**(4), 1061–1106.
- Herdegen, M., & Schweizer, M. (2016). Strong bubbles and strict local martingales. *International Journal of Theoretical and Applied Finance*, **19**(04), 1650022.
- Heston, S. L. (1993), ‘A closed-form solution for options with stochastic volatility with applications to bond and currency options’, *The Review of Financial Studies* **6**(2), 327–343.
- Hull, J. and White, A. (1988), ‘An analysis of the bias in option pricing caused by a stochastic volatility’, *Advances in Futures and Options Research* **3**, 29–61.
- Jacobson, D. H. (1974), ‘Extensions of Linear-Quadratic Control; Optimization and Matrix Theory’, *Academic Press, London*
- Jarrow, R. A., Protter, P., & Shimbo, K. (2010). Asset price bubbles in incomplete markets. *Mathematical Finance: An International Journal of Mathematics, Statistics and Financial Economics*, **20**(2), 145–185.
- Jørgensen, B. (1982), ‘Statistical Properties of the Generalized Inverse Gaussian Distribution’, *Springer Science & Business Media*
- Jonsson, M. and Sircar, K. R. (2002), ‘Partial hedging in a stochastic volatility environment’, *Mathematical Finance* **12**(4), 375–409.
- Karasinski, P., and Sepp, A. (2012), ‘Beta stochastic volatility model’, *Risk Magazine* 66–71.
- Karatzas, I. and Shreve, S. E. (1991), *Brownian motion and stochastic calculus*, Graduate Texts in Mathematics, Springer-Verlag, New York.

- Karlin, S. and Taylor, H. E. (1981), *A second course in stochastic processes*, Elsevier.
- Kaye, G. J. (2012), *Value Of Uncertainty, The: Dealing With Risk In The Equity Derivatives Market*, World Scientific Publishing Company.
- Keller-Ressel, M. and Mayerhofer, E. (2015), ‘Exponential moments of affine processes’, *The Annals of Applied Probability* **25**(2), 714–752.
- Jarrow, R. A., & Larsson, M. (2012). The meaning of market efficiency. *Mathematical Finance: An International Journal of Mathematics, Statistics and Financial Economics*, 22(1), 1–30.
- Lewis, A. L. (2000), *Option Valuation under Stochastic Volatility*, Finance Press.
- Lewis, A. L. (2016), *Option Valuation under Stochastic Volatility II*, Finance Press.
- Lewis, A. L. (2018), ‘Exact solutions for a gbm-type stochastic volatility model having a stationary distribution’, *arXiv preprint arXiv:1809.08635*.
- Lions, P.-L. and Musiela, M. (2007), ‘Correlations and bounds for stochastic volatility models’, *24*(1), 1–16.
- Lipton, A. (2001), *Mathematical methods for foreign exchange: A financial engineer’s approach*, World Scientific.
- Lipton, A. (2002), ‘The vol smile problem’, *Risk* 61–65.
- Lipton, A. and Sepp, A. (2008), ‘Stochastic volatility models and Kelvin waves’, *Journal of Physics A: Mathematical and Theoretical* **41**(34), P344012.
- Lucic, V. (2021), ‘BTC inverse call and the standard fx framework’, Available at SSRN 4113726.
- Masoliver, J. and Perelló, J. (2006), ‘Multiple time scales and the exponential ornstein–uhlenbeck stochastic volatility model’, *Quantitative Finance* **6**(5), 423–433.
- Merton, R. C. (1973), ‘Theory of rational option pricing’, *The Bell Journal of economics and management science* 141–183.
- Musiela, M. and Rutkowski, M. (2009), *Martingale Methods in Financial Modelling*, Vol. 36, Springer Science & Business Media.
- Neuenkirch, A. and Szpruch, L. (2014), ‘First order strong approximations of scalar SDEs defined in a domain’, *Numerische Mathematik* **128**(1), 103–136.
- Pan, J. & Singleton, K. J. (2008), ‘Default and recovery implicit in the term structure of sovereign CDS spreads’, *Journal of Finance* **63**(1), 2345–2384.
- Perelló, J., Sircar, R. and Masoliver, J. (2008), ‘Option pricing under stochastic volatility: the exponential Ornstein–Uhlenbeck model’, *Journal of Statistical Mechanics* **2008**(06), P06010.
- Protter P. (2001), ‘A partial introduction to financial asset pricing theory’, *Risk Magazine* 138–143.
- Ren, Y., Madan, D. and Qian, M. Q. (2007), ‘Calibrating and pricing with embedded local volatility models’, *Risk Magazine* 138–143.
- Sepp, A. (2007), ‘Variance swaps under no conditions’, *Risk Magazine* 82–87.
- Sepp, A. (2008), ‘Pricing options on realized variance in the Heston model with jumps in returns and volatility’, *Journal of Computational Finance* **11**(4), 33–70.

- Sepp, A. (2012), ‘Pricing Options on Realized Variance in the Heston Model with Jumps in Returns and Volatility – Part II: An Approximate Distribution of Discrete Variance’, *Journal of Computational Finance* **16**(22), 3–32.
- Shephard, N. (2005), *Stochastic volatility: Selected Readings*, Oxford University Press.
- Sin, C. A. (1998), ‘Complications with stochastic volatility models’, *Advances in Applied Probability* **30**(1), 256–268.
- Stein, E. M. & Stein, J.C. (1991), ‘Stock price distributions with stochastic volatility: an analytic approach’, *Review of Financial Studies* **4**, 727–752.
- Tegner, M. & Poulsen, R. ‘Volatility is Log-Normal–But Not for the Reason You Think’, *Risk* **6**(2).
- Wu, L., Luo, H., & Fu, Z. ‘Positive Return-Volatility Correlation and Short Sale Constraints: Evidence from the Chinese Market’, *Asia-Pacific Journal of Financial Studies* **47**(1).